Natural Secretory Immunoglobulins Facilitate Enteric Viral Infection

by

Holly Turula

A dissertation submitted in partial fulfillment
of the requirements for the degree of
Doctor of Philosophy
(Immunology)
in the University of Michigan
2019

Doctoral Committee:

Associate Professor Christiane E. Wobus, Co-Chair
Professor Bethany B. Moore, Co-Chair
Associate Professor Yasmina Laouar
Associate Professor Steven K. Lundy
Professor Asma Nusrat

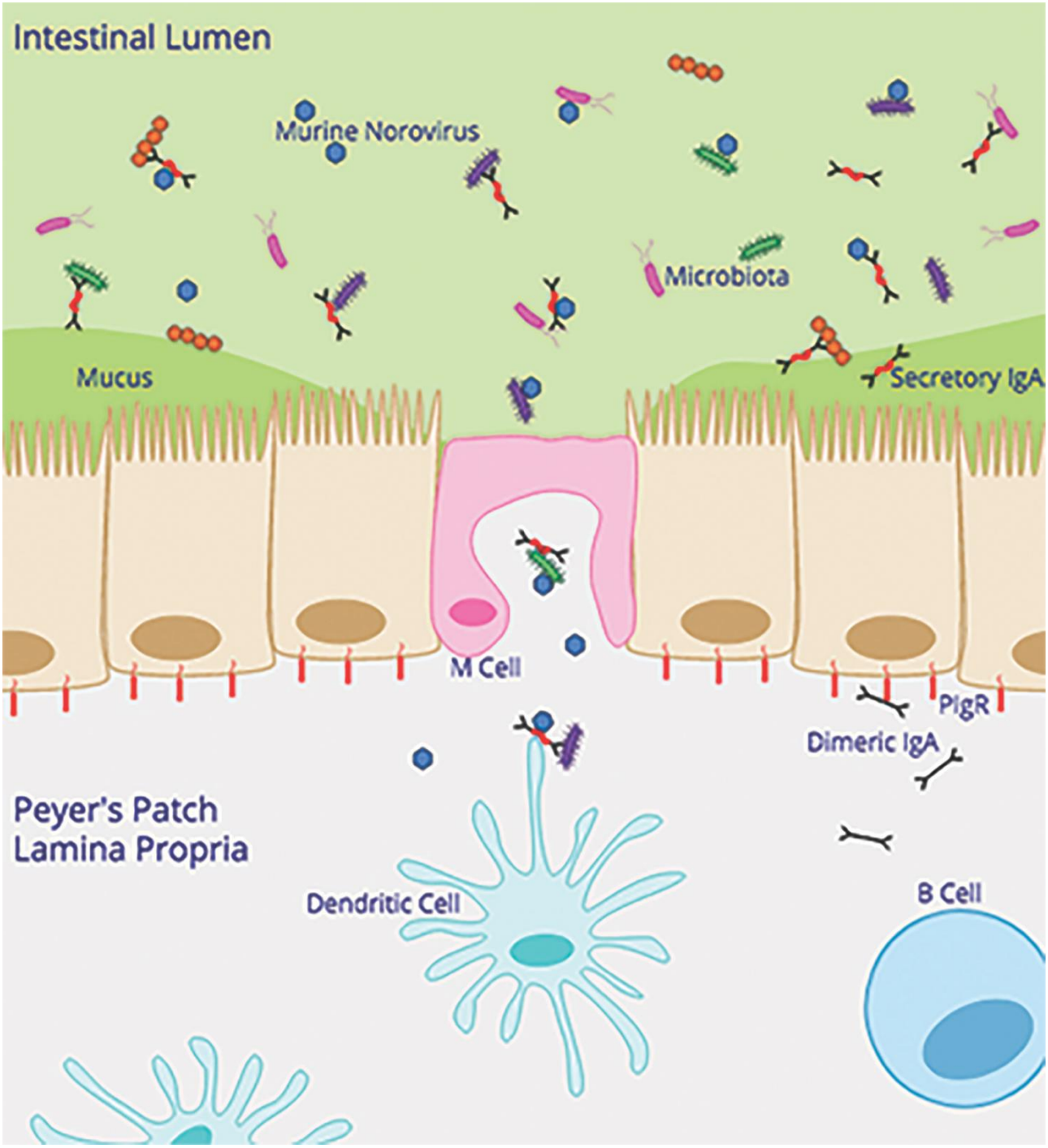
Intestinal Lumen
Murine Norovirus
Microbiota
Mucus
Secretory IgA
M Cell
PIgR
Dimeric IgA
Peyer's Patch
Lamina Propria
Dendritic Cell
B Cell

Holly Turula

hturula@umich.edu

ORCID iD: 0000-0001-5502-311X

Dedication

I would like to dedicate my doctoral dissertation to
the underprivileged youth of the United States of America and beyond.
It is my sincerest hope that I have helped in some small way
to pave the road to your future success.

Acknowledgements

My first scientific mentor Dr. Ann Hill gave me several opportunities to foster my scientific pursuits. She allowed me the opportunity to attend a scientific conference, in the beautiful surroundings of Banff Canada, without the pressure of presenting my work. This opportunity allowed me to get comfortable with listening to and engaging in scientific discussions and gave me confidence when it was finally time to present my own work at a conference. She also allowed me to audit several immunology courses at Oregon Health & Sciences University and gave me the opportunity to attend a week-long immunology short course through the American Association of Immunologists. These opportunities allowed me to gain a better understanding of the complex field of immunology and gave me a marked advantage over other students when I joined the Immunology program here at UM. I would also like to thank Mary Wittig for hiring me initially and training me on laboratory techniques, Dr. Amelia Pinto for teaching me what it means to be a good lab citizen, and Dr. Carmen Doom for allowing me to help her with her doctoral project. Working in Dr. Hill's lab I was trusted to generate data for publication and train new lab members in immunologic and virologic techniques. It was during these training experiences that I first realized my skills as a teacher.

Dr. Christopher Snyder was a post-doc throughout my 4 years in Dr. Hill's lab. When he was offered a position to start his own lab at Thomas Jefferson University in Philadelphia he offered me a chance to join him. To help me successfully transition to my new life across the country, he moved my belongings, allowed me to drive his family car (and dog) across the

country, let me stay with his family in New Jersey until I found an apartment, and even loaned me money for my security deposit so I could move in! I cannot imagine a more supportive mentor. For many months I was the sole generator of data for the Snyder lab and Chris and I would routinely find ourselves in long "science talks" trying to figure out what our data meant and how to proceed. I really treasure these interactions as they helped me to think critically about data and take intellectual responsibility for my data. I advanced greatly in his lab and as a result was very well prepared for graduate school. Chris was a strong advocate in my pursuit of graduate school and helped me tremendously during the application process. I am incredibly thankful for all he has done to support me throughout the years, and I feel incredibly lucky to have met him.

I would also like to thank Dr. Christiane Wobus for taking a chance on me and allowing me to join her laboratory as a doctoral student in the field of immunology. I have learned an incredible amount in her lab. She inspires excellence in her employees and fosters an inclusive environment where all members of the lab have equal contribution to scientific discussions. Upon joining the Wobus lab I informed Christiane that my career goal was to teach. Contrary to what I expected she was highly supportive and allowed me to take a significant amount of time away from the lab to hone my teaching skills both here at UM and in Ethiopia. She has not only tolerated my teaching endeavors but has informed me of other opportunities and seminars to advance my skills still further and has nominated me for several awards to assure I receive recognition for my efforts.

Communication is instrumental to teaching, and Christiane has helped me to communicate my ideas clearly and concisely in both my scientific seminars, and in my writing. I have advanced greatly as a scientific writer due to her guidance and I am very grateful for her willingness to pass her skills onto me. The Wobus lab takes great pride in presenting data clearly and effectively and I have received invaluable feedback regarding how to share my data with the scientific community. I often remark that they lovingly tear my presentations to shreds, only to make them stronger going forward reminding me of the military adage "the more you sweat in training the less you bleed in war". Together with her thoughtful and considerate lab, Christiane has undoubtedly prevented many "injuries" during my presentations.

The freedom Christiane has allowed me in creating my own schedule has been instrumental to my success. She has allowed me to work non-traditional hours and has been flexible regarding my working from home. This has been really wonderful for me and allowed me to reach my goals with relative ease. She has also allowed me the freedom to volunteer at UM and the surrounding community to enhance diversity in the sciences, work which is both rewarding and rejuvenating to me.

In addition to Christiane, the senior scientists in the Wobus lab, Dr. Abimbola "Ola" Kolawole and Dr. Karla Passalacqua, have been incredible mentors to me. They have been quick to help answer my scientific questions and offer invaluable advice. My favorite advice from Karla came as I was preparing for my qualifying exam to become a PhD candidate. I was feeling a lot of stress and anxiety because I felt that other students knew more than I did. Her advice was "Don't look left, don't look right, just look forward". This has turned out to be great life advice

over the years and I find myself repeating it to any student that will listen. She is always available for me to complain about the crumbling state of our society, or to offer valuable insight regarding rigor and reproducibility in my scientific endeavors. I trust her judgement tremendously. Ola is my perpetual ray of sunshine and has an uncanny ability to make me laugh even at the darkest of times. He has helped calm me after countless mishaps in the lab and is always encouraging and kind.

My doctoral thesis committee has been wonderful in regard to helping me and Christiane throughout the tumbling and whirling that was my PhD. Their guidance has saved me from going down some very silly rabbit holes by keeping an eye always on the bigger picture. Of note I would like to especially thank Dr. Beth Moore, my doctoral committee co-chair. She has always made time in her absurdly busy schedule to meet with me to discuss not only how to improve my scientific work, but also the Immunology program as a whole. She has been a true advocate for me and has nominated me for several awards and taken the time to attend the awards ceremonies to help me celebrate. I feel very fortunate to have had essentially two doctoral thesis committees, my traditional committee, and the mentors in our bi-weekly virology joint lab meeting called "IT'S WOW" so named after doctors Imperiale, Tai, Spindler, Weinberg, Ono and Wobus (previously "SWIVL" including Dr. Lauring). They have seen my data from its infancy and have helped to guide me throughout my entire PhD. Of note, Dr. Spindler has gone above and beyond in helping me to achieve my career goals and I am very grateful for her guidance along the way.

I have had several amazing teaching mentors that have allowed me several hands-on opportunities to enhance my teaching skills. I would like to thank Dr. Victor DiRita for agreeing

to be my teaching mentor and helping to guide me through difficult situations with students. He has also given me much great career advice, along with Dr. Thomas Moore. Tom really trusted me to take on larger than normal teaching tasks which allowed me the experience I needed to move into my next position with confidence and I am very grateful. Dr. Venkat Keshamouni and Michal Olszewski have also allowed me an amazing opportunity to gain valuable one-on-one teaching mentorship and have helped me to realize what it takes to be an effective teacher.

I would also like to thank Tracey Shultz for her kind ear and her zany antics. I am also indebted to Dr. Malini Raghavan for noticing my need for support and taking the time to meet with me privately to help. She introduced me to the healing power of taking a moment for myself every day in the form of yoga and has forever changed my life. I would also like to thank Zarinah Aquil who has always been so proud of my accomplishments and has always been available to listen and praise me liberally, which is something every graduate student needs!

I have been fortunate to receive much love and compassion from my great aunt Jan and uncle Gerry Nelson. They have been a wonderful source of support throughout my life and have taught me that it is your actions and not where you come from that defines you. They have given me hope in the darkest moments of my life and have shown me the path of love and kindness and I am forever grateful.

I am also very grateful to Brian Gregorka. He has taught me what it means to be a loving and supportive partner. My zest for self-improvement is matched in him and I am so thankful to have the opportunity to grow with him in the future. His goofy nature keeps me upbeat and his acceptance of my emotions and my past allows me the courage to heal and become a more

balanced person. His intelligence, diligence, and love of learning have motivated me tremendously to explore my passions and develop my extracurricular skills. His love of nature surpasses even my own and I have learned so much from him about the planet, the forests, biochemistry, and Michigan. He is a patient and enthusiastic teacher and I look forward to learning all he has to teach me in the coming years.

I first met Dr. Juliana Bragazzi-Cunha in Christiane Wobus's lab where she was a graduate student. We immediately bonded over our detail-oriented approach to the lab and our overenthusiastic nature. She is the only person I know who uses more exclamation points than me! Throughout graduate school she has been my +1 at countless events which helped motivate me to be social and to have a life outside of lab. I highly value her honesty and compassion and she has been an amazing friend over the years. I can always count on her to help me be impartial in my thinking and to help me understand my own emotions. She has been a great scientific ally as well and has insisted on attending all my presentations well after moving on from the Wobus lab. She is an amazing person, scientist, and friend.

I have made more friends in graduate school than I have in my entire life, and the quality of these friendships can hardly compare to those of my youth. I would like to specifically thank my Immunology Program friends Dr. Peter Chockley for his astounding mind, Dr. Amanda Wong and Dr. Julia Wu for their continued support and friendship, and soon to be Dr. Emily Yarosz for her compassion and understanding. I would also like to thank my "townie" friends Andy Hosford for being always accepting and kind, and Maggie Halpern for her advice and giggles. I would like to acknowledge Jared Carpenter for his enthusiasm, unfailing good nature,

and love of Minnesota. My roommate Martha Alves and I have developed a close bond over the years and I am very proud of our ability to be open with one another. She is kind to a fault and I have been fortunate enough to benefit from that “defect”. I would also like to thank my Philadelphia friends Ryan McKelvey and Justin “Judd” Hill for their support and awe over the years. They have helped me see just how special I am. Lastly, I would like to thank my dog George for teaching me patience and compassion. He is always there to go adventuring, make me smile, and to lick my tears and I am so grateful for him.

Table of Contents

List of Figures

Abstract

Noroviruses are enteric pathogens causing significant morbidity, mortality and economic losses worldwide. Secretory immunoglobulins (SIg) are a first line of mucosal defense against enteric pathogens. They are secreted into the intestinal lumen via the polymeric immunoglobulin receptor (pIgR), where they bind to antigens. However, whether natural SIg protect against norovirus infection remains unknown. To determine if natural SIg alter murine norovirus (MNV) pathogenesis, I infected pIgR knockout (KO) mice, which lack SIg in mucosal secretions. Acute MNV infection was significantly reduced in pIgR KO mice compared to controls, despite increased MNV target cells in the Peyer's patch. Natural SIg did not alter MNV binding to, or crossing, of the follicle-associated epithelium (FAE) into the lymphoid follicle. Instead, naïve pIgR KO mice have enhanced levels of the antiviral inflammatory molecules interferon gamma (IFN-g) and inducible nitric oxide synthase (iNOS) in the ileum compared to controls. Strikingly, depletion of the intestinal microbiota in pIgR KO and control mice resulted in comparable IFN-g and iNOS levels, as well as MNV infectious titers. IFN-g treatment of WT mice and neutralization of IFN-g in pIgR KO mice modulated MNV titers, implicating this antiviral cytokine in the phenotype. Reduced gastrointestinal infection in pIgR KO mice was also observed with another enteric virus, reovirus. Collectively, my findings suggest that natural SIg are not protective during enteric virus infection, but rather that SIg promote enteric viral infection through alterations in microbial immune responses.

Chapter 1: Introduction

The Immunological Threesome of Norovirus, Secretory Immunoglobulins, and Enteric Bacteria

The text and figures presented in this chapter were recently published in Viruses, Volume 10, Issue 5, Pages 237-252; 2018 and Trends in Molecular Medicine, Volume 22, Issue 12, Pages 1047-1059; 2016

INTRODUCTION

1.1 Human Norovirus is an Emerging Pathogen

The gastrointestinal tract is the largest mucosal surface in the body [1]. The gastrointestinal lumen houses a large number and variety of commensal microbes (bacteria, viruses, fungi, protozoa, and single-celled archaea species), collectively referred to as the microbiome. In addition to the commensal microbiome, pathogenic microbes can also populate the GI tract. One such microbe, Norovirus, is the primary cause of gastroenteritis worldwide. In the United States alone, human noroviruses (HNoVs) are responsible for approximately 20 million cases of acute gastroenteritis

annually, leading to over 70,000 hospitalizations and nearly 800 deaths [2]. HNoV infections are also a global problem, causing approximately US$60 billion in societal costs every year [3]. NoV is a genus in the *Caliciviridae* family. These non-enveloped, icosahedral viruses have a single-stranded, positive-sense RNA genome, and are classified into at least six genogroups on the basis of their nucleotide sequence [4]. Genogroup I (GI), GII, and GIV viruses infect humans, with GII being the most prevalent, while GV viruses infect rodents [5]. The NoV genome contains three to four open reading frames (ORFs) (**Figure 1.1**). ORF1 encodes nonstructural proteins including viral protein, genome-linked (VPg) and the RNA-dependent RNA polymerase (RdRp). ORF2 and ORF3 encode the major and minor structural capsid proteins VP1 and VP2, respectively [4]. ORF4 is only found in MNVs and encodes virulence factor VF1 [6].

NoV transmission typically occurs by the fecal–oral route from contaminated surfaces, food or water, and by person-to-person spread [4], but transmission via droplets, through aerosolization of HNoV-containing vomitus, can also occur [7, 8]. Outbreaks occur in places where people gather (e.g., cruise ships, day-care centers, hospitals). They are facilitated by the low numbers of virions able to cause infections (i.e., low infectious dose) [9, 10], high amounts of viral shedding [11], high environmental stability of HNoV [12], and a relative viral resistance to disinfectants [13]. After an average 29-hour incubation period, HNoV infection induces symptoms including abdominal pain, nausea, vomiting, and diarrhea, which typically resolve within 1–4 days [11, 14, 15]. However, viral shedding may occur for weeks to months in asymptomatic healthy hosts [16], and years in immunocompromised patients [17]. The latter have been postulated to serve as a reservoir for future outbreaks [18]. There is no significant correlation between presentation of symptoms and viral burden, duration, or magnitude of NoV shedding, but enhanced cytokine responses correlate with HNoV symptoms and suggest immune

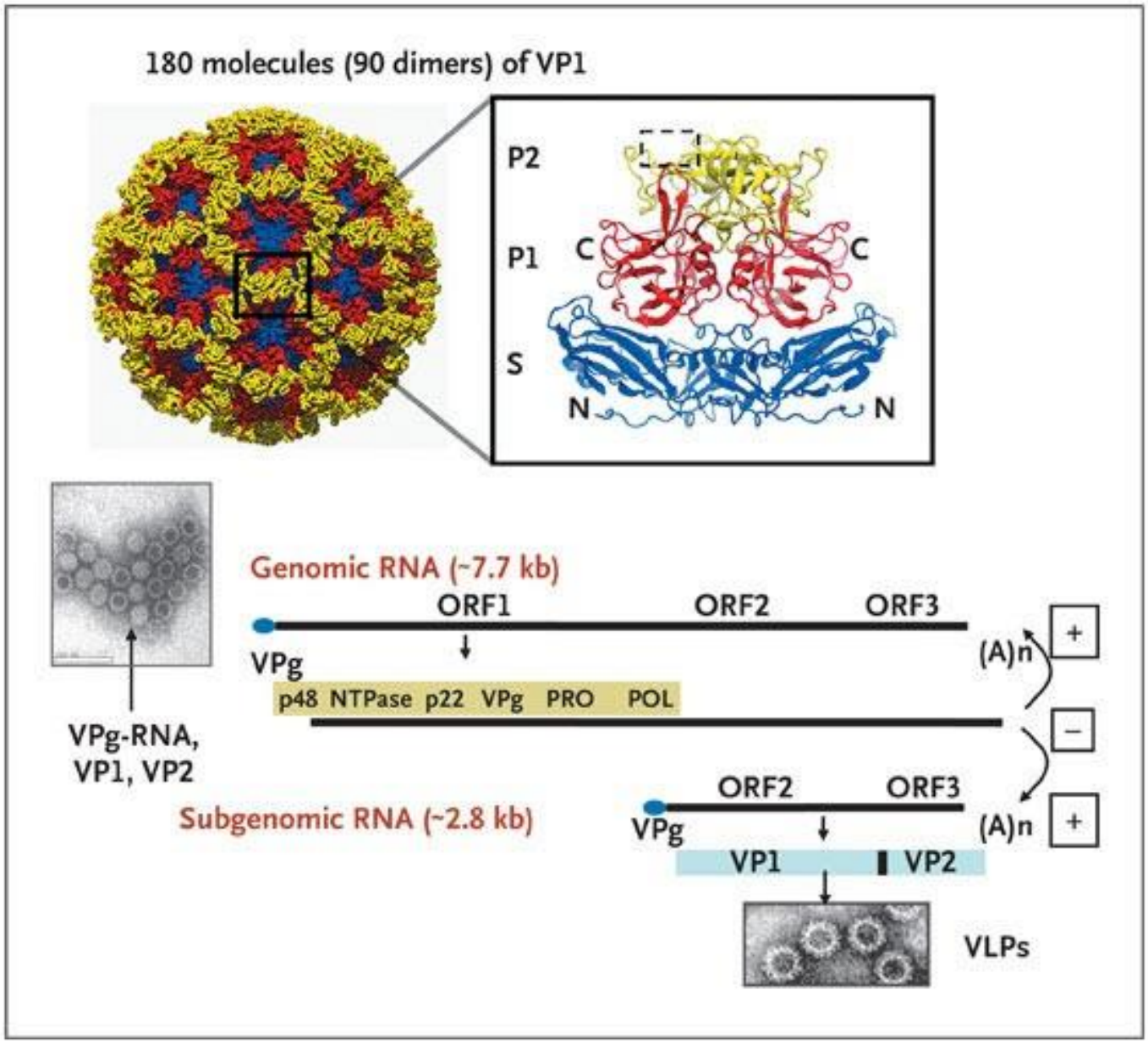

Figure 1.1: Human norovirus (HuNoV) virion and genome structure. TOP. Color coded ribbon structure of the murine norovirus shell (S)- and protruding (P)-domain of the virus capsid protein 1, dashed box indicates histo-blood group antigen binding sites. **BOTTOM.** Transmission electron micrograph of HuNoV as well as genomic organization and genome replication of HuNoV, a positive-sense single stranded RNA virus. (from Glass et. al. 2009)

mediated symptomology [11]. Complications can occur following acute infection and includepost-infectious irritable bowel syndrome [19, 20], life-threatening dehydration [21], necrotizing enterocolitis [22], and exacerbation of Crohn's disease [23].

Recent developments in HNoV research are overcoming the historical lack of cell culture and small animal models [24-26]. Nevertheless, the direct study of factors regulating HNoV pathogenesis in the natural host will always be limited. To counter this limitation, HNoV infections are studied in non-human hosts or related NoVs are investigated in their natural hosts. HNoVs can infect animal models, but only those with drastically reduced immune responses [24]. Alternatively, models relying on the natural infection of surrogate viruses can be used (recently reviewed [27]).

1.2 Murine Norovirus Provides a Model to Study Norovirus Biology

Murine norovirus (MNV), a natural mouse pathogen first described in 2003 [28], is endemic to animal facilities throughout the world [29-31]. MNV cultivation in multiple cell types in vitro, the ability to genetically manipulate both virus and host, and the use of acute [murine norovirus 1 (MNV-1)] and chronic (e.g., MNV-CR6, MNV-CR3) MNV strains add to the strengths of this model system [18, 27]. Together, these studies have revealed novel host pathways critical to the regulation of NoV infection and facilitated the exploration of NoV interactions with the commensal microbiome, a critically important player in mucosal infection. MNV provides the most widely used, readily tractable model system to explore viral factors regulating NoV infection.

The MNV system can also be used to determine host factors contributing to NoV infection. Cellular tropism of NoVs is determined at the level of virus entry [32]. This was confirmed recently following the identification of CD300LF and CD300LD as functional receptors for MNV [33, 34]. Expression of murine CD300LF and CD300LD in multiple non-susceptible cells, including HeLa or HEK293T cells from nonmurine hosts, supported MNV infection, while infection could be reduced by competition with soluble protein or antibody [33, 34]. Expression of the human homologue CD300F was unable to substitute for murine CD300LF, nor was anti-human CD300F antibody able to block infection, indicating that restriction of NoVs may be due to species- specific variation in these molecules, rendering them determinants of species specificity. CD300LF and CD300LD belong to a family of type I transmembrane proteins with an immunoglobulin-like extracellular domain that can bind lipids in the plasma membrane [35]. Both proteins are expressed in myeloid cells, which are known MNV target cells [36, 37]. These findings raise questions regarding their physiological role during MNV infection *in vivo*. Preincubation of MNV-1 with soluble CD300LF prevents mortality of Stat1- deficient mice, and *Cd300lf*$^{-/-}$ mice are resistant to viral shedding following oral infection with MNV.CR6 [33]. Whether MNV establishes tissue infection in *Cd300lf*$^{-/-}$ or *cd300ld*$^{-/-}$ mice, however, has not been reported.

1.3 Reovirus is an Enteric Pathogen

Respiratory enteric orphan virus (reovirus) is a double-stranded RNA virus in the family *Reoviridae*. Reovirus is non-enveloped, and the outer capsid and the protein core surround the segmented viral genome (**Figure 1.2**). As the name suggests, infection is initiated via the respiratory or gastrointestinal tract and is mostly asymptomatic, but can result in hematogenous

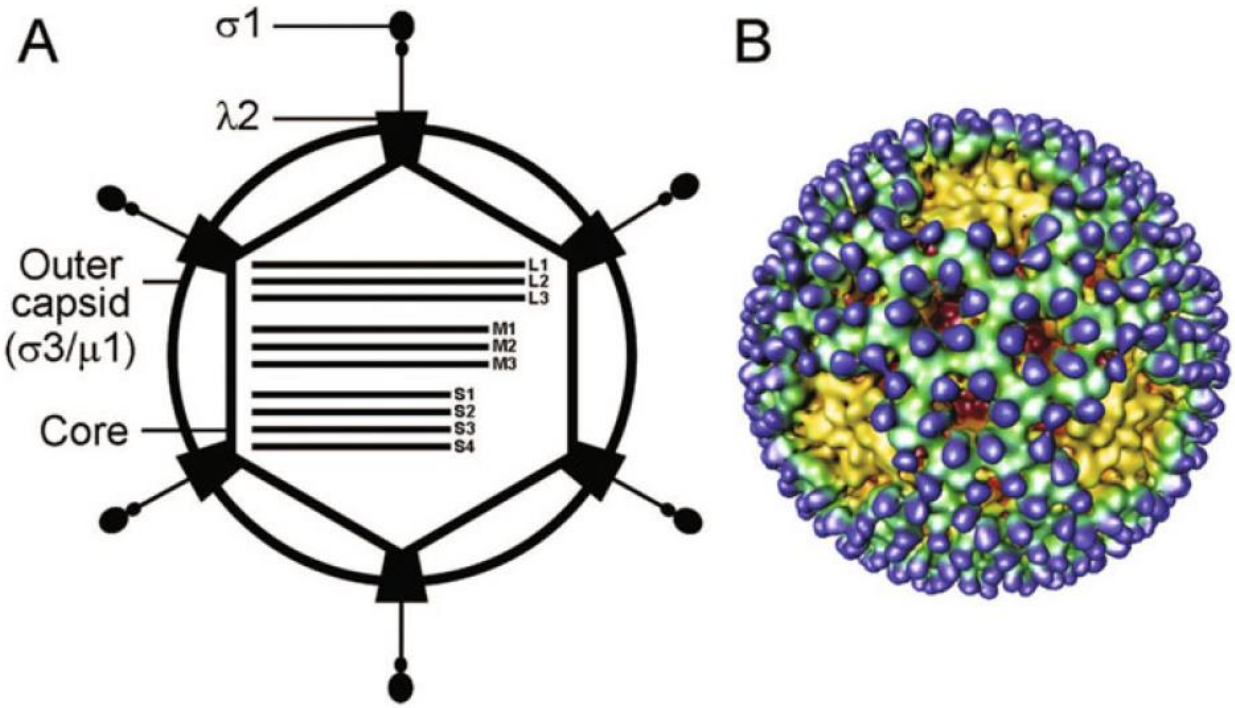

Figure 1.2: Reovirus virion and genome structure. A. Schematic of reovirus capsid and capsid proteins including attachment protein σ1, as well as the reovirus core and segmented double-stranded RNA genome. **B.** Reconstitution of Cryo-electron micrograph image of reovirus virion at 23 Å resolution. (from Danthi et. al 2013)

dissemination and myocarditis [38, 39], as well as central nervous system spread and hydrocephaly [40]. Reovirus attaches to epithelial cells via the attachment protein σ1 interaction with epithelial basolateral surface protein junction adhesion molecule-A (JAM-A) [41]. Endocytosis of reovirus into the host cell via σ1 interaction with β1 integrins stimulates cathepsin-mediated digestion of the outer protein shell. Reovirus uncoating results in exposure of viral protein μ1 which mediates endosomal membrane pore formation and viral core release into the cytosol [42, 43]. Once in the cytosol, the transcriptionally active viral core initiates mRNA formation and protein synthesis [44]. In addition to epithelial cells, reovirus may also infect dendritic cells via JAM-A at the initial site of pathogen entry [45], which could aid in viral spread to the draining mesenteric lymph nodes and distal sites such as ependymal cells of the brain [46].

1.4 Mucosal Defenses Against Pathogens

To combat enteric viruses and other microbes, the GI tract has evolved several host defense mechanisms to prevent their entry into the host. The intestinal epithelial layer that separates the intestinal lumen (the space where food passes through) and the interior of the body is only a single cell layer thick [1] (**Figure 1.3**). To protect itself from these microbes, the epithelial barrier has developed an array of defense mechanisms. Epithelial cells connected by tight junction complexes are a critical barrier that separate the host interior, termed lamina propria, from the outside world. Tight junctions, coupled with mucus production by goblet cells, make the intestine relatively impermeable to pathogens and antigens. The protective capacity of this physical barrier is further enhanced by innate and adaptive immune responses. The intestinal

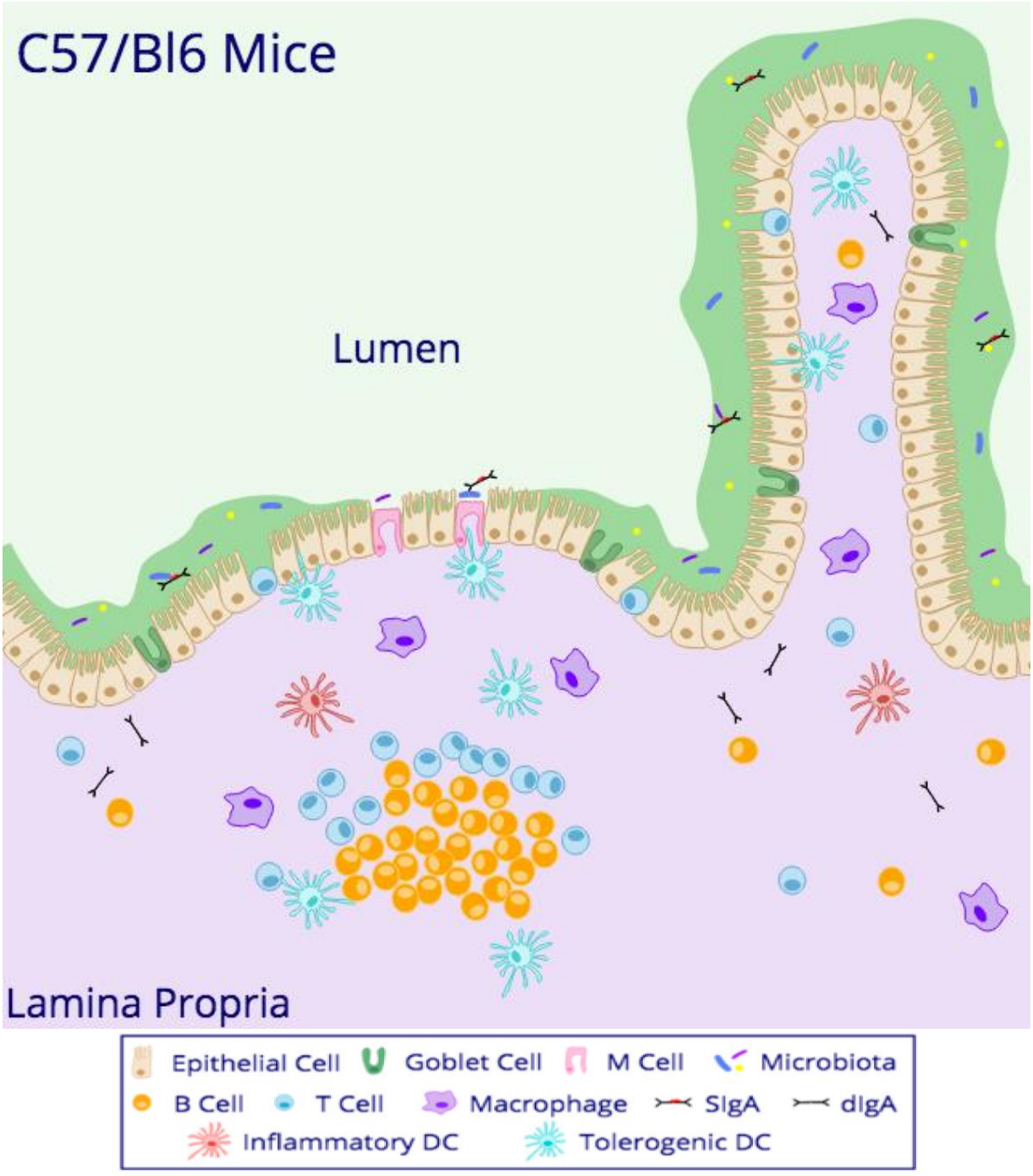

Figure 1.3: Mucosal defense against enteric pathogens. Schematic representation of small intestinal tissue including intestinal vili and Peyer's patch. The intestinal epithelial barrier is a single cell layer thick. Through mucosal defenses such as epithelial cell tight junctions, mucus production by goblet cells. Dimeric immunoglobulin A (dIgA) is secreted from the intestinal lamina propria into the lumen to form secretory immunoglobulin A (SIgA). SIgA binds to intestinal antigens and is transcytosed through highly transcytotic microfold (M cells) overlying the Peyer's patch. Dendritic cells (DC) immediately underlying the M cells uptake SIg immune complexes and generate tolerogenic immune responses.

epithelium and underlying lamina propria has the largest population of T cells, B cells and macrophages in the body [1]. They are primarily localized in lymphoid follicles, where both local and systemic immune responses are initiated.

1.5 Microfold (M) Cells Mediate Transcytosis of Lumenal Contents

Immune cell sampling of the luminal contents is necessary for generating both tolerogenic and inflammatory immune responses [47], a process primarily mediated by Microfold (M) cells [48]. M cells are specialized epithelial cells found on mucosal surfaces. M cells are primarily localized overlying the mucosa-associated lymphoid tissue in the follicle-Associated Epithelium (FAE) of the small intestine, colon, tonsils, rectum, and respiratory system (**Figure 1.4**) [49, 50]. M cells function in the FAE barrier to transport luminal antigens across the intestinal epithelium to the antigen-presenting cells within the lymphoid follicle [48]. M cells are highly endocytic, and can transport macromolecules and microorganisms through the M cell in 10-15 minutes [48]. The M cell morphology is specifically tailored for this purpose. The apical surface has truncated microvilli and a reduced mucus layer, which allows luminal contents access to the cell surface, unlike the rest of the mucosal epithelium [51]. The basolateral surface of the M cell plasma membrane is invaginated, forming a "pocket" (**Figure 1.4**). The pocket increases the transcytosis rate of the M cells by minimizing the intracellular distance necessary to reach the basolateral surface.

The fate of SIg-immune complexes in the lumen is not only restricted to immune exclusion, SIgA-immune complexes are also sampled by the host via M cells and contribute to maintaining homeostasis of the mucosa. ‘Retrotranscytosis’ (apical to basolateral) of SIgA

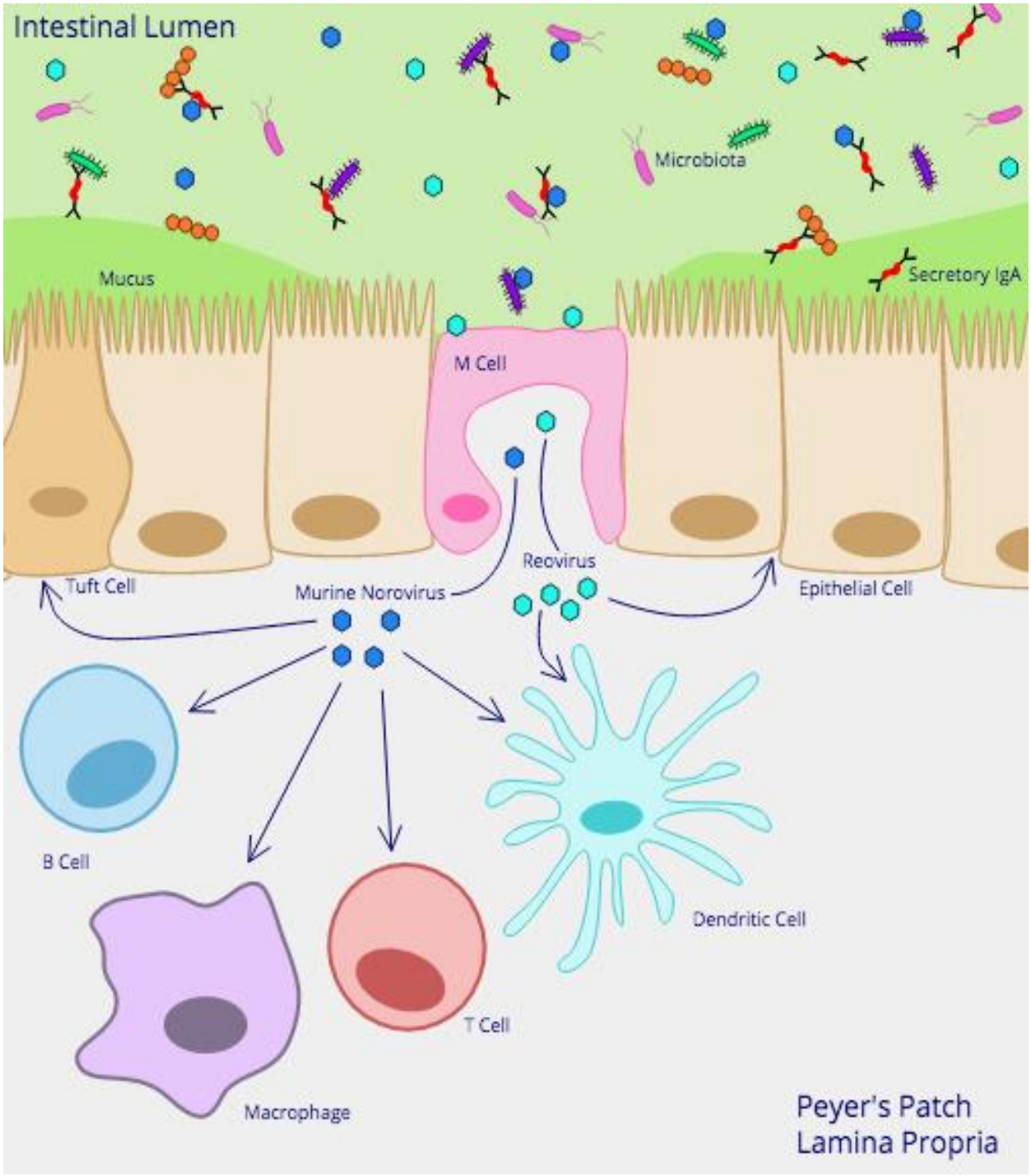

Figure 1.4: Norovirus and reovirus utilize microfold (M) cells to facilitate infection. Both viruses rely on M cells to cross the follicle associated epithelial (FAE) barrier and gain access to virus susceptible cells. Once across the FAE barrier, murine norovirus is free to infect immune cells (B cells, macrophages, T cells and dendritic cells) as well as specialized chemosensory epithelial (tuft) cells. Reovirus can also infect dendritic cells but primarily infects intestinal epithelial cells via basolatterally expressed tight junction proteins.

complexes across the epithelial barrier is mediated by M cells located in the mucosal-associated lymphoid tissue [5]. Although the identity of the receptor that mediates SIgA transcytosis on M cells remains unknown, the asialoglycoprotein receptor (ASGPR), a lectin-like receptor, or FcαRI (CD89) were ruled out as candidates [5]. Upon internalization through the M cell, "tolerogenic" DCs immediately underlying the M cell phagocytose SIgA-immune complexes [94,95]. Although binding to CD4+ T cells was noted, complexes were not internalized. Uptake of SIgA-immune complexes by mouse or human DCs is mediated via specific intercellular adhesion molecule-3 grabbing non-integrin receptor (SIGNR) 1 or the human homolog DC-SIGN, respectively [96,97]. SIgA-immune complexes can further bind to murine intestinal DCs via Dectin-1, and SIGNR3 [98].

1.6 Microfold (M) Cells are Necessary for Efficient Norovirus and Reovirus Infection

Despite their primary role as a sentinel cell involved in immune surveillance, several bacteria, viruses, and even prions, hijack the highly endocytic nature of M cells, and use them to invade the FAE [47]. In this context, M cells act as a gateway for pathogen entry, rather than a gatekeeper. For example, Reovirus σ1 protein facilitates selective binding to M cells allowing for viral entry into the host interior (**Figure 1.4**) [52-55]. The enhanced access to the cell surface, easy entry into the lamina propria, and localization of potential target cells to the site of antigen crossing all make M cells ideal ports of pathogen entry for noroviruses. Recently, a model was proposed based on experimental evidence, whereby MNVs use lymphoid follicle M cells to overcome the epithelial barrier in order to infect B cells, macrophages, and dendritic cells (DCs) in the intestine, before being trafficked to local lymph nodes and distal sites by DCs [25, 55-59]

(**Figure 1.4**). B cells are also targets for HNoVs [25], but other targets exist, since humans deficient in B cells are still susceptible to HNoV infection [60]. Recent immunofluorescence analysis of small intestinal biopsy samples from HNoV-infected immunocompromised patients revealed the presence of HNoV infection in intestinal epithelial cells, CD68+ or DC-SIGN+ phagocytes (e.g., macrophages, DCs), and CD3+ cells (T cells or intraepithelial lymphocytes) [61]. A tropism of HNoV for enterocytes was subsequently confirmed by cultivating HNoV in human intestinal enteroid monolayer cultures [26]. MNV antigen is also observed in small intestinal epithelial cells of immunodeficient signal transducer and activator of transcription 1 (Stat1)- and recombination activating gene (Rag1)/Stat1-deficient mice [62, 63]. Whether these cells are intestinal chemosensory cells (tuft cells), identified subsequently as a MNV target cell during persistent infection [64] remains unknown. Taken together, the data indicate that both MNV and HNoVs share a tropism for intestinal immune cell subsets found underlying the M cells within lymphoid structures of the GI tract and cells of intestinal epithelial origin.

1.7 Interferon Gamma (IFN-γ) Inhibits Reovirus and Norovirus Infection

Interferon-gamma (IFN-γ) is a cytokine with known antiviral effects. Exogenous treatment of cells with IFN-γ results in direct inhibition of reovirus binding and infection in vitro [65]. These findings have yet to be tested directly in vivo, however reduction of IFN-γ responses mediated by fungal Fusarium spp. T-2 mycotoxin administration resulted in enhanced reovirus infection, suggesting IFN-γ also reduces reovirus infection *in vivo* [66]. The role of IFN-γ in controlling norovirus infection has been studied for the past 15 years. Direct testing of IFN-γ effects on MNV-1 infection in primary and transformed cells revealed a dose-dependent decrease in MNV genome translation after IFN-γ treatment compared to untreated controls [67].

Additionally, pretreatment with as little as 1 unit of IFN-γ was sufficient to significantly reduce MNV-1 infection in vitro [68]. Human norovirus consensus sequence replicon-transduced cells treated with IFN-γ exhibited reduced RNA production compared to untreated cells, suggesting human norovirus is also susceptible to IFN-γ [69]. Furthermore, activation of transcription factors Stat 1 and interferon regulatory factor 1 (IRF1) downstream of IFN-γ signaling results in transcription of cytokines, chemokines, and interferon-stimulated genes, which mediate anti-MNV activity in vitro and in vivo, further implicating IFN-γ in noroviral immunity [70, 71]. However these transcription factors are also activated by type I interferons, and host IFN-γ serum cytokine responses were unchanged during d1-4 of human norovirus infection in both symptomatic and asymptomatic individuals as compared to their pre-challenge IFN-γ levels [11], highlighting the need for further studies into IFN-γ mediated nororvirus immunity.

The above data clearly demonstrate the antiviral role of IFN-γ in norovirus infection, however the mechanism behind norovirus translation inhibition was not elucidated fully. Interestingly, it was determined that IFN-γ exerts its antiviral activity against MNV by disruption of the MNV replication complex. Replication complexes (RC) are intracellular host membranes utilized by positive-sense RNA viruses to facilitate viral replication. MNV RCs organize close to the nucleus and contain all MNV non-structural proteins [72]. Upon IFN-γ treatment, ubiquitin-like LC3-II is ligated to the surface of the MNV RC via the E3 ligase-like autophagy complex Atg:12Atg5:Atg16L1 (**Figure 1.5**) [68, 73]. Rather than degrading the RC through the canonical autophagy pathway [68], LC3-II recruits granulocyte binding proteins (GBP) and immune related GTPases (IRGs) to the vacuolar membrane of the RC resulting in vessiculation and MNV RC disruption [73]. Together these data point to a model in which IFN-γ directly inhibits norovirus translation by disruption of the intracellular norovirus replication complex.

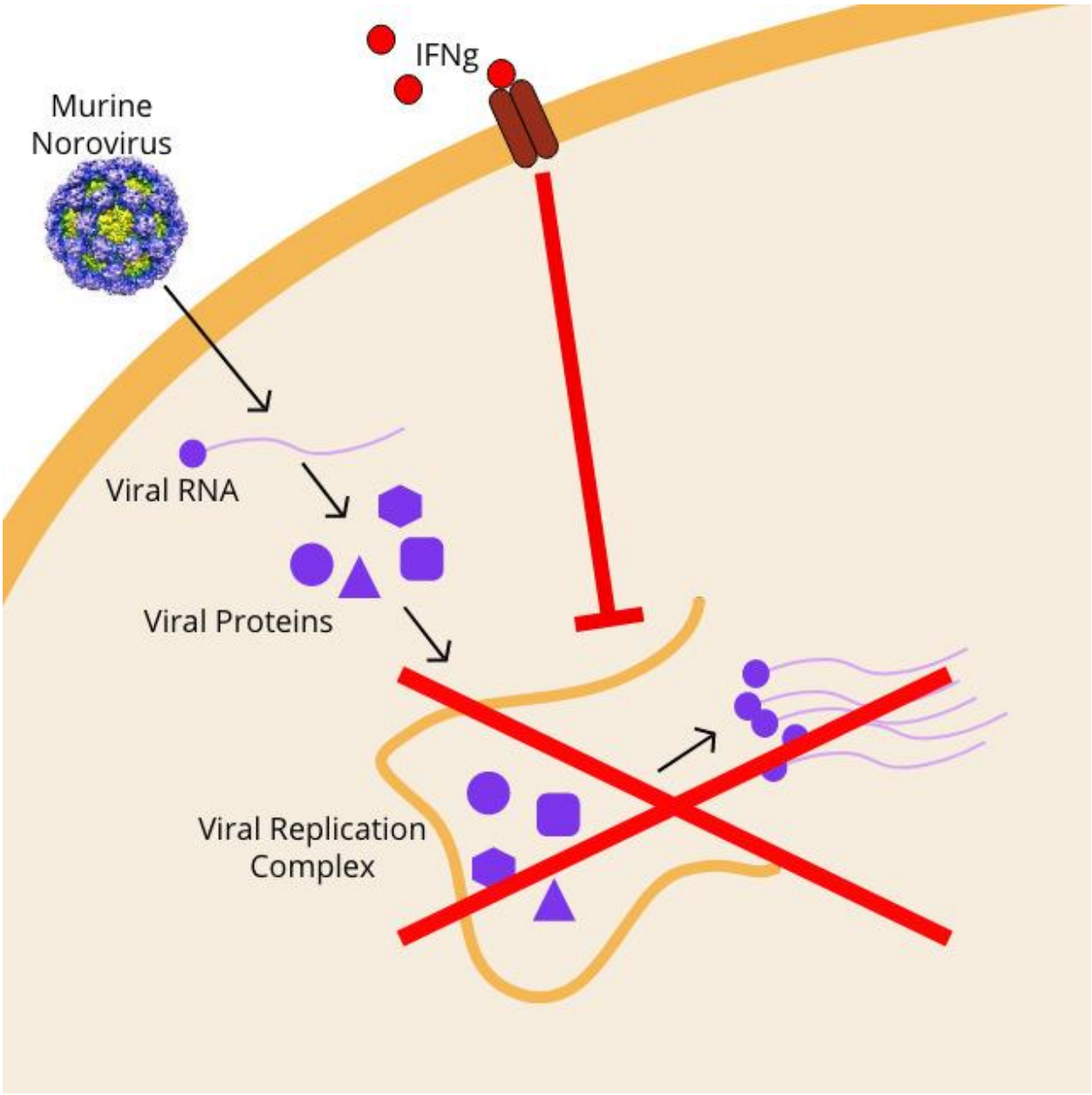

Figure 1.5: Model of interferon-gamma induced disruption of murine norovirus replication complex. Interferon-gamma induced GTPases inhibit murine norovirus replication complex formation within target cells resulting in inhibition of viral replication. Figure modeled from Biering et al. 2017.

1.8 Polymeric Immunoglobulin Receptor (pIgR) Structure and Expression

In addition to cytokines, cells at mucosal surfaces also respond to secretory immunoglobulins (SIgs) resulting in immune-mediated pathogen regulation. SIgs elicit both innate and adaptive immunologic mechanisms at mucosal barriers. Polymeric immunoglobulins (pIg), specifically dimeric immunoglobulin A and polymeric immunoglobulin M, are made by plasma cells in the lamina propria underlying the epithelial barrier (**Figure 1.6**). They are then transported across the epithelial barrier with the help of the polymeric immunoglobulin receptor (pIgR). PIgR is a highly glycosylated [74, 75], type I transmembrane protein with a predicted molecular mass of ~81 kDa that is conserved among all vertebrates [76]. NoV are known to bind to glycosylated molecules. However, if NoV can interact with SIg carbohydrate residues, and what role this plays in viral sequestration, if any, within the mucus layer or NoV transcytosis across the barrier remains to be determined.

PIgR protein expression and SIg secretion are modulated by multiple factors: immunological, microbial, hormonal and environmental [77]. A main regulator of pIgR expression are immune system mediators, including IFNγ and tumor necrosis factor alpha (TNFα) [78]. Regulation occurs at the transcriptional level and several transcription factor binding sites, including nuclear factor κ-light-chain-enhancer of activated B cells (NF-kB) and interferon regulatory factor 1 (IRF1), are found near the 5' end of the PIGR gene. Thus, PIGR gene transcription and subsequently pIgR:pIg transcytosis are upregulated following NF-κB activation [79]. Several immune signaling cascades, including toll-like receptor (TLR) activation and inflammatory cytokine signaling, converge on NF-κB and have been demonstrated to directly upregulate PIGR gene expression and pIgR:pIg transcytosis both in vivo [80, 81] and in

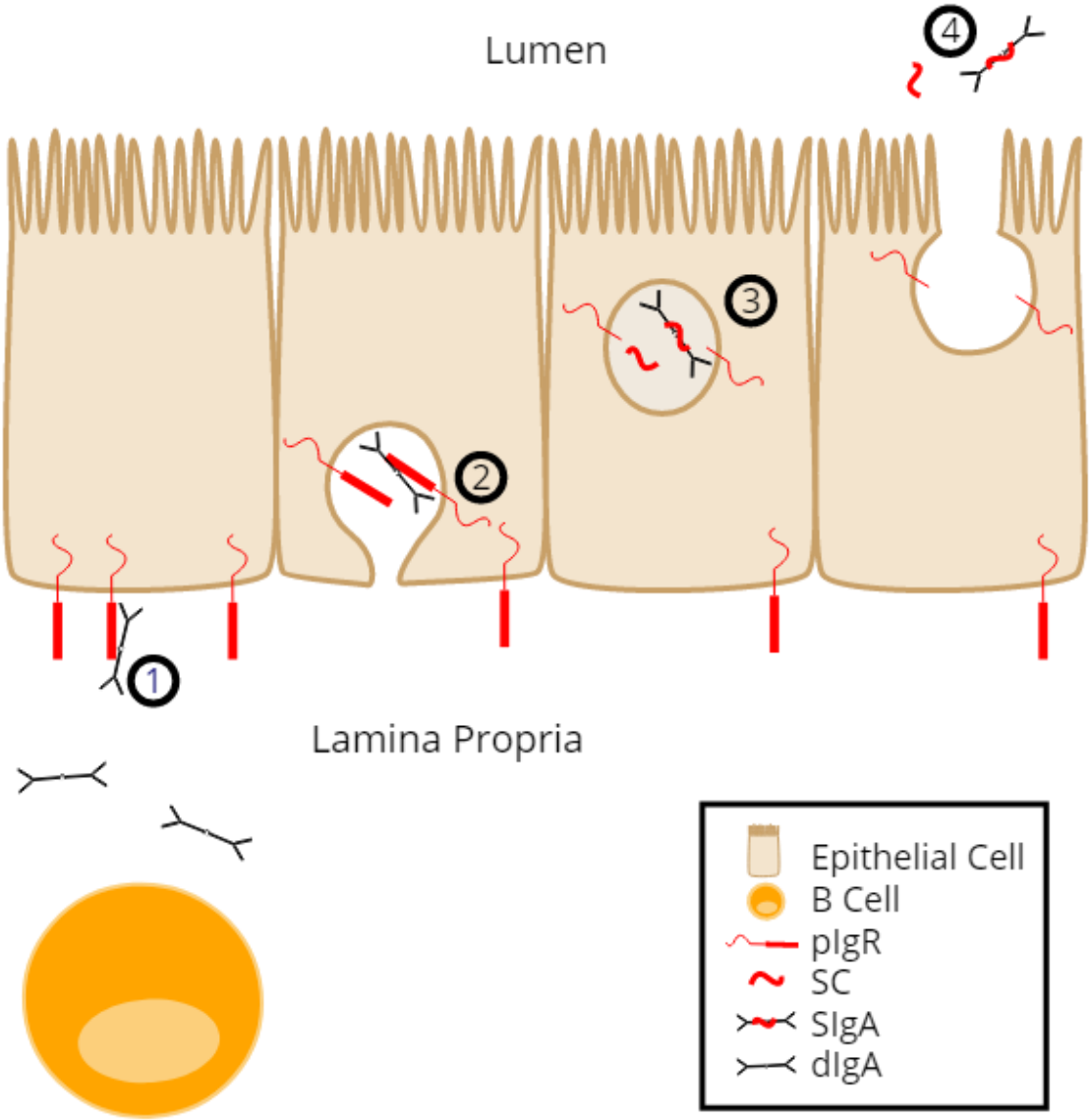

Figure 1.6: Transport of polymeric immunoglobulins (pIg) to the mucosal surface. **(1)** PIg (dimeric IgA (dIgA) [shown] or pentameric IgM [not shown]) made in the lamina propria bind to polymeric immunoglobulin receptor (pIgR). **(2)** Endocytosis and transcytosis of the pIg:pIgR complex from the basolateral to the apical side of the mucosal epithelium. **(3)** Intracellular proteolytic cleavage of pIgR creating secretory component (SC) and secretory IgA (SIgA). **(4)** Release of SC and SIgA to the mucosal surface.

vitro [82-84]. Thus, it is not surprising that bacteria, bacterial products, and viruses also stimulate pIgR in vitro [80, 85, 86]. This was also confirmed *in vivo*. For example, bacterial upregulation of pIgR expression during infection was observed during *Chlamydia* infection in the epithelium of the human reproductive tract [87]. In addition, pIgR expression increases distally throughout the small intestine of mice, correlating with increasing concentrations of bacteria [1, 88]. Hormones, such as estrogen, progesterone and androgen, are another group of host factors that regulates PIGR gene expression [89]. Thus, pIgR levels change during the estrous cycle, and pIgR is upregulated in mammary glands during lactation [90]. Furthermore, environmental factors such as diet [91], exercise [92], alcohol consumption [93], and likely smoking [94] also alter pIgR levels. For completeness, we note that recent work also indicates modulation of pIgR expression in cancer [95-97]. Hence, the functions of pIgR go beyond the mucosal surface. Nevertheless, most studies to date have focused on the critical role of pIgR as a key mucosal defense mediator.

1.9 Polymeric Immunoglobulin Receptor (pIgR) Mediated Polymeric Immunoglobulin (pIg) Transport

The extracellular portion of pIgR is composed of six domains: five immunoglobulin-like domains, and a sixth, which contains a highly conserved cleavage signal [78]. The intracellular domain contains signals for endocytosis, intracellular sorting and transcytosis. PIgR is expressed on the basolateral surface of ciliated epithelial cells in the mucosal epithelium [82]. Expression is inhibited in mucus-producing goblet cells by secretory leukocyte protease inhibitor (SLPI) via the NFkB pathway [98]. The main function of pIgR is to transport dimeric immunoglobulin A (dIgA) and polymeric immunoglobulin M (pIgM) from the lamina propria across the epithelial

barrier to mucosal surfaces in four main steps (**Figure 1.6**) [99]. 1. PIg made in the lamina propria binds non-covalently via the joining (J) chain to the extracellular domain 1 of pIgR, on the basolateral surface of the epithelial layer [100, 101]. 2. Once bound, the receptor and Ig undergo clathrin-mediated endocytosis, and are transcytosed through the epithelial cell to the mucosa [76]. 3. Upon approaching the apical surface, the pIg bound domain of the receptor undergoes endoproteolytic cleavage, likely by a host serine proteinase [102], and disassociates from the membrane-bound domain, forming secretory component (SC). SC remains associated with pIg, forming SIg. Unbound pIgR can also be transcytosed via the endosome to the luminal side of the epithelium alongside with pIg-bound pIgR. It similarly undergoes endoproteolytic cleavage forming SC and releasing free, unbound SC. 4. Upon release, SC and SIg diffuse into the mucus layer [103]. Therefore, pIgR plays a vital role during the generation of SIgs and becomes a part of SIgs. The clinical importance of pIgR is further underscored by the finding that multiple polymorphisms in the PIGR gene are linked with immunoglobulin A nephropathy [104]. Additionally, inflammatory diseases such as chronic obstructive pulmonary disease [105-107], DSS-induced and T-cell-mediated colitis in mice [108, 109], as well as Crohn's disease and ulcerative colitis in humans [110, 111] are highly prevalent when SIgs are absent or reduced.

1.10 The Multiple Functions of Secretory Component (SC)

SC has multiple functions beyond facilitation of pIg transport and is critically important for the function of SIg [89, 112]. First, SC enhances SIg stability. While SC does not alter SIg antigen affinity [113, 114], SC is thought to help SIg resist proteolytic degradation by host and bacterial enzymes in the intestinal lumen [115, 116]. However, at least one pathogen has evolved ways to overcome the enhanced resistance to proteolysis. Specifically, streptococcus-specific

proteases degrade pIg and SIg similarly [117]. Second, SC aids in appropriately localizing SIg in the mucus layer. Both the SC and pIg are glycosylated via N- and O-linkages [74, 75]. These glycosylations aid in transcytosis and release of SIg from the epithelial cells [118]. In the distal gastrointestinal tract, SIg diffuses through the thick inner mucus layer and adheres to the outer mucus layer where intestinal bacteria are localized via binding to these carbohydrates [103]. Third, SC is a non-specific microbial scavenger. Both N- and O-linked glycosylations mediate attachment of bacteria, aiding in sequestration of bacteria in the mucus layer [119]. Thus, SC promotes intralumenal sequestration of bacteria. Fourth, SC can also neutralize the effect of toxins and prevent infections [120, 121]. Fifth, SC has homeostatic functions in the epithelium. For example, it can prevent activation of neutrophil effector functions [122] and neutralize IL-8 activity [123]. Taken together, SC is a critical player in the mucosal defense arsenal. MNV has been shown to bind to N- and O-linked glycosylations [124], however, whether MNV binds to SIg and SC, remains to be determined. Additionally, the role SIg and SC may play in preventing MNV crossing the epithelial barrier is unknown.

1.11 Lessons from Polymeric Immunoglobulin Receptor-Deficient (pIgR KO) Mice

PIgR is critical for the protective function of the GI tract as SIg and SC can mediate host protection through specific and non-specific pathogen interactions [125, 126]. In order to directly assess the role of pIgR/SC/SIg in mucosal homeostasis, pIgR-deficient (pIgR KO) mice were generated [127]. Although an initial littermate-controlled study found no alteration in bacterial communities in mice lacking PIgR [128], these findings have a caveat, namely, since SIg can pass through the digestive system [129], it may have been passed along from pIgR-sufficient littermate controls to pIgR KO mice obscuring any potential changes. Consistent with that, a

subsequent, non-littermate study using 16S rRNA analysis did reveal alterations in the feces and cecal microbiota in pIgR KO vs. WT B6 mice and suggested an overall 7% change in intestinal bacterial communities in the absence of pIgR [108]. Despite differences in microbial communities, colonic mucus thickness is similar in pIgR KO mice compare to controls [103]. Small intestinal mucus thickness has not been directly assessed; however, small intestinal permeability may increase with age in pIgR KO mice compared to controls [130]. These studies demonstrate that removal of pIgR, and therefore SIg and SC, results in alterations in the commensal microbiota. The role that SIg and SC play in modulating bacterial communities has been well demonstrated, however, the indirect role that this interaction has on enteric viral infections remains undetermined.

Although there are many similarities to WT B6 control mice, pIgR KO mice exhibit several key differences in addition to the aforementioned alterations in microbial communities (**Figure 1.7, point 1**). The lack of pIgR results in a lack of secretion of dIgA into the mucosa, and a buildup of serum IgA compared to WT mice (**Figure 1.7, point 2**) [127, 131]. Serum IgA levels may be further augmented in pIgR KO mice due to elevated numbers of B cells in the lamina propria compared to controls (**Figure 1.7, point 3**) [132]**.** Although no differences were found in CD4 T cells of the Peyer's patch, spleen, and mesenteric lymph nodes [132], increased quantities of small intestinal intraepithelial lymphocytes (IELs) in pIgR KO mice have been reported (**Figure 1.7, point 4**) [133]. The latter is thought to be mediated through the enhanced differentiation of immature hematopoietic precursor cells, but it was not due to changes in proliferative capacities, ex vivo cytotoxicity, or migration into the intestinal epithelium [133]. In the lung, lack of SIgs through pIgR depletion (pIgR KO) results in an upregulation of pulmonary natural killer cells [105]. PIgR KO mice have enhanced lymphocytes compared to controls,

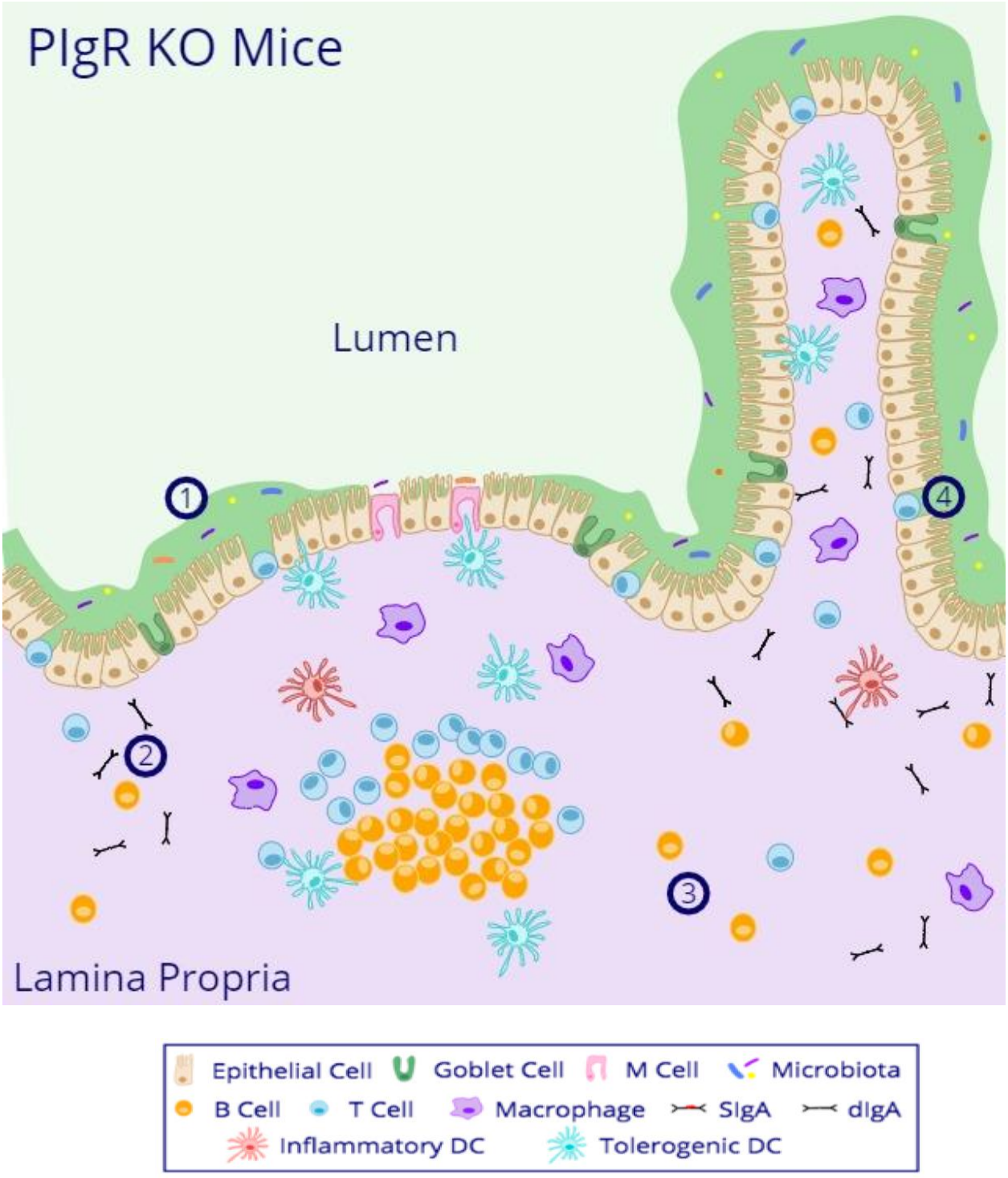

Figure 1.7: Previously reported small intestinal alterations in polymeric immunoglobulin receptor-deficient (pIgR KO) mice compared to C57/Bl6 (WT B6) control mice. PIgR KO mice exhibit: **(1)** alterations in intestinal microbial communities, **(2)** enhanced serum IgA, as well as enhanced numbers of intestinal **(3)** B cells, and **(4)** intraepithelial lymphocytes.

which could contribute to the enhanced susceptibility to inflammatory diseases seen in pIgR KO mice.

1.12 The Multiple Functions of Secretory immunoglobulins (SIg)

SIgs in the gastrointestinal tract are polyreactive against several bacterial species and primarily target intestinal commensal bacteria [134]. Most of these "natural" anti-commensal SIg are made through T cell-independent B cell responses [135]. Despite the lack of T cell help, these natural polyreactive SIgs can bind to antigens with high affinity, sometimes equivalent to that of T cell-dependent SIgs [136]. SIgs, of which SIgA is the most abundant, and SC mediate innate protection of the host via immune exclusion, neutralization, and complement activation, but also aid in adaptive immunity by modulating immune cell activation and function, and by maintaining homeostasis.

1.12.1 Agglutination and Exclusion of Pathogens from Mucosal Surfaces (Immune Exclusion)

An important defense mechanism of the pIgR/SIg cycle is via agglutination of pathogens and subsequent exclusion from mucosal surfaces. This mechanism has been generally demonstrated for bacterial pathogens. One example of a bacteria modulated by SIg is *Helicobacter pylori* (*H. pylori*), a common pathogen that causes gastric mucosal inflammation, gastric cancers and peptic ulcers [137]. Indications that naturally produced SIg modulate *H. pylori* infection come from studies in pIgR KO mice [138]. These mice exhibit enhanced susceptibility to *H. pylori* infection, increased weight loss and delayed clearance compared to

WT C57BL/6. Furthermore, intestinal IgA concentrations inversely correlated with *H. pylori* gastric bacterial load in C57BL/6 mice. A potential mechanism for the pIgR/SIg-mediated control of *H. pylori* infection was suggested by in vitro experiments, which demonstrated that human colostrum SIgA inhibited bacterial binding to human stomach tissue sections in a glycan-dependent manner [139]. The protective effect of this process in the human host is unclear since *H. pylori*-infected human gastric mucosa samples show increased levels of SC and IgA [140, 141]. Thus, given the ability by *H. pylori* to establish an infection, these findings suggest that pre-existing SC and SIg were unable to prevent infection. However, whether SC and antigen-specific SIg modulate the level of *H. pylori* infection, remains to be resolved. Immune exclusion and host protection mediated by pathogen-specific SIg was directly demonstrated for several bacterial pathogens. For example, *Vibrio cholerae*-specific SIgA also mediate in vivo agglutination and immune exclusion [142], and reduced diarrhea severity [143] and mortality [144] in mouse models.

Another example is *Shigella flexneri*, the causative agent of dysentery. *Shigella* LPS-specific SIgA protected the intestinal epithelial barrier in rabbit ileal loops from destruction by virulent *Shigella flexneri* via trapping of the bacteria in the lumen and reducing inflammation [145]. Similar findings of SIgA- and SIgM-mediated bacterial agglutination, reduced inflammation and protection of the epithelial barrier were also made in polarized Caco-2 cell monolayers [146, 147]. Consistent with immune exclusion is the finding that SIgA targeting *Chlamydia trachomatis* outer membrane protein reduces infection in vitro and in vivo when binding the antigen extra-epithelially but not intra-epithelially [148]. SC and SIg may also bind pathogens during infection of naïve individuals. This scavenger function is mediated through glycosylation of SC and Ig molecules. For example, SC, through non-specific glycan

interactions, agglutinates and neutralizes *Clostridium difficile* toxin A [120, 149]. In addition, the glycan binding capabilities of enteropathogenic *Escherichia coli* intimin protein and type 1 fimbral lectin mediate SIgA binding, which in turn agglutinates the bacteria and prevents epithelial cell damage in vitro [150].

Natural, non-specific SIgA also reduces *Vibrio cholerae* bacterial loads *in vivo*, and inhibits biofilm formation in vitro [151]. Inhibition of biofilm formation is dependent on mannose-containing oligosaccharides present on SC. Natural SIgA further mediates *in vivo* agglutination and intra-lumenal immune exclusion of *Enterococcus faecium* [152], and *Salmonella enterica typhimurium* resulting in reduced infection and inflammation of both pathogens [153]. Taken together, these examples indicate that SC, natural SIg, and pathogen-specific SIg can mediate immune exclusion of mucosal pathogens and protect the host by a combination of innate and adaptive mechanisms. While the listed examples for immune exclusion are for bacterial pathogens, the same mechanism can be envisioned for other microbes. In fact, the microbial-scavenger function of SIgA also extends to commensal bacterial strains [119]. However, it is not universal for all microbes. SC did not bind to three rotavirus strains and in vitro infection was not impacted [149]. Thus, it will be of interest in the future to determine whether other viral or fungal mucosal infections can be controlled by SIg-mediated agglutination.

1.12.2 Intracellular Neutralization and Excretion of Pathogens

In addition to protecting the epithelial surface via extracellular complex formation, SIgA may also neutralize pathogens intracellularly while being transcytosed to the apical surface. For

example, anti-Sendai virus or anti-influenza hemagglutinin specific IgA supplied to the basolateral side of polarized MCDK cells expressing pIgR was able to reduce virus infection from the apical side [154, 155]. Immunofluorescence analysis demonstrated intracellular co-localization of virus and IgA, suggesting neutralization occurred inside cells. Neutralization was not observed for IgG, indicating a role for pIgR-mediated transcytosis of IgA. Similar findings were obtained with measles virus, HIV, and rotavirus [156-159]. In vitro studies of measles virus and HIV in epithelial monolayers further showed that antigen-specific IgA can bind virus on the basolateral side and mediate excretion of the immune complexes via pIgR through basolateral to apical transcytosis [156-160]. These data suggest the potential for IgA to trap pathogens that have breached the epithelial barrier and expel them from the mucosal lamina propria. Whether these principles extend to events *in vivo* has not been investigated in depth. In future, it will be of interest to determine if basolateral to apical excretion of SIgA-immune complexes extend to non-viral infections, and what affect it has on within or between host spread.

Consistent with intracellular inactivation of virus by SIgA *in vivo* is a set of studies of rotavirus infection in mice [159, 161]. Using a murine hybridoma backpack tumor model, which secretes a given monoclonal antibody onto mucosal surfaces via the normal epithelial transport pathway, the authors showed that rotavirus-specific IgA antibodies inhibited primary infections, resolved chronic rotavirus infections, and protected newborn mice from diarrhea upon oral challenge. Inhibition of rotavirus infection in this model was not observed with non-antigen-specific SIgA, anti-rotavirus IgG, or when antibodies were delivered directly into the intestinal lumen. Studies from knock-out mice suggest that non-antigen-specific, natural SIgA and J chain-mediated transcytosis play some role during rotavirus infection, since naïve J chain-deficient mice lacking SIg exhibited enhanced shedding and delayed clearance of rotavirus as compared to

wild-type mice [162]. Taken together, these studies implicate intracellular neutralization by SIgA and basolateral to apical excretion of SIgA-immune complexes as a potential mechanism for protection of mucosal surfaces from viral infection. Whether these mechanisms apply broadly to all viruses infecting via mucosal surfaces or to other non-viral pathogens, or play a major role *in vivo* remains to be determined in future studies.

1.12.3 SIg-Mediated Immune Modulation via Microfold Cells

Uptake of SIgA alone or SIgA-immune complexes by DCs is critical for dampening inflammatory immune responses in the intestinal mucosa and in turn mediating intestinal homeostasis. For example, SIgA-primed DCs exhibited reduced DC maturation and inflammatory cytokine secretion upon TLR stimulation compared to untreated DCs [163]. These DCs further induced the expansion of Foxp3+ regulatory T cells via IL-10 and TGF-β secretion in vitro and in vivo [163]. Furthermore, *Shigella flexneri*:SIgA immune complexes reduced expression of pro-inflammatory molecules by DCs and epithelial monolayers in vitro compared to the bacterium alone [146, 164]. Importantly, Peyer's patches exposed to *Shigella flexneri*:SIgA immune complexes showed reduced induction of inflammatory mediators and tissue damage as compared to bacteria alone [145]. The anti-inflammatory effect appears to be specific to SIgA, as serum IgA-immune complexes enhance production of pro-inflammatory cytokines by monocytes and macrophages [165]. These data highlight the important role of SIgA in directly downregulating immune responses in the intestinal mucosa, thereby contributing to mucosal homeostasis.

1.12.4 SIg-Induced Complement Activation and Immune Pathology

Once the pathogen has crossed the epithelial barrier, complement activation and antibody-mediated phagocytosis are important host effector functions [166]. Therefore, SIgs may also protect the mucosal surface SIgA by these effector mechanisms. Consistent with such effector functions, SIgA agglutinates *Streptococcus pneumoniae* and opsonizes the bacteria in a complement-dependent manner [117]. However, the importance of these host defenses during bacterial pathogenesis remain to be determined. Similarly, the ability of human SIgM to activate human complement was recently demonstrated [167]. It will now be interesting to see whether SIgM mediates efficient opsonophagocytosis of pathogens at mucosal surfaces and any inflammatory consequences that might result from complement activation. Thus, the possibility exists that SIg is not always protective but may instead contribute to disease under some circumstances. One example for the detrimental effects of SIgs comes from herpes simplex virus 2 (HSV-2), the common cause of genital herpes. J chain-deficient mice intravaginally infected with HSV-2 exhibited reduced vaginal symptoms (erythema, swelling, and ulceration) and hind limb paralysis, despite equivalent viral titers in the vaginal fluid compared to controls [168]. Additionally, treatment of intestinal organoid and immune cell co-cultures with uncomplexed SIgA triggers enhanced production of the pro-inflammatory cytokines interleukin 8 and tumor necrosis factor alpha, and increased mucus production and pIgR expression [169]. These responses were attenuated when SIgA was complexed with a commensal *Escherichia coli*, suggesting SIg elicits distinct immune responses upon antigen binding. These data highlight that depending on the circumstances, SIg can be protective for the host via induction of immune tolerance or immune exclusion, or it can also have negative consequences for the host through activation of complement or immune-mediated histopathology.

1.13 Subversion of the pIgR/SIg System by Pathogens

Given the critical defensive role of pIgR and SIg, some pathogens have evolved strategies to hijack this system to enhance their own infection. Chiefly among those is *Streptococcus pneumoniae* (*S. pneumoniae*)—a gram-positive bacterium and a leading cause of invasive disease in children and adults worldwide [170]. *S. pneumoniae* binds to human SC [171]. Binding to pIgR aids in attachment and infection of human nasopharyngeal epithelial cells in vitro by reverse transcytosis [172]. Sensing of the infection by the host cells mobilizes intracellular calcium stores and reduces *S. pneumoniae* internalization in vitro [173]. Lack of SC in both pIgR KO and p62yesKO mice resulted in reduced *S. pneumoniae* lung infection [172]. Thus, high expression of pIgR in the nasopharynx is thought to promote *S. pneumoniae* colonization of the upper respiratory tract [106]. Antigen-specific SIgA is further important in protecting the host from nasal colonization [174]. It is known that NoV can bind to carbohydrate residues similar to those on pIgR, but the role pIgR plays in NoV epithelial cell infection is unknown.

Consistent with the immunologic upregulation of pIgR, overexpression of pIgR was observed in a mouse model of chronically inflamed lungs (i.e., SPC-HAxTCR-HA mice) [175]. However, chronic inflammation resulted in resistance rather than susceptibility to infection by *S. pneumonia*, likely because of increased levels of airway mucosal SIgA or SIgM. PIgR may also aid in *S. pneumoniae* meningitis, as pIgR was found to colocalize with *S. pneumoniae* in brain samples from human patients who had succumbed to meningitis, and anti-pIgR antibodies administered intravenously prior to infection prevented pneumococcal entry into the brain and subsequent meningitis in mice [176]. Thus, the capability of *S. pneumonia* to bind pIgR is a

virulence determinant. Another pathogen that binds to SC is *Candida albicans*—an opportunistic pathogen and important cause of vaginal infections [177]. Earlier work showed that *C. albicans* attachment to epithelial cells in vitro is aided by a component of human saliva [178]. Recently, *C. albicans* cells were demonstrated to specifically bind to free SC in saliva, and this interaction aids in epithelial cell attachment in vitro [179]. However, whether SC also aids in *C. albicans* internalization and/or infection remains to be determined.

Epstein–Barr virus (EBV)—the causative agent of infectious mononucleosis [180]—successfully hijacks the immune defense function of SIgA to expand its cell tropism. Specifically, EBV:EBV-specific SIgA immune complexes bind to pIgR on non-susceptible epithelial cells and are internalized to initiate infections in vitro [181, 182]. Subsequent *in vivo* experiments showed that pIgR-mediated the transcytosis of EBV immune complexes via hepatocytes and aided in dissemination [183]. The ability of EBV immune complexes to be translocated from the basal to the apical side without infection was confirmed in vitro in polarized pIgR-expressing MDCK cells. In contrast, infection was observed when the cells remained unpolarized, suggesting loss of polarization predisposes epithelial cells to EBV infection following reactivation from latency in the presence of anti-EBV-specific SIgA. In contrast to hijacking the pIgR/SIg system for their own benefit, some pathogens appear to evade the anti-microbial function by suppressing pIgR. For example, enterotoxigenic *E. coli* suppresses pIgR mRNA expression *in vivo* [184]. Similarly, simian immunodeficiency virus (SIV) and chimeric simian/human immunodeficiency virus (S/HIV) was able to downregulate pIgR mRNA expression in the gastrointestinal and respiratory mucosa of infected rhesus macaques [185, 186], suggesting HIV may also use pIgR downregulation as an immune evasion tactic. Taken together, these examples suggest that some bacterial, viral and fungal pathogens can subvert the protective

functions of pIgR and SIg to facilitate their own infections or inhibit their defense response. It will be interesting to see in the future whether additional mucosal pathogens have evolved similar or different pIgR/SIg subversion or evasion mechanisms.

1.14 Conclusions

Taken together, overwhelming evidence supports that SC, natural SIg, and pathogen-specific SIg binding is an essential host defense mechanism. SIgs bind pathogens either specifically through their antigen-binding domain, or non-specifically via carbohydrate residues resulting in pathogen agglutination and immune-mediated exclusion of pathogens from mucosal surfaces. As SIg are being formed, they mediate intracellular neutralization and excretion of pathogens. Despite potential NoV binding sites on pIgR, SC and SIg nothing is known regarding their role in innate enteric defense against NoV. Specifically, it is known that NoV can bind to carbohydrate residues similar to those on pIgR [74, 187, 188], but the role pIgR plays in NoV epithelial barrier crossing is unknown. Intestinal microbiota also express carbohydrate residues and HNoV binding to certain intestinal bacteria enhances NoV infection [25, 189]. The microbiome is a critical regulator of pIgR and SIg expression, which in turn then modulates the microbiome. Whether NoV infection is regulated directly by natural non-specific SIg or SC through immune exclusion or neutralization, or indirectly through modulation of intestinal microbial communities remains unexplored. These findings highlight the need to further study complex, trans-kingdom interactions and their effects on the host.

The cellular and tissue tropism is a critical determinant of pathogenesis and an active area of investigation in the NoV field [190]. In addition to potential modulation of NoV infection by

innate SIg functions, adaptive immune functions may also control NoV infection. SC and natural SIg are also capable of manipulating host immunity mucosal tolerance via modulation of cytokines and regulatory immune cell development. Immune cell subsets of the gastrointestinal tract are in highest abundance in the lymphoid tissue, and most reside immediately underlying the M cells allowing them direct access to newly transcytosed antigens. M cells retrotranscytose SIg into the lymphoid follicles allowing direct sampling of SIg-immune complexes by intestinal antigen-presenting cells. The antigen-sensitized cells stimulate local immune responses in the lymphoid follicle and can migrate to the lymph nodes to generate systemic responses [191]. The role that SIg and SC play in modulating bacterial communities has been well demonstrated, however, the indirect role that this interaction has on enteric viral infections remains unexplored.

Despite several mechanisms of SIg-mediated mucosal protection, pathogens are still able to modulate SIg and utilize it to facilitate infection. Studies that address SIg and SC subversion or evasion mechanisms among mucosal pathogens are less explored. It would be interesting to know if different kingdoms have shared or specific evasion strategies. Addressing these and other future studies on how pathogens modulate and subvert SC and the SIg cycle will aid in further dissecting the complex roles of SIg in mucosal defense and infection. Future studies of the multifaceted regulation of NoV infection using existing and newly developed models will undoubtedly yield new scientific insights that may ultimately reduce the global burden of disease.

1.15 References

1. Mowat, A.M. and W.W. Agace, *Regional specialization within the intestinal immune system.* Nat Rev Immunol, 2014. **14**(10): p. 667-85.
2. Hall, A.J., et al., *Norovirus disease in the United States.* Emerg Infect Dis, 2013. **19**(8): p. 1198-205.

3. Bartsch, S.M., et al., *Global Economic Burden of Norovirus Gastroenteritis.* PLoS One, 2016. **11**(4): p. e0151219.
4. Fields, B.N., D.M. Knipe, and P.M. Howley, *Fields virology*. 2007, Philadelphia: Wolters Kluwer Health/Lippincott Williams & Wilkins.
5. Vinje, J., *Advances in laboratory methods for detection and typing of norovirus.* J Clin Microbiol, 2015. **53**(2): p. 373-81.
6. McFadden, N., et al., *Norovirus regulation of the innate immune response and apoptosis occurs via the product of the alternative open reading frame 4.* PLoS Pathog, 2011. **7**(12): p. e1002413.
7. Jones, R.M. and L.M. Brosseau, *Aerosol transmission of infectious disease.* J Occup Environ Med, 2015. **57**(5): p. 501-8.
8. Kirby, A.E., A. Streby, and C.L. Moe, *Vomiting as a Symptom and Transmission Risk in Norovirus Illness: Evidence from Human Challenge Studies.* PLoS One, 2016. **11**(4): p. e0143759.
9. Atmar, R.L., et al., *Determination of the 50% human infectious dose for Norwalk virus.* J Infect Dis, 2014. **209**(7): p. 1016-22.
10. Teunis, P.F., et al., *Norwalk virus: how infectious is it?* J Med Virol, 2008. **80**(8): p. 1468-76.
11. Newman, K.L., et al., *Norovirus in symptomatic and asymptomatic individuals: cytokines and viral shedding.* Clin Exp Immunol, 2016. **184**(3): p. 347-57.
12. Colas de la Noue, A., et al., *Absolute Humidity Influences the Seasonal Persistence and Infectivity of Human Norovirus.* Appl Environ Microbiol, 2014. **80**(23): p. 7196-205.
13. Tung, G., et al., *Efficacy of commonly used disinfectants for inactivation of human noroviruses and their surrogates.* J Food Prot, 2013. **76**(7): p. 1210-7.
14. Kaufman, S.S., K.Y. Green, and B.E. Korba, *Treatment of norovirus infections: moving antivirals from the bench to the bedside.* Antiviral Res, 2014. **105**: p. 80-91.
15. Lee, R.M., et al., *Incubation periods of viral gastroenteritis: a systematic review.* BMC Infect Dis, 2013. **13**: p. 446.
16. Teunis, P.F., et al., *Shedding of norovirus in symptomatic and asymptomatic infections.* Epidemiol Infect, 2015. **143**(8): p. 1710-7.
17. Echenique, I.A., et al., *Prolonged norovirus infection after pancreas transplantation: a case report and review of chronic norovirus.* Transpl Infect Dis, 2016. **18**(1): p. 98-104.
18. Karst, S.M., S. Zhu, and I.G. Goodfellow, *The molecular pathology of noroviruses.* J Pathol, 2015. **235**(2): p. 206-16.
19. Bonani, M., et al., *Chronic Norovirus Infection as a Risk Factor for Secondary Lactose Maldigestion in Renal Transplant Recipients: A Prospective Parallel Cohort Pilot Study.* Transplantation, 2017. **101**(6): p. 1455-1460.
20. Futagami, S., T. Itoh, and C. Sakamoto, *Systematic review with meta-analysis: post-infectious functional dyspepsia.* Aliment Pharmacol Ther, 2015. **41**(2): p. 177-88.
21. Glass, R.I., U.D. Parashar, and M.K. Estes, *Norovirus gastroenteritis.* N Engl J Med, 2009. **361**(18): p. 1776-85.
22. Pelizzo, G., et al., *Isolated colon ischemia with norovirus infection in preterm babies: a case series.* J Med Case Rep, 2013. **7**: p. 108.
23. Hubbard, V.M. and K. Cadwell, *Viruses, autophagy genes, and Crohn's disease.* Viruses, 2011. **3**(7): p. 1281-311.
24. Taube, S., et al., *A mouse model for human norovirus.* MBio, 2013. **4**(4).

25. Jones, M.K., et al., *Enteric bacteria promote human and mouse norovirus infection of B cells.* Science, 2014. **346**(6210): p. 755-9.
26. Ettayebi, K., et al., *Replication of human noroviruses in stem cell-derived human enteroids.* Science, 2016. **353**(6306): p. 1387-1393.
27. Karst, S.M., et al., *Advances in norovirus biology.* Cell Host Microbe, 2014. **15**(6): p. 668-80.
28. Wobus, C.E., L.B. Thackray, and H.W.t. Virgin, *Murine norovirus: a model system to study norovirus biology and pathogenesis.* J Virol, 2006. **80**(11): p. 5104-12.
29. Hsu, C.C., et al., *Development of a microsphere-based serologic multiplexed fluorescent immunoassay and a reverse transcriptase PCR assay to detect murine norovirus 1 infection in mice.* Clin Diagn Lab Immunol, 2005. **12**(10): p. 1145-51.
30. Kim, J.R., et al., *Prevalence of murine norovirus infection in Korean laboratory animal facilities.* J Vet Med Sci, 2011. **73**(5): p. 687-91.
31. McInnes, E.F., et al., *Prevalence of viral, bacterial and parasitological diseases in rats and mice used in research environments in Australasia over a 5-y period.* Lab Anim (NY), 2011. **40**(11): p. 341-50.
32. Guix, S., et al., *Norwalk virus RNA is infectious in mammalian cells.* J Virol, 2007. **81**(22): p. 12238-48.
33. Orchard, R.C., et al., *Discovery of a proteinaceous cellular receptor for a norovirus.* Science, 2016. **353**(6302): p. 933-6.
34. Haga, K., et al., *Functional receptor molecules CD300lf and CD300ld within the CD300 family enable murine noroviruses to infect cells.* Proc Natl Acad Sci U S A, 2016. **113**(41): p. E6248-e6255.
35. Borrego, F., *The CD300 molecules: an emerging family of regulators of the immune system.* Blood, 2013. **121**(11): p. 1951-60.
36. Tian, L., et al., *Enhanced efferocytosis by dendritic cells underlies memory T-cell expansion and susceptibility to autoimmune disease in CD300f-deficient mice.* Cell Death Differ, 2016. **23**(6): p. 1086-96.
37. Albino, D., et al., *ESE3/EHF controls epithelial cell differentiation and its loss leads to prostate tumors with mesenchymal and stem-like features.* Cancer Res, 2012. **72**(11): p. 2889-900.
38. Hassan, S.A., E.R. Rabin, and J.L. Melnick, *REOVIRUS MYOCARDITIS IN MICE: AN ELECTRON MICROSCOPIC, IMMUNOFLUORESCENT, AND VIRUS ASSAY STUDY.* Exp Mol Pathol, 1965. **4**: p. 66-80.
39. Davis, J.F., A. Kulkarni, and O. Fletcher, *Myocarditis in 9- and 11-day-old broiler breeder chicks associated with a reovirus infection.* Avian Dis, 2012. **56**(4): p. 786-90.
40. Weiner, H.L., et al., *Molecular basis of reovirus virulence: role of the S1 gene.* Proc Natl Acad Sci U S A, 1977. **74**(12): p. 5744-8.
41. Barton, E.S., et al., *Junction adhesion molecule is a receptor for reovirus.* Cell, 2001. **104**(3): p. 441-51.
42. Maginnis, M.S., et al., *Beta1 integrin mediates internalization of mammalian reovirus.* J Virol, 2006. **80**(6): p. 2760-70.
43. Ivanovic, T., et al., *Peptides released from reovirus outer capsid form membrane pores that recruit virus particles.* Embo j, 2008. **27**(8): p. 1289-98.
44. L. A. Schiff, M.L.N.a.K.L.T., *Orthoreoviruses and Their Replication.* Fields Virology, 2007. **5th Edition**: p. pp. 1853-1915. .

45. Vedula, S.R., et al., *A comparative molecular force spectroscopy study of homophilic JAM-A interactions and JAM-A interactions with reovirus attachment protein sigma1.* J Mol Recognit, 2008. **21**(4): p. 210-6.
46. Weiner, H.L., M.L. Powers, and B.N. Fields, *Absolute linkage of virulence and central nervous system cell tropism of reoviruses to viral hemagglutinin.* J Infect Dis, 1980. **141**(5): p. 609-16.
47. Mabbott, N.A., et al., *Microfold (M) cells: important immunosurveillance posts in the intestinal epithelium.* Mucosal Immunol, 2013. **6**(4): p. 666-77.
48. Owen, R.L., *Sequential uptake of horseradish peroxidase by lymphoid follicle epithelium of Peyer's patches in the normal unobstructed mouse intestine: an ultrastructural study.* Gastroenterology, 1977. **72**(3): p. 440-51.
49. Kobayashi, A., et al., *Identification of novel genes selectively expressed in the follicle-associated epithelium from the meta-analysis of transcriptomics data from multiple mouse cell and tissue populations.* DNA Res, 2012. **19**(5): p. 407-22.
50. Giannasca, P.J., et al., *Regional differences in glycoconjugates of intestinal M cells in mice: potential targets for mucosal vaccines.* Am J Physiol, 1994. **267**(6 Pt 1): p. G1108-21.
51. Owen, R.L. and A.L. Jones, *Epithelial cell specialization within human Peyer's patches: an ultrastructural study of intestinal lymphoid follicles.* Gastroenterology, 1974. **66**(2): p. 189-203.
52. Mah, D.C., et al., *The N-terminal quarter of reovirus cell attachment protein sigma 1 possesses intrinsic virion-anchoring function.* Virology, 1990. **179**(1): p. 95-103.
53. Turner, D.L., R. Duncan, and P.W. Lee, *Site-directed mutagenesis of the C-terminal portion of reovirus protein sigma 1: evidence for a conformation-dependent receptor binding domain.* Virology, 1992. **186**(1): p. 219-27.
54. Wolf, J.L., et al., *Intestinal M cells: a pathway for entry of reovirus into the host.* Science, 1981. **212**(4493): p. 471-2.
55. Gonzalez-Hernandez, M.B., et al., *Efficient norovirus and reovirus replication in the mouse intestine requires microfold (M) cells.* J Virol, 2014. **88**(12): p. 6934-43.
56. Wobus, C.E., et al., *Replication of Norovirus in cell culture reveals a tropism for dendritic cells and macrophages.* PLoS Biol, 2004. **2**(12): p. e432.
57. Elftman, M.D., et al., *Multiple effects of dendritic cell depletion on murine norovirus infection.* J Gen Virol, 2013. **94**(Pt 8): p. 1761-8.
58. Karst, S.M. and C.E. Wobus, *A working model of how noroviruses infect the intestine.* PLoS Pathog, 2015. **11**(2): p. e1004626.
59. Gonzalez-Hernandez, M.B., et al., *Murine norovirus transcytosis across an in vitro polarized murine intestinal epithelial monolayer is mediated by M-like cells.* J Virol, 2013. **87**(23): p. 12685-93.
60. Brown, J.R., K. Gilmour, and J. Breuer, *Norovirus Infections Occur in B-Cell-Deficient Patients.* Clin Infect Dis, 2016. **62**(9): p. 1136-1138.
61. Karandikar, U.C., et al., *Detection of human norovirus in intestinal biopsies from immunocompromised transplant patients.* J Gen Virol, 2016. **97**(9): p. 2291-300.
62. Mumphrey, S.M., et al., *Murine norovirus 1 infection is associated with histopathological changes in immunocompetent hosts, but clinical disease is prevented by STAT1-dependent interferon responses.* J Virol, 2007. **81**(7): p. 3251-63.

63. Ward, J.M., et al., *Pathology of immunodeficient mice with naturally occurring murine norovirus infection.* Toxicol Pathol, 2006. **34**(6): p. 708-15.
64. Wilen, C.B., et al., *Tropism for tuft cells determines immune promotion of norovirus pathogenesis.* Science, 2018. **360**(6385): p. 204-208.
65. Rubin, B.Y., et al., *The anticellular and protein-inducing activities of human gamma interferon preparations are mediated by the interferon.* J Immunol, 1983. **130**(3): p. 1019-20.
66. Li, M., C.F. Cuff, and J.J. Pestka, *T-2 toxin impairment of enteric reovirus clearance in the mouse associated with suppressed immunoglobulin and IFN-gamma responses.* Toxicol Appl Pharmacol, 2006. **214**(3): p. 318-25.
67. Changotra, H., et al., *Type I and type II interferons inhibit the translation of murine norovirus proteins.* J Virol, 2009. **83**(11): p. 5683-92.
68. Hwang, S., et al., *Nondegradative role of Atg5-Atg12/ Atg16L1 autophagy protein complex in antiviral activity of interferon gamma.* Cell Host Microbe, 2012. **11**(4): p. 397-409.
69. Chang, K.O. and D.W. George, *Interferons and ribavirin effectively inhibit Norwalk virus replication in replicon-bearing cells.* J Virol, 2007. **81**(22): p. 12111-8.
70. Karst, S.M., et al., *STAT1-dependent innate immunity to a Norwalk-like virus.* Science, 2003. **299**(5612): p. 1575-8.
71. Maloney, N.S., et al., *Essential cell-autonomous role for interferon (IFN) regulatory factor 1 in IFN-gamma-mediated inhibition of norovirus replication in macrophages.* J Virol, 2012. **86**(23): p. 12655-64.
72. Hyde, J.L., et al., *Mouse norovirus replication is associated with virus-induced vesicle clusters originating from membranes derived from the secretory pathway.* J Virol, 2009. **83**(19): p. 9709-19.
73. Biering, S.B., et al., *Viral Replication Complexes Are Targeted by LC3-Guided Interferon-Inducible GTPases.* Cell Host Microbe, 2017. **22**(1): p. 74-85 e7.
74. Huang, J., et al., *Site-specific glycosylation of secretory immunoglobulin A from human colostrum.* J Proteome Res, 2015. **14**(3): p. 1335-49.
75. Pierce-Cretel, A., et al., *Primary structure of the N-glycosidically linked sialoglycans of secretory immunoglobulins A from human milk.* Eur J Biochem, 1982. **125**(2): p. 383-8.
76. Stadtmueller, B.M., et al., *The structure and dynamics of secretory component and its interactions with polymeric immunoglobulins.* Elife, 2016. **5**: p. e10640.
77. Kaetzel, C.S., *Cooperativity among secretory IgA, the polymeric immunoglobulin receptor, and the gut microbiota promotes host-microbial mutualism.* Immunol Lett, 2014. **162**(2 Pt A): p. 10-21.
78. Asano, M. and K. Komiyama, *Polymeric immunoglobulin receptor.* J Oral Sci, 2011. **53**(2): p. 147-56.
79. Bruno, M.E., et al., *Regulation of the polymeric immunoglobulin receptor by the classical and alternative NF-kappaB pathways in intestinal epithelial cells.* Mucosal Immunol, 2011. **4**(4): p. 468-78.
80. Bruno, M.E., et al., *Regulation of the polymeric immunoglobulin receptor in intestinal epithelial cells by Enterobacteriaceae: implications for mucosal homeostasis.* Immunol Invest, 2010. **39**(4-5): p. 356-82.
81. Frantz, A.L., et al., *Targeted deletion of MyD88 in intestinal epithelial cells results in compromised antibacterial immunity associated with downregulation of polymeric*

immunoglobulin receptor, mucin-2, and antibacterial peptides. Mucosal Immunol, 2012. **5**(5): p. 501-12.
82. Schneeman, T.A., et al., *Regulation of the polymeric Ig receptor by signaling through TLRs 3 and 4: linking innate and adaptive immune responses.* J Immunol, 2005. **175**(1): p. 376-84.
83. Blanch, V.J., J.F. Piskurich, and C.S. Kaetzel, *Cutting edge: coordinate regulation of IFN regulatory factor-1 and the polymeric Ig receptor by proinflammatory cytokines.* J Immunol, 1999. **162**(3): p. 1232-5.
84. Moon, C., et al., *Development of a primary mouse intestinal epithelial cell monolayer culture system to evaluate factors that modulate IgA transcytosis.* Mucosal Immunol, 2014. **7**(4): p. 818-28.
85. Kvale, D. and P. Brandtzaeg, *Butyrate differentially affects constitutive and cytokine-induced expression of HLA molecules, secretory component (SC), and ICAM-1 in a colonic epithelial cell line (HT-29, clone m3).* Adv Exp Med Biol, 1995. **371A**: p. 183-8.
86. Pal, K., et al., *Regulation of polymeric immunoglobulin receptor expression by reovirus.* J Gen Virol, 2005. **86**(8): p. 2347-57.
87. Armitage, C.W., C.P. O'Meara, and K.W. Beagley, *Chlamydial infection enhances expression of the polymeric immunoglobulin receptor (pIgR) and transcytosis of IgA.* Am J Reprod Immunol, 2017. **77**(1): p. e12611.
88. Godinez-Victoria, M., et al., *Modulation by bovine lactoferrin of parameters associated with the IgA response in the proximal and distal small intestine of BALB/c mice.* Immunopharmacol Immunotoxicol, 2017. **39**(2): p. 66-73.
89. Kaetzel, C.S., *The polymeric immunoglobulin receptor: bridging innate and adaptive immune responses at mucosal surfaces.* Immunol Rev, 2005. **206**: p. 83-99.
90. Rincheval-Arnold, A., L. Belair, and J. Djiane, *Developmental expression of pIgR gene in sheep mammary gland and hormonal regulation.* J Dairy Res, 2002. **69**(1): p. 13-26.
91. Godinez-Victoria, M., et al., *Intermittent fasting promotes bacterial clearance and intestinal IgA production in Salmonella typhimurium-infected mice.* Scand J Immunol, 2014. **79**(5): p. 315-24.
92. Kurimoto, Y., et al., *Voluntary exercise increases IgA concentration and polymeric Ig receptor expression in the rat submandibular gland.* Biosci Biotechnol Biochem, 2016. **80**(12): p. 2490-2496.
93. Lopez, M.C., *Chronic alcohol consumption regulates the expression of poly immunoglobulin receptor (pIgR) and secretory IgA in the gut.* Toxicol Appl Pharmacol, 2017. **333**: p. 84-91.
94. Rusznak, C., et al., *Cigarette smoke decreases the expression of secretory component in human bronchial epithelial cells, in vitro.* Acta Microbiol Immunol Hung, 2001. **48**(1): p. 81-94.
95. Arumugam, P., et al., *Expression of polymeric immunoglobulin receptor and stromal activity in pancreatic ductal adenocarcinoma.* Pancreatology, 2017. **17**(2): p. 295-302.
96. Qi, X., X. Li, and X. Sun, *Reduced expression of polymeric immunoglobulin receptor (pIgR) in nasopharyngeal carcinoma and its correlation with prognosis.* Tumour Biol, 2016. **37**(8): p. 11099-104.
97. Yue, X., et al., *Polymeric immunoglobulin receptor promotes tumor growth in hepatocellular carcinoma.* Hepatology, 2017. **65**(6): p. 1948-1962.

98. Mikami, Y., et al., *Secretory leukocyte protease inhibitor inhibits expression of polymeric immunoglobulin receptor via the NF-kappaB signaling pathway.* Mol Immunol, 2015. **67**(2 Pt B): p. 568-74.
99. Kaetzel, C.S., et al., *The polymeric immunoglobulin receptor (secretory component) mediates transport of immune complexes across epithelial cells: a local defense function for IgA.* Proc Natl Acad Sci U S A, 1991. **88**(19): p. 8796-800.
100. Bakos, M.A., A. Kurosky, and R.M. Goldblum, *Characterization of a critical binding site for human polymeric Ig on secretory component.* J Immunol, 1991. **147**(10): p. 3419-26.
101. Johansen, F.E., R. Braathen, and P. Brandtzaeg, *The J chain is essential for polymeric Ig receptor-mediated epithelial transport of IgA.* J Immunol, 2001. **167**(9): p. 5185-92.
102. Pilette, C., et al., *Secretory component is cleaved by neutrophil serine proteinases but its epithelial production is increased by neutrophils through NF-kappa B- and p38 mitogen-activated protein kinase-dependent mechanisms.* Am J Respir Cell Mol Biol, 2003. **28**(4): p. 485-98.
103. Rogier, E.W., et al., *Secretory IgA is Concentrated in the Outer Layer of Colonic Mucus along with Gut Bacteria.* Pathogens, 2014. **3**(2): p. 390-403.
104. Obara, W., et al., *Association of single-nucleotide polymorphisms in the polymeric immunoglobulin receptor gene with immunoglobulin A nephropathy (IgAN) in Japanese patients.* J Hum Genet, 2003. **48**(6): p. 293-9.
105. Richmond, B.W., et al., *Bacterial-derived Neutrophilic Inflammation Drives Lung Remodeling in a Mouse Model of COPD.* Am J Respir Cell Mol Biol, 2018: p. [Epub ahead of print].
106. Polosukhin, V.V., et al., *Bronchial secretory immunoglobulin a deficiency correlates with airway inflammation and progression of chronic obstructive pulmonary disease.* Am J Respir Crit Care Med, 2011. **184**(3): p. 317-27.
107. Gohy, S.T., et al., *Polymeric immunoglobulin receptor down-regulation in chronic obstructive pulmonary disease. Persistence in the cultured epithelium and role of transforming growth factor-beta.* Am J Respir Crit Care Med, 2014. **190**(5): p. 509-21.
108. Reikvam, D.H., et al., *Epithelial-microbial crosstalk in polymeric Ig receptor deficient mice.* Eur J Immunol, 2012. **42**(11): p. 2959-70.
109. Frantz, A.L., et al., *Multifactorial patterns of gene expression in colonic epithelial cells predict disease phenotypes in experimental colitis.* Inflamm Bowel Dis, 2012. **18**(11): p. 2138-48.
110. Arsenescu, R., et al., *Signature biomarkers in Crohn's disease: toward a molecular classification.* Mucosal Immunol, 2008. **1**(5): p. 399-411.
111. Bruno, M.E., et al., *Correlation of Biomarker Expression in Colonic Mucosa with Disease Phenotype in Crohn's Disease and Ulcerative Colitis.* Dig Dis Sci, 2015. **60**(10): p. 2976-84.
112. Phalipon, A. and B. Corthesy, *Novel functions of the polymeric Ig receptor: well beyond transport of immunoglobulins.* Trends Immunol, 2003. **24**(2): p. 55-8.
113. Lullau, E., et al., *Antigen binding properties of purified immunoglobulin A and reconstituted secretory immunoglobulin A antibodies.* J Biol Chem, 1996. **271**(27): p. 16300-9.
114. Phalipon, A., et al., *Secretory component: a new role in secretory IgA-mediated immune exclusion in vivo.* Immunity, 2002. **17**(1): p. 107-15.

115. Crottet, P. and B. Corthesy, *Secretory component delays the conversion of secretory IgA into antigen-binding competent F(ab')2: a possible implication for mucosal defense.* J Immunol, 1998. **161**(10): p. 5445-53.
116. Duc, M., F.E. Johansen, and B. Corthesy, *Antigen binding to secretory immunoglobulin A results in decreased sensitivity to intestinal proteases and increased binding to cellular Fc receptors.* J Biol Chem, 2010. **285**(2): p. 953-60.
117. Fasching, C.E., et al., *Impact of the molecular form of immunoglobulin A on functional activity in defense against Streptococcus pneumoniae.* Infect Immun, 2007. **75**(4): p. 1801-10.
118. Matsumoto, N., et al., *Release of non-glycosylated polymeric immunoglobulin receptor protein.* Scand J Immunol, 2003. **58**(4): p. 471-6.
119. Mathias, A. and B. Corthesy, *Recognition of gram-positive intestinal bacteria by hybridoma- and colostrum-derived secretory immunoglobulin A is mediated by carbohydrates.* J Biol Chem, 2011. **286**(19): p. 17239-47.
120. Dallas, S.D. and R.D. Rolfe, *Binding of Clostridium difficile toxin A to human milk secretory component.* J Med Microbiol, 1998. **47**(10): p. 879-88.
121. de Oliveira, I.R., et al., *Binding of lactoferrin and free secretory component to enterotoxigenic Escherichia coli.* FEMS Microbiol Lett, 2001. **203**(1): p. 29-33.
122. Motegi, Y. and H. Kita, *Interaction with secretory component stimulates effector functions of human eosinophils but not of neutrophils.* J Immunol, 1998. **161**(8): p. 4340-6.
123. Marshall, L.J., et al., *IL-8 released constitutively by primary bronchial epithelial cells in culture forms an inactive complex with secretory component.* J Immunol, 2001. **167**(5): p. 2816-23.
124. Taube, S., et al., *Murine noroviruses bind glycolipid and glycoprotein attachment receptors in a strain-dependent manner.* J Virol, 2012. **86**(10): p. 5584-93.
125. Wijburg, O.L., et al., *Innate secretory antibodies protect against natural Salmonella typhimurium infection.* J Exp Med, 2006. **203**(1): p. 21-6.
126. Davids, B.J., et al., *Polymeric immunoglobulin receptor in intestinal immune defense against the lumen-dwelling protozoan parasite Giardia.* J Immunol, 2006. **177**(9): p. 6281-90.
127. Shimada, S., et al., *Generation of polymeric immunoglobulin receptor-deficient mouse with marked reduction of secretory IgA.* J Immunol, 1999. **163**(10): p. 5367-73.
128. Sait, L., et al., *Secretory antibodies do not affect the composition of the bacterial microbiota in the terminal ileum of 10-week-old mice.* Appl Environ Microbiol, 2003. **69**(4): p. 2100-9.
129. Van de Perre, P., *Transfer of antibody via mother's milk.* Vaccine, 2003. **21**(24): p. 3374-6.
130. Kato-Nagaoka, N., et al., *Enhanced differentiation of intraepithelial lymphocytes in the intestine of polymeric immunoglobulin receptor-deficient mice.* Immunology, 2015. **146**(1): p. 59-69.
131. Johansen, F.E., et al., *Absence of epithelial immunoglobulin A transport, with increased mucosal leakiness, in polymeric immunoglobulin receptor/secretory component-deficient mice.* J Exp Med, 1999. **190**(7): p. 915-22.
132. Uren, T.K., et al., *Role of the polymeric Ig receptor in mucosal B cell homeostasis.* J Immunol, 2003. **170**(5): p. 2531-9.

133. Yamazaki, K., et al., *Accumulation of intestinal intraepithelial lymphocytes in association with lack of polymeric immunoglobulin receptor.* Eur J Immunol, 2005. **35**(4): p. 1211-9.
134. Bunker, J.J., et al., *Natural polyreactive IgA antibodies coat the intestinal microbiota.* Science, 2017. **358**(6361).
135. Macpherson, A.J., et al., *A primitive T cell-independent mechanism of intestinal mucosal IgA responses to commensal bacteria.* Science, 2000. **288**(5474): p. 2222-6.
136. Quan, C.P., et al., *Natural polyreactive secretory immunoglobulin A autoantibodies as a possible barrier to infection in humans.* Infection and Immunity, 1997. **65**(10): p. 3997-4004.
137. Testerman, T.L. and J. Morris, *Beyond the stomach: an updated view of Helicobacter pylori pathogenesis, diagnosis, and treatment.* World J Gastroenterol, 2014. **20**(36): p. 12781-808.
138. Gorrell, R.J., et al., *Contribution of secretory antibodies to intestinal mucosal immunity against Helicobacter pylori.* Infect Immun, 2013. **81**(10): p. 3880-93.
139. Falk, P., et al., *An in vitro adherence assay reveals that Helicobacter pylori exhibits cell lineage-specific tropism in the human gastric epithelium.* Proc Natl Acad Sci U S A, 1993. **90**(5): p. 2035-9.
140. Ahlstedt, I., et al., *Role of local cytokines in increased gastric expression of the secretory component in Helicobacter pylori infection.* Infect Immun, 1999. **67**(9): p. 4921-5.
141. Kaneko, T., et al., *Helicobacter pylori infection produces expression of a secretory component in gastric mucous cells.* Virchows Arch, 2000. **437**(5): p. 514-20.
142. Fubara, E.S. and R. Freter, *Protection against enteric bacterial infection by secretory IgA antibodies.* J Immunol, 1973. **111**(2): p. 395-403.
143. Tokuhara, D., et al., *Secretory IgA-mediated protection against V. cholerae and heat-labile enterotoxin-producing enterotoxigenic Escherichia coli by rice-based vaccine.* Proc Natl Acad Sci U S A, 2010. **107**(19): p. 8794-9.
144. Winner, L., 3rd, et al., *New model for analysis of mucosal immunity: intestinal secretion of specific monoclonal immunoglobulin A from hybridoma tumors protects against Vibrio cholerae infection.* Infect Immun, 1991. **59**(3): p. 977-82.
145. Boullier, S., et al., *Secretory IgA-mediated neutralization of Shigella flexneri prevents intestinal tissue destruction by down-regulating inflammatory circuits.* J Immunol, 2009. **183**(9): p. 5879-85.
146. Mathias, A., S. Longet, and B. Corthesy, *Agglutinating secretory IgA preserves intestinal epithelial cell integrity during apical infection by Shigella flexneri.* Infect Immun, 2013. **81**(8): p. 3027-34.
147. Longet, S., et al., *Reconstituted human polyclonal plasma-derived secretory-like IgM and IgA maintain the barrier function of epithelial cells infected with an enteropathogen.* J Biol Chem, 2014. **289**(31): p. 21617-26.
148. Armitage, C.W., et al., *Evaluation of intra- and extra-epithelial secretory IgA in chlamydial infections.* Immunology, 2014. **143**(4): p. 520-30.
149. Perrier, C., N. Sprenger, and B. Corthesy, *Glycans on secretory component participate in innate protection against mucosal pathogens.* J Biol Chem, 2006. **281**(20): p. 14280-7.
150. Wold, A.E., et al., *Secretory immunoglobulin A carries oligosaccharide receptors for Escherichia coli type 1 fimbrial lectin.* Infect Immun, 1990. **58**(9): p. 3073-7.

151. Murthy, A.K., et al., *Mannose-containing oligosaccharides of non-specific human secretory immunoglobulin A mediate inhibition of Vibrio cholerae biofilm formation.* PLoS ONE, 2011. **6**(2): p. e16847.
152. Hendrickx, A.P., et al., *Antibiotic-Driven Dysbiosis Mediates Intraluminal Agglutination and Alternative Segregation of Enterococcus faecium from the Intestinal Epithelium.* MBio, 2015. **6**(6): p. e01346-15.
153. Bioley, G., et al., *Plasma-Derived Polyreactive Secretory-Like IgA and IgM Opsonizing Salmonella enterica Typhimurium Reduces Invasion and Gut Tissue Inflammation through Agglutination.* Front Immunol, 2017. **8**: p. e1043.
154. Mazanec, M.B., et al., *Intracellular neutralization of virus by immunoglobulin A antibodies.* Proc Natl Acad Sci U S A, 1992. **89**(15): p. 6901-5.
155. Mazanec, M.B., C.L. Coudret, and D.R. Fletcher, *Intracellular neutralization of influenza virus by immunoglobulin A anti-hemagglutinin monoclonal antibodies.* J Virol, 1995. **69**(2): p. 1339-43.
156. Wright, A., et al., *Immunoglobulin A antibodies against internal HIV-1 proteins neutralize HIV-1 replication inside epithelial cells.* Virology, 2006. **356**(1-2): p. 165-70.
157. Yan, H., et al., *Multiple functions of immunoglobulin A in mucosal defense against viruses: an in vitro measles virus model.* J Virol, 2002. **76**(21): p. 10972-9.
158. Corthesy, B., et al., *Rotavirus anti-VP6 secretory immunoglobulin A contributes to protection via intracellular neutralization but not via immune exclusion.* J Virol, 2006. **80**(21): p. 10692-9.
159. Ruggeri, F.M., et al., *Antirotavirus immunoglobulin A neutralizes virus in vitro after transcytosis through epithelial cells and protects infant mice from diarrhea.* J Virol, 1998. **72**(4): p. 2708-14.
160. Wright, A., M.E. Lamm, and Y.T. Huang, *Excretion of human immunodeficiency virus type 1 through polarized epithelium by immunoglobulin A.* J Virol, 2008. **82**(23): p. 11526-35.
161. Burns, J.W., et al., *Protective effect of rotavirus VP6-specific IgA monoclonal antibodies that lack neutralizing activity.* Science, 1996. **272**(5258): p. 104-7.
162. Schwartz-Cornil, I., et al., *Heterologous protection induced by the inner capsid proteins of rotavirus requires transcytosis of mucosal immunoglobulins.* J Virol, 2002. **76**(16): p. 8110-7.
163. Diana, J., et al., *Secretory IgA induces tolerogenic dendritic cells through SIGNR1 dampening autoimmunity in mice.* J Immunol, 2013. **191**(5): p. 2335-43.
164. Mikulic, J., G. Bioley, and B. Corthesy, *SIgA-Shigella Immune Complexes Interact with Dectin-1 and SIGNR3 to Differentially Regulate Mouse Peyer's Patch and Mesenteric Lymph Node Dendritic Cell's Responsiveness.* J Mol Biol, 2017. **429**(15): p. 2387-2400.
165. Hansen, I.S., et al., *Serum IgA Immune Complexes Promote Proinflammatory Cytokine Production by Human Macrophages, Monocytes, and Kupffer Cells through FcalphaRI-TLR Cross-Talk.* J Immunol, 2017. **199**(12): p. 4124-4131.
166. Lu, L.L., et al., *Beyond binding: antibody effector functions in infectious diseases.* Nat Rev Immunol, 2018. **18**(1): p. 46-61.
167. Michaelsen, T.E., et al., *Human Secretory IgM Antibodies Activate Human Complement and Offer Protection at Mucosal Surface.* Scand J Immunol, 2017. **85**(1): p. 43-50.
168. Hendrickson, B.A., et al., *Decreased vaginal disease in J-chain-deficient mice following herpes simplex type 2 genital infection.* Virology, 2000. **271**(1): p. 155-62.

169. Salerno-Goncalves, R., et al., *Free and complexed-secretory immunoglobulin A triggers distinct intestinal epithelial cell responses.* Clin Exp Immunol, 2016. **185**(3): p. 338-47.
170. Deng, X., et al., *Streptococcus pneumoniae infection: a Canadian perspective.* Expert Rev Anti Infect Ther, 2013. **11**(8): p. 781-91.
171. Hammerschmidt, S., et al., *SpsA, a novel pneumococcal surface protein with specific binding to secretory immunoglobulin A and secretory component.* Mol Microbiol, 1997. **25**(6): p. 1113-24.
172. Zhang, J.R., et al., *The polymeric immunoglobulin receptor translocates pneumococci across human nasopharyngeal epithelial cells.* Cell, 2000. **102**(6): p. 827-37.
173. Asmat, T.M., et al., *Streptococcus pneumoniae infection of host epithelial cells via polymeric immunoglobulin receptor transiently induces calcium release from intracellular stores.* J Biol Chem, 2011. **286**(20): p. 17861-9.
174. Sun, K., et al., *An important role for polymeric Ig receptor-mediated transport of IgA in protection against Streptococcus pneumoniae nasopharyngeal carriage.* J Immunol, 2004. **173**(7): p. 4576-81.
175. Boehme, J.D., et al., *Chronic lung inflammation primes humoral immunity and augments antipneumococcal resistance.* Sci Rep, 2017. **7**(1): p. 4972.
176. Iovino, F., et al., *pIgR and PECAM-1 bind to pneumococcal adhesins RrgA and PspC mediating bacterial brain invasion.* J Exp Med, 2017. **214**(6): p. 1619-1630.
177. Poulain, D., *Candida albicans, plasticity and pathogenesis.* Crit Rev Microbiol, 2015. **41**(2): p. 208-17.
178. Holmes, A.R., B.M. Bandara, and R.D. Cannon, *Saliva promotes Candida albicans adherence to human epithelial cells.* J Dent Res, 2002. **81**(1): p. 28-32.
179. van der Wielen, P.A., A.R. Holmes, and R.D. Cannon, *Secretory component mediates Candida albicans binding to epithelial cells.* Oral Dis, 2016. **22**(1): p. 69-74.
180. Vetsika, E.K. and M. Callan, *Infectious mononucleosis and Epstein-Barr virus.* Expert Rev Mol Med, 2004. **6**(23): p. 1-16.
181. Sixbey, J.W. and Q.Y. Yao, *Immunoglobulin A-induced shift of Epstein-Barr virus tissue tropism.* Science, 1992. **255**(5051): p. 1578-80.
182. Lin, C.T., et al., *The mechanism of Epstein-Barr virus infection in nasopharyngeal carcinoma cells.* Am J Pathol, 1997. **150**(5): p. 1745-56.
183. Gan, Y.J., et al., *Epithelial cell polarization is a determinant in the infectious outcome of immunoglobulin A-mediated entry by Epstein-Barr virus.* J Virol, 1997. **71**(1): p. 519-26.
184. Liu, G., et al., *L-Glutamine and L-arginine protect against enterotoxigenic Escherichia coli infection via intestinal innate immunity in mice.* Amino Acids, 2017. **49**(12): p. 1945-1954.
185. Li, D., et al., *Expression of pIgR in the tracheal mucosa of SHIV/SIV-infected rhesus macaques.* Zool Res, 2017. **38**(1): p. 44-48.
186. Wang, Y. and G.B. Yang, *Alteration of Polymeric Immunoglobulin Receptor and Neonatal Fc Receptor Expression in the Gut Mucosa of Immunodeficiency Virus-Infected Rhesus Macaques.* Scand J Immunol, 2016. **83**(4): p. 235-43.
187. Taube, S., et al., *Murine noroviruses bind glycolipid and glycoprotein attachment receptors in a strain-dependent manner.* J Virol, 2012. **86**(10): p. 5584-93.
188. Taube, S., et al., *Ganglioside-linked terminal sialic acid moieties on murine macrophages function as attachment receptors for murine noroviruses.* J Virol, 2009. **83**(9): p. 4092-101.

189. Karst, S.M., *The influence of commensal bacteria on infection with enteric viruses.* Nat Rev Microbiol, 2016. **14**(4): p. 197-204.
190. Karst, S.M. and S.A. Tibbetts, *Recent advances in understanding norovirus pathogenesis.* J Med Virol, 2016. **88**(11): p. 1837-43.
191. Wang, J., et al., *Convergent and divergent development among M cell lineages in mouse mucosal epithelium.* J Immunol, 2011. **187**(10): p. 5277-85.

Chapter 2: Results

Natural Secretory Immunoglobulins Promote Enteric Viral Infection

Some text and figures presented in this chapter were published as a "Spotlight" article of significant interest in The Journal of Virology 92:e00826-18. https://doi.org/10.1128/JVI.00826-18

2.1 Introduction

The mucosal surface of the gastrointestinal tract is a potential entry point for many pathogens. To protect itself from pathogen attack, the host has evolved multiple mechanisms, including the secretion of immunoglobulins (i.e., secretory immunoglobulins (SIg). SIg neutralize microorganisms in the intestinal lumen and reduce the immunogenicity of remaining bacteria [1]. Intestinal epithelial cells transcytose polymeric IgA (pIgA) and pIgM from the lamina propria via the basolaterally expressed polymeric immunoglobulin receptor (pIgR). Once the pIgR:pIgA/M complex reaches the intestinal lumen, the receptor is cleaved, and SIgA and SIgM are released [1]. Pathogens that have crossed the epithelial barrier and those present in intestinal

epithelial cells can also be expelled by this transcytotic process [2]. Highlighting the defense function of this process are studies demonstrating that deletion of pIgR results in increased pathogen loads for *Helicobacter pylori* [3], *Giardia muris* [4], *Salmonella* spp. [5] and *Clostridium difficile* [6].

SIgA are the predominant species of immunoglobulins in the intestine [7]. In addition to their host defense function, they also play an immunomodulatory role [7]. The follicle-associated epithelium (FAE) of Peyer's patches (PP) and other mucosal-associated lymphoid follicles contain transcytotic microfold (M) cells. SIgA aid in the luminal sampling and the initiation of mucosal immune responses. Selective adherence of luminal SIgA to the M cell surface triggers uptake of SIgA immune complexes into the PP [8], resulting in 'retrograde' SIgA sampling by dendritic cells (DC) [9], non-inflammatory activation of DC, and induction of regulatory T cells [7]. The SIgA-induced anti-pathogenic immune responses also, non-specifically, reduce the inflammatory potential of macrophages via upregulation of inhibitory receptors [10].

Noroviruses are the leading cause of acute gastroenteritis worldwide [11, 12]. Targeting host entry and infection initiation may provide an avenue for intervention, as they are instrumental in determining host range, initiation of immune responses, and pathogenesis. However, limited information is available about factors that promote or inhibit norovirus infection. To gain a better understanding of the early events during norovirus infection in a natural host, I took advantage of murine norovirus (MNV), a well-established and highly tractable animal model for studying norovirus biology [13-15]. The first MNV strain to be discovered, MNV-1 [16], initiates infection in the ileum [17] but is cleared within days [18].

Infection is primarily detected in antigen-presenting cells (APCs) (i.e. dendritic cells [DCs] and macrophages) and lymphocytes (T and B cells) [19-21]. To reach these target cells, MNV-1 hijacks M cells for targeted delivery [17, 22, 23]. Reovirus is another enteric virus, which uses M cells during infection of the intestine [17, 24], and both viruses require enteric bacteria for optimal pathogenesis [25-27].

No information is available about the role of natural SIg during enteric virus infection. Therefore, I infected mice deficient in pIgR (pIgR KO) with MNV and reovirus. Surprisingly, and contrary to previous studies [4, 5, 28], MNV-1 and reovirus T1L loads were reduced in the gastrointestinal tract of pIgR KO mice compared to C57BL/6 controls (WT B6). This was despite enhanced numbers of DCs, macrophages, and B cells, MNV target cells, in the PP of pIgR KO mice. However, compared to WT B6 mice, naive pIgR KO mice had enhanced baseline levels of inducible nitric oxide synthase (iNOS) and interferon gamma (IFN-ɣ), a cytokine with known anti-MNV and anti-reovirus activities [29-33]. Neutralization of IFN-ɣ in pIgR KO mice or addition of IFN-ɣ to WT B6 mice resulted in modulated MNV-1 viral loads. Taken together, our findings support a model whereby SIg downmodulates antiviral cytokine levels, thereby promoting enteric viral infection.

2.2 Results

2.2A Acute Norovirus Infection is Reduced in Polymeric Immunoglobulin Receptor KO Mice

To investigate the role of SIg during norovirus infection, I analyzed MNV-1 infection in mice lacking the polymeric Ig receptor (pIgR) [34]. Since assessment of viral replication in the intestine is confounded by the lingering presence of the inoculum, neutral red, a light-sensitive

dye, was incorporated into MNV-1 virions (MNV-1-NR). Exposure to white light inactivates MNV-1-NR virions in a time-dependent manner resulting in a 3-log reduction in viral titers versus virus exposed to red light only (**Figure 2.1A**). A preliminary experiment (n=1) suggested maximum inactivation occurs between 20-30 minutes of white light exposure, and longer exposure to white light did not inactivate the virus further (**Figure 2.1B**). In vivo, newly replicated MNV-1 particles in the animal will be devoid of NR providing a means to differentiate between input (i.e., light-sensitive) and replicated (i.e., light-tolerant) virus [35].

To determine the kinetics of acute MNV-1 infection in WT B6 mice, a previous graduate student, Dr. Juliana Bragazzi-Cunha, first performed a time-course of MNV-1-NR infection via oral gavage (o.g.). Viral loads were measured at 9, 12, 18, and 24 Hours post-infection (hpi). These results suggest that the first round of MNV-1 replication occurs within 9 hpi in the distal small intestine and mesenteric lymph node (MLN) after oral infection of WT B6 mice (data not shown). Next, I compared MNV-1 infection in naïve pIgR KO and WT B6 mice. In collaboration with Sadeesh Ramakrishnan from the Shah laboratory at University of Michigan, we first confirmed that fecal levels of IgA were undetectable in pIgR KO mice, while serum IgA levels were significantly increased compared to WT B6 mice (data not shown) in accordance with the literature [36, 37]. Then, I measured MNV-1-NR viral loads in the intestinal tract and draining lymph nodes of pIgR KO and WT B6 mice at 9, 18 and 48 hpi.

Consistent with previous results, infection was detected in the MLN at 18 hpi and viral loads were maintained at 48 hpi in WT B6 mice. However, infection in pIgR KO mice was delayed and did not reach WT B6 levels until 48 hpi (**Figure 2.2A**). Consistent virus replication was not detected in the duodenum at any time point tested for either mouse strain (**Figure 2.2B**). Jejunal MNV-1 replication peaked at 18 hpi in WT B6 mice, while no consistent replication was

A.

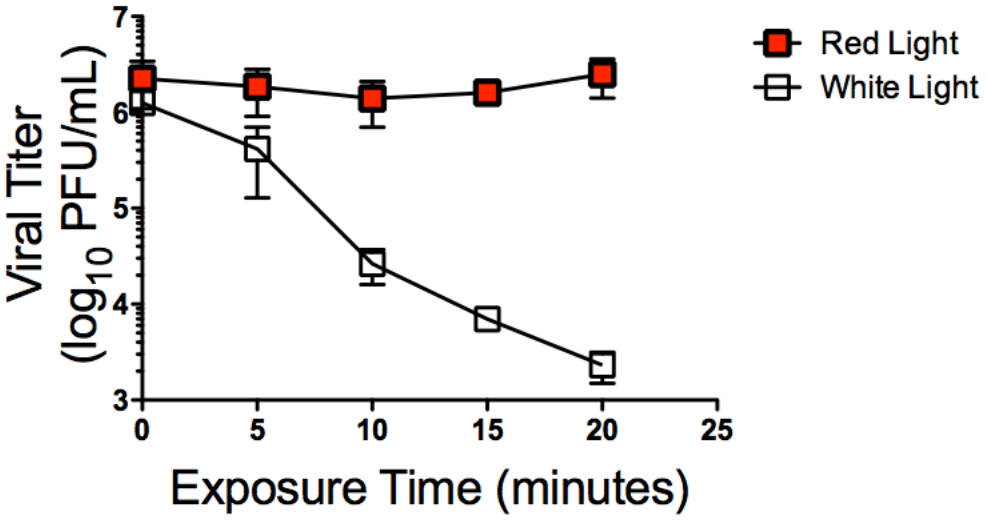

B.

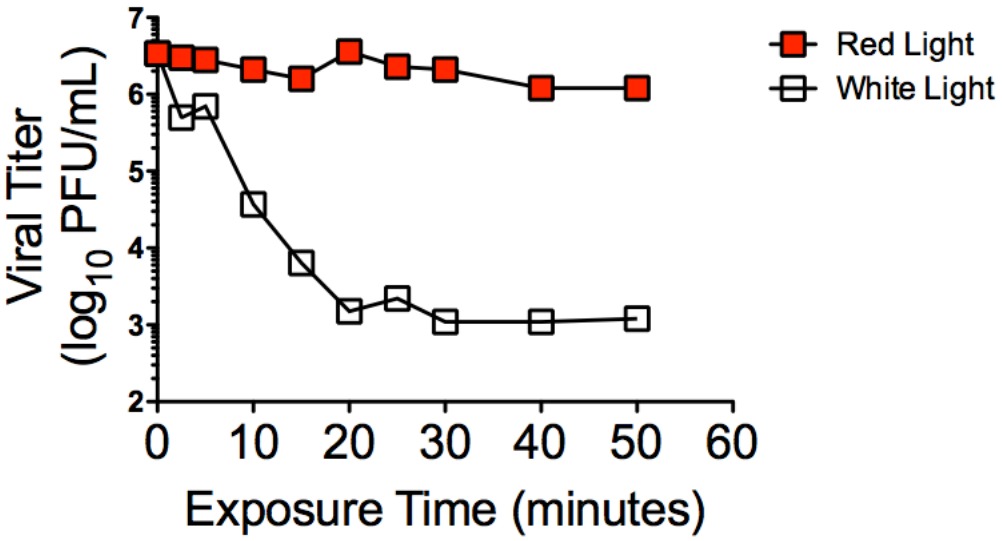

Figure 2.1: Kinetics of MNV-1-neutral red light sensitivity
A-B. Neutral red labeled MNV-1 was protected from, or exposed to, white light for the indicated minutes. Viral titers were assessed via plaque assay performed in a darkened room using a red photolight. **A.** Data are from three independent experiments. Error bars are standard error of the mean (SEM). **B.** Data are from one experiment.

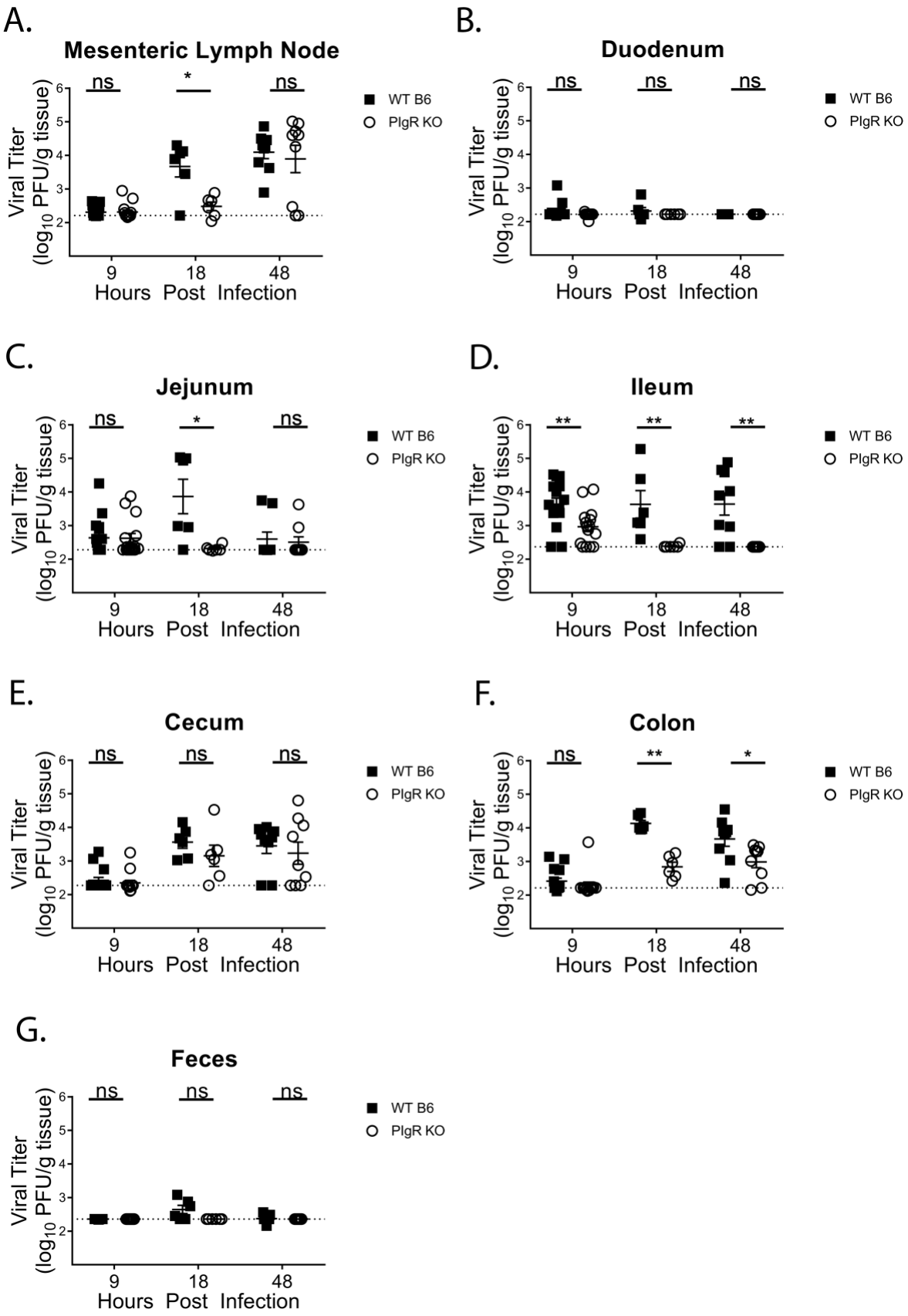
A.
Mesenteric Lymph Node
B.
Duodenum
C.
Jejunum
D.
Ileum
E.
Cecum
F.
Colon
G.
Feces
Viral Titer
(log10 PFU/g tissue)
Hours Post Infection
9
18
48
ns
*
**
WT B6
PIgR KO

Figure 2.2: Acute MNV-1 infection is reduced in pIgR KO mice

A-G. Mice were infected by oral gavage with $3.8x10^5$ PFU/animal neutral red labeled MNV-1, and tissues were harvested at 9, 18 and 48 hpi in a darkened room using a red photolight. The tissue homogenates were serially diluted and exposed to white light for 30 min. Replicated viral titers in the indicated tissue of WT B6 and pIgR KO mice were assessed via plaque assay. The sensitivity threshold for each graph is indicated by the dashed line and is as follows (log PFU/g tissue): **A.** 2.17 **B.** 2.21 **C.** 2.3 **D.** 2.37 **E.** 2.27 **F.** 2.22 **G.** 2.37**.** Data are pooled from at least two independent experiments and each symbol is a data point from an individual animal. Error bars are standard error of the mean (SEM). Data were analyzed using Mann Whitney U test. *= $P<0.05$. **= $P<0.01$. ns = not statistically significant.

observed in pIgR KO mice after 9 hpi (**Figure 2.2C**). Surprisingly, MNV-1 replication was significantly reduced in the ileum of pIgR KO mice compared to WT B6 at all time points tested (**Figure 2.2D**). Cecal MNV-1 replication increased throughout the time course in pIgR KO mice, but was not significantly different from WT B6 mice (**Figure 2.2E**). In contrast, colon titers were significantly reduced in pIgR KO mice at 18 and 48 hpi compared to WT B6 mice (**Figure 2.2F**). Fecal shedding was only detectable in WT B6 mice at 18 hpi and below the limit of detection in pIgR KO mice (**Figure 2.2G**). Taken together, these data demonstrate that pIgR KO mice have reduced viral loads, suggesting that natural, non-MNV specific, SIg are not protective, but instead enhance acute norovirus infection in vivo.

To determine if another strain of MNV will recapitulate the reduced MNV-1 viral loads in pIgR KO mice compared to controls, I used MNV-CR3 complexed with Neutral Red (MNV-CR3-NR), a strain of MNV with different infection kinetics and pathogenesis features than MNV-1. MNV-CR3 replicates slower and establishes a persistent infection in vivo [17]. Experiments to determine the kinetics of oral MNV-CR3-NR infection in WT B6 mice were performed in the lab previously by Dr. Juliana Bragazzi-Cunha. Using MNV-CR3-NR she determined that replicated MNV-CR3 was first detected in the cecum at 12 hpi (data not shown). By 24 hpi replicated virus was also detectable in the ileum and ascending colon in the majority of mice and had started spreading to the jejunum in some mice (data not shown). The spleen, MLN, stomach, duodenum, and descending colon failed to replicate MNV-CR3 within 24 hpi (data not shown). Using 12 hpi time point for MNV-CR3-NR, I sought to determine if reduced MNV infection in pIgR KO mice is MNV strain-dependent. Similar to the kinetics experiments performed previously, I detected very little MNV-CR3 replication in the small intestine and feces (**Figure 2.3A-C, 2.3F**). Robust viral replication was detected in the cecum, and infection had

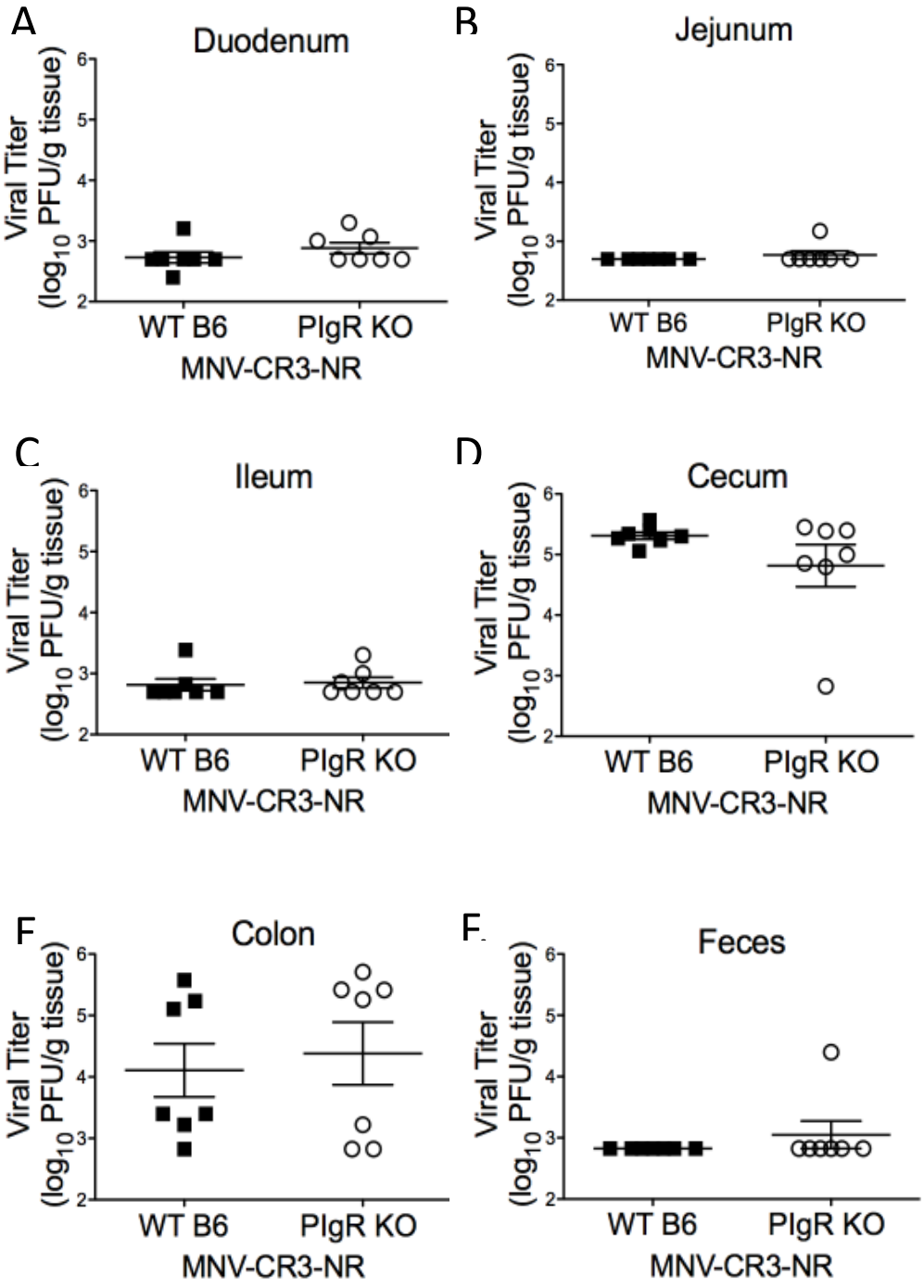

Figure 2.3: PIgR is dispensable for acute MNV-CR3 infection

A-G. Mice were infected by oral gavage with $2.6x10^5$ PFU/animal neutral red labeled MNV-CR3, and tissues were harvested at 24 hpi in a darkened room using a red photolight. The tissue homogenates were serially diluted and exposed to white light for 30 min. Replicated viral titers in the indicated tissue of WT B6 and pIgR KO mice were assessed via plaque assay. The sensitivity threshold for each graph is indicated by the dashed line and is as follows (log PFU/g tissue): **A.** 2.7 **B.** 2.7 **C.** 2.7 **D.** 2.82 **E.** 2.82 **F.** 2.82**.** Data are pooled from two independent experiments and each symbol is a data point from an individual animal. Error bars are standard error of the mean (SEM). Data were analyzed using Mann Whitney U test. ns = not statistically significant.

spread to the colon in some animals (**Figure 2.3D, 2.3E**). Interestingly however, no differences in viral loads were observed between mouse strains throughout the GI tract during MNV-CR3 infection, suggesting that reduced MNV infection in pIgR KO mice is strain-dependent.

2.2B Acute Reovirus Infection is Reduced in Polymeric Immunoglobulin Receptor KO Mice

To determine if the observed pIgR KO phenotype extended to another virus, pIgR KO and WT B6 mice were infected with reovirus T1L and tissues were harvested at 24 hpi. Our collaborator Dr. Bernardo Mainou (Emory University) measured reoviral loads in the intestinal tract and mesenteric lymph nodes. Reovirus T1L infection was similar in the mesenteric lymph nodes, duodenum, jejunum, and feces of both mouse strains (**Figures 2.4A-C, 2.4G**). However, pIgR KO mice had significantly reduced infection in the ileum, cecum, and ascending colon compared to controls (**Figure 2.4D-F**). Taken together, these data demonstrate that similar to MNV-1, natural SIg are not protective during reovirus infection. In summary, our findings show that pIgR and SIg do not directly inhibit enteric viral infection, instead SIg promote enteric viral infection. To investigate the mechanism behind this enhancement in viral infection we chose to use MNV-1 as the MNV-1 infection model is established in the Wobus lab.

2.2C Natural Secretory Immunoglobulins Do Not Facilitate Norovirus Access to Peyer's Patches

To determine if the effect of reduced MNV-1 infection following oral infection seen in pIgR KO mice is specific to the intestinal mucosa, I infected pIgR KO and control mice intraperitoneally with MNV-1-NR and assessed viral replication at 9 hpi. These data show no

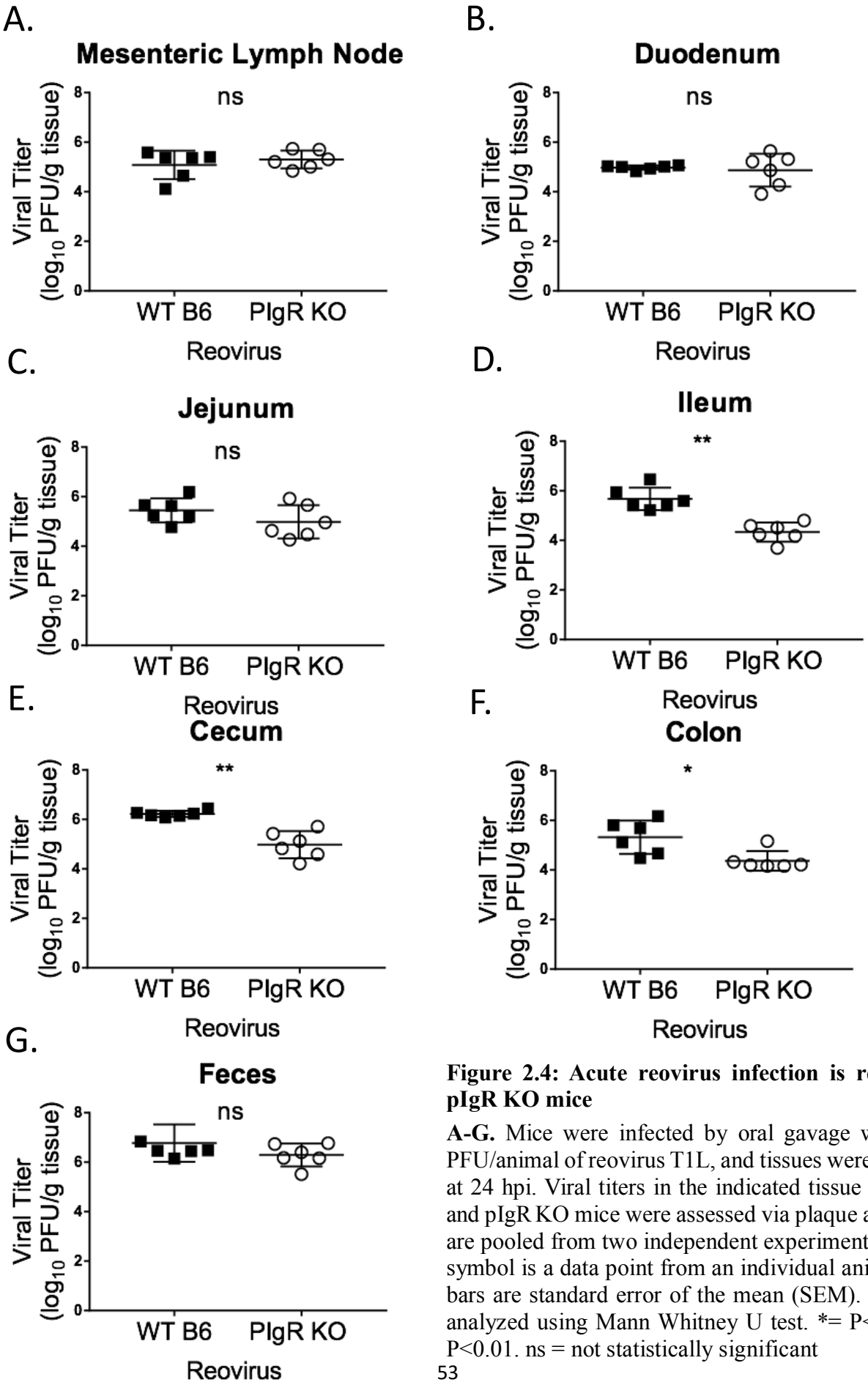

Figure 2.4: Acute reovirus infection is reduced in pIgR KO mice

A-G. Mice were infected by oral gavage with $2x10^6$ PFU/animal of reovirus T1L, and tissues were harvested at 24 hpi. Viral titers in the indicated tissue of WT B6 and pIgR KO mice were assessed via plaque assay. Data are pooled from two independent experiments and each symbol is a data point from an individual animal. Error bars are standard error of the mean (SEM). Data were analyzed using Mann Whitney U test. *= $P<0.05$. **= $P<0.01$. ns = not statistically significant

significant differences in viral load in the small intestine at 9 hpi (**Fig 2.5**), suggesting the defect in oral MNV-1 infection of pIgR KO mice may be localized to the epithelial barrier. This defect in oral infection is consistent with the role of SIg at mucosal surfaces and could be a result of reduced epithelial barrier crossing, or localized mis regulation of immunity within the PP in the absence of tolerizing SIg. To determine if reduced access to the distal small intestine was the cause of reduced MNV-1 replication in pIgR KO mice, I determined intestinal peristalsis rates in pIgR KO and WT B6 mice. Using Evans Blue dye as a marker of intestinal transit, I found that small intestinal transit was equivalent in pIgR KO mice compared to controls (**Figure 2.6A**). These data suggest that access to the distal small intestine cannot account for the reduced MNV-1 replication seen in pIgR KO mice.

M cells are necessary for efficient MNV infection [17, 22], so I next investigated M cell-associated gene expression. Host mRNA was isolated from PP in the ileum of naïve pIgR KO and WT B6 mice and analyzed for transcript levels of SpiB (a transcription factor required during M cell development) and GP2 (a marker of mature M cells) [38]. No differences in expression levels were observed for both genes between both groups (**Figure 2.6B**). These data suggest that the virus encounters similar levels of functional M cells during infection of both mouse strains, suggesting the reduced MNV-1 infection in pIgR KO mice is not due to reduced viral transcytosis. It further suggests that the lack of immune complex sensing by the intestinal immune cells does not significantly affect M cell gene transcription.

SIg are taken up by M cells and sampled by an underlying network of MNV-susceptible APCs [7]. To determine whether natural SIg aid in viral targeting to and transcytosis across the FAE, a previous graduate student Dr. Mariam Gonzalez-Hernandez, first determined whether MNV-1 was capable of interacting with non-NoV specific, recombinant sIgA. These data

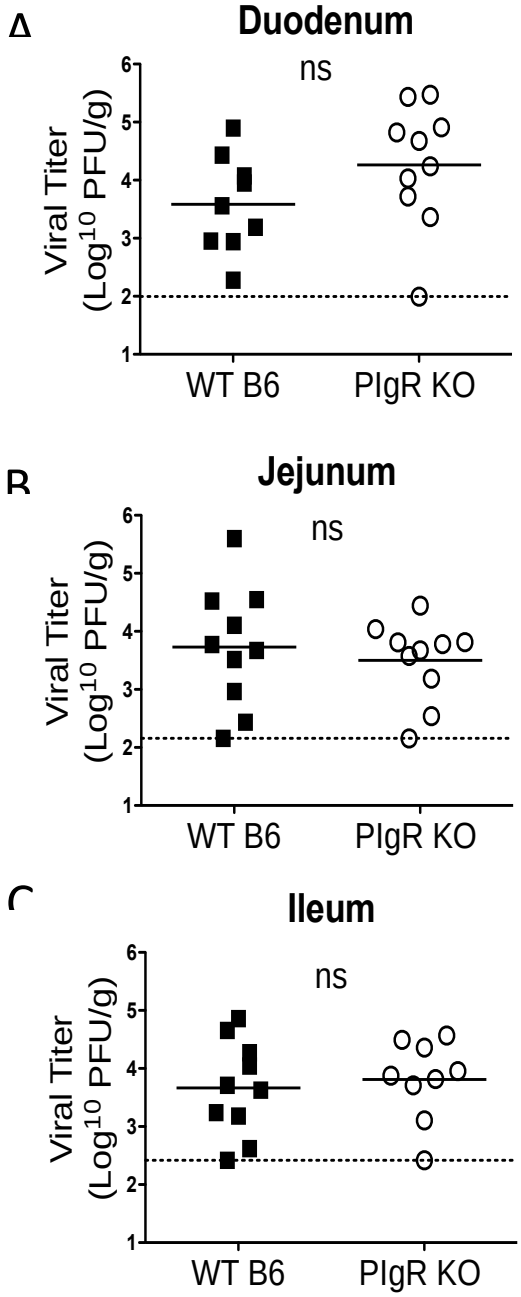

Figure 2.5: PIgR is dispensable for intraperitoneal MNV-1 infection

A-C. Mice were infected intraperitoneally with $3.8x10^5$ PFU/animal neutral red labeled MNV-1, and tissues were harvested at 9 hpi in a darkened room using a red photolight. The tissue homogenates were serially diluted and exposed to white light for 30 min. Replicated viral titers in the indicated tissue of WT B6 and pIgR KO mice were assessed via plaque assay. The sensitivity threshold for each graph is indicated by the dashed line and is as follows (log PFU/g tissue): **A.** 2.00 **B.** 2.16 **C.** 2.42. Data are pooled from three independent experiments and each symbol is a data point from an individual animal. Error bars are standard error of the mean (SEM). Data were analyzed using Mann Whitney U test. ns = not statistically significant.

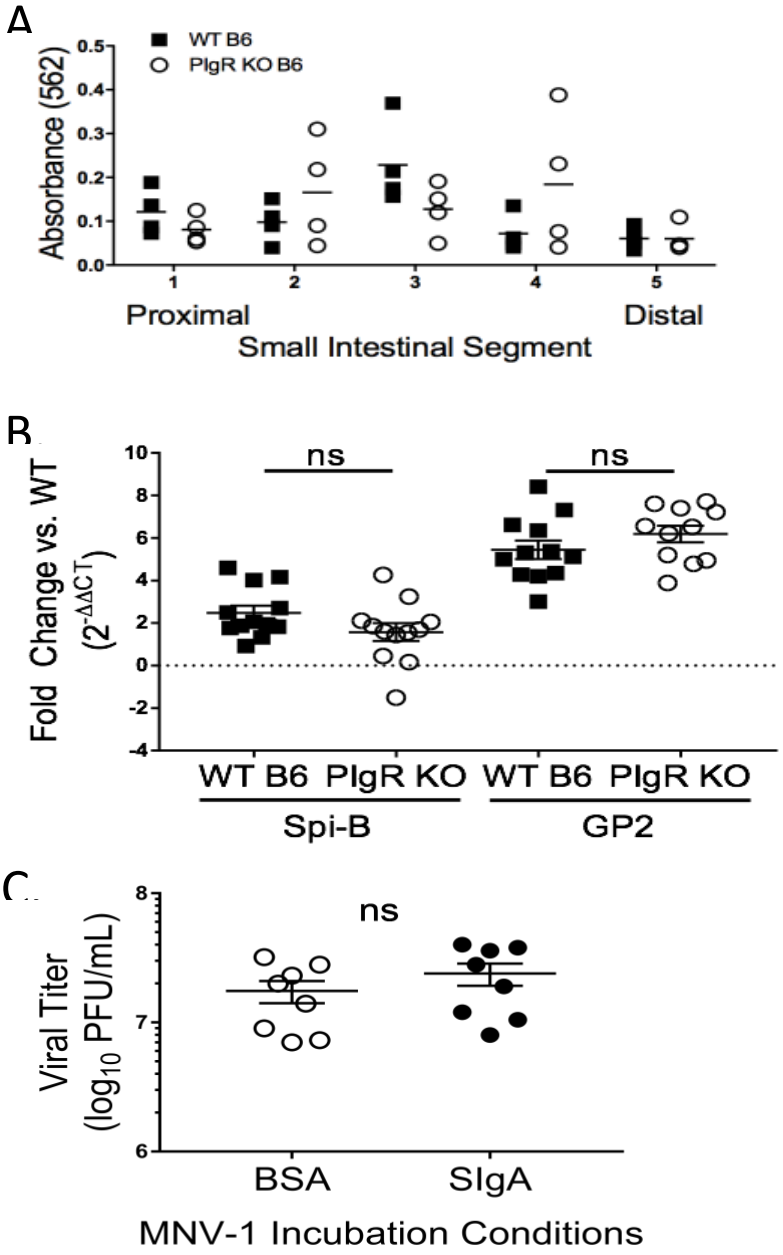

Figure 2.6: Natural SIgA biding to MNV-1 fails to neutralize infection *in vitro*

A. Evans blue dye was administered to fasting pIgR KO and B6 mice. After 15 minutes the stomach and small intestine were harvested. The small intestine was divided into fifths and transit of the dye was measured by absorbance at 562 nm. Data are pooled from two independent experiments and each symbol is a data point from an individual animal. Data was analyzed using 2-way ANOVA. **B.** Transcript levels of M cell-related genes, Spi-B and GP2, from WT B6 and pIgR KO Peyer's patches over GAPDH transcript levels are shown as 2^-(ΔΔCT) in reference to WT B6. ΔCT values were analyzed for statistical significance. Each symbol is a data point from an individual animal. Data were analyzed using Mann Whitney U test. ns = not statistically significant. **C.** MNV-1 ($2.8x10^7$ PFU) was pre-incubated with 0.25 mg/ml recombinant SIgA or bovine serum albumin for 1 hour in 37°C water bath, and neutralization was assessed via plaque assay. Error bars represent standard error of the mean (SEM) and each data pint represents an individual animal. Data were analyzed using Mann Whitney U test. ns = not statistically significant.

demonstrated the MNV interaction with natural SIgA is restricted to the P domain (data not shown), which also interacts with host cell receptors and contains neutralizing antibody epitopes [39]. Furthermore, SIgA did not affect viral infection in vitro, since no difference was observed in MNV-1 titers by plaque assay when complexed with recombinant, non-antigen specific SIgA compared to protein control (**Figure 2.6C**).

Since MNV-1 was able to bind to recombinant, non-MNV specific SIgA, I next performed ligated ileal loop assays to determine whether MNV-1 uptake was altered by the presence or absence of non-specific SIg. A potential caveat in assessing MNV-1 FAE binding and crossing, is that MNV binds mucus [40] which could potentially trap the virus confounding our results of FAE binding. Dithiothreitol (DTT) has been shown to degrade mucus and should remove any mucin bound MNV from the PP [41]. Nothing is known regarding the effect of DTT on MNV cell surface binding, so to assure that DTT treatment would not remove virions bound to the cell surface a binding assay was performed in the macrophage like cell line, RAW26.7 cells. MNV-1 was allowed to bind to RAW26.7 cells for one hour on ice. After washing unbound virus, cells were treated with DTT and bound viral genome copies were assessed via RT-qPCR. I found no differences in MNV-1 binding of DTT-treated cells as compared to untreated control cells (**Figure 2.7A**). These data suggest that DTT will not remove virus bound to the PP FAE.

To investigate potential differences in MNV PP access, ileal PP of naïve pIgR KO and WT B6 mice were ligated to create a ~2 cm closed loop, and virus was injected as the loop was sealed (Diagram **Figure 2.7B**). After 25 minutes, whole PP were excised, and mucus-bound virions were removed prior to measuring viral genome titers by qRT-PCR. No difference was

observed in viral genome copies between the two groups (**Figure 2.7C**) suggesting similar amounts of virions bound and/or entered the PP in either mouse strain.

Since MNV-1 primarily infects immune cells [19], I further assessed the amount of virions that reach PP lamina propria. To determine if I could distinguish between virus bound to the FAE, and virus that had crossed the barrier into the PP lamina propria, I digested the PP FAE with 2 mM EDTA. This resulted in a ~5 fold reduction in epithelial cells (EpCam+) as measured by flow cytometry (data not shown). Although these results are preliminary (n=1), they suggest that separation of the FAE from the lamina propria is possible. Ileal loops were performed, and after 25 or 40 minutes of virus incubation the PP FAE was digested away from the PP lamina propria with 5 mM EDTA, and viral genome levels were determined by RT-qPCR. There were no significant differences in the amount of virus that associated with the PP FAE between mouse strains at either timepoint (**Figure 2.7D**). More uniform FAE binding was seen after 40 minutes, however overall virus attachment was not enhanced above 25 minutes of virus incubation (**Figure 2.7D**). There was also no difference in MNV-1 crossing the FAE into the PP lamina propria in pIgR KO compared to WT B6 mice at either timepoint (**Figure 2.7E**). These data suggest that MNV-1 access to the PP lamina propria is not altered in pIgR KO mice compared to controls.

However, one limitation of the previous experiment is the short interaction time between MNV-1 and SIg compared to a natural, oral infection, during which the virus travels through the intestinal tract. Therefore, we hypothesized that pre-incubation of MNV-1 with natural SIgA may boost virus internalization if performed prior to the ileal loop ligation. Nevertheless, similar MNV levels were detected in the PP lamina propria in WT B6 and pIgR KO mice when MNV-1 was pre-complexed with non-MNV specific SIgA or bovine serum albumin (BSA) as negative

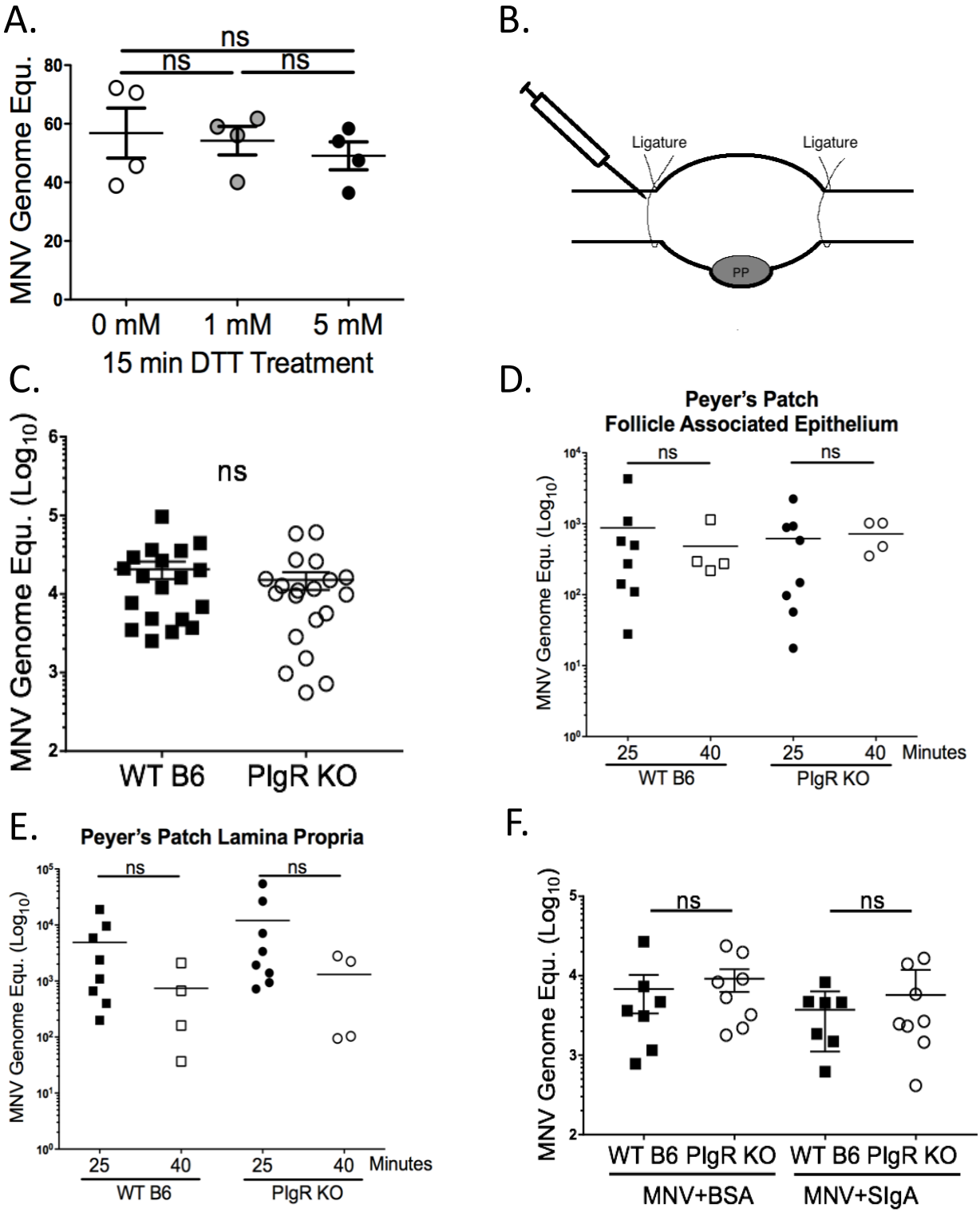
A.
ns
ns
ns
MNV Genome Equ.
80
60
40
20
0
0 mM
1 mM
5 mM
15 min DTT Treatment
B.
Ligature
Ligature
PP
C.
MNV Genome Equ. (Log10)
ns
6
5
4
3
2
WT B6
PIgR KO
D.
Peyer's Patch
Follicle Associated Epithelium
MNV Genome Equ. (Log10)
ns
ns
25
40
25
40
Minutes
WT B6
PIgR KO
E.
Peyer's Patch Lamina Propria
MNV Genome Equ. (Log10)
ns
ns
25
40
25
40
Minutes
WT B6
PIgR KO
F.
MNV Genome Equ. (Log10)
ns
ns
WT B6 PIgR KO
WT B6 PIgR KO
MNV+BSA
MNV+SIgA

Figure 2.7: Natural secretory immunoglobulins do not aid in MNV-1 access to the Peyer's patch

A. RAW264.7 cells were exposed to MNV-1 for one hour on ice to allow virus attachment. Unbound virus was removed, and dithiothreitol (DTT) was added at varying concentrations for 15 minutes at 37°C. Cells were frozen at -80°C after washing and MNV-1 genome copies were determined via RT-qPCR. **B-F.** Intestinal ileal loop assay in WT B6 and pIgR KO mice. 100 µl ($3.8x10^5$ PFU) MNV-1 was injected into the closed loop and incubated for 25 or 40 min. Viral genome copy equivalents were measured by RT-qPCR in Peyer's patches. **B.** Model of intestinal loop assay. **C.** MNV-1 bound to and internalized into the Peyer's patch (PP). Data are pooled from four independent experiments. **D-E.** MNV-1 genomes bound to the follicle-associated epithelium (FAE binding) and internalized into the PP lamina propria (FAE crossing) after 25 or 40 minutes. Data are pooled from two independent experiments. **F.** MNV-1 was pre-incubated with rotavirus-specific secretory IgA (SIgA) or bovine serum albumin (BSA) for 1 hour at 37°C before injecting the complex into the loop. Data are pooled from two independent experiments. Error bars represent standard error of the mean (SEM) and each datapoint represents an individual PP. Data were analyzed using Mann Whitney U test. ns = not statistically significant.

control for MNV-1 binding (**Figure 2.7F**). Taken together, these data demonstrate that, although MNV-1 can interact with recombinant non-specific SIg, natural SIg does not facilitate MNV-1 binding to or crossing of the intestinal epithelial barrier.

2.2D Polymeric Immunoglobulin Receptor KO Mice Have Increased Numbers of Small Intestinal Antigen Presenting Cell (APC) Subsets

Since access to the site of primary viral infection, the PP, cannot account for the reduced infection seen in pIgR KO mice, I next investigated whether an absolute or relative reduction in the number of B cells, macrophages and DC, established MNV target cells [20, 21] in the small intestine, might provide an explanation. Small intestines and their PP were collected from naïve mice, tissues were digested to create single cell suspensions, and cellularity was analyzed via flow cytometry. To determine the correct digestion time to preserve immune cells viability, I digested PP samples for 10 to 20 minutes [42] and assessed cellular viability via flow cytometry. I determined that cellular viability decreased with increasing digestion time, and that the optimal digestion time occurred between 10-13 minutes (data not shown). After harvest and digestion of naïve tissues, no difference was detected in the percentage of B cells (CD19+/CD11b-), macrophages (CD19-/CD11b+/CD64+), and DCs (CD19-/CD11b+/CD64-/CD11c+) in the villous or PP lamina propria (**Figure 2.8A-B**). No difference was further observed in the number of the three APC subsets in the villous lamina propria (**Figure 2.8C**). Interestingly, all three APC subsets were increased roughly 2.5-fold in the PP lamina propria of pIgR KO mice compared to controls (**Figure 2.8D**). These data demonstrate that pIgR KO mice have increased numbers of MNV-susceptible cell types at the site of infection.

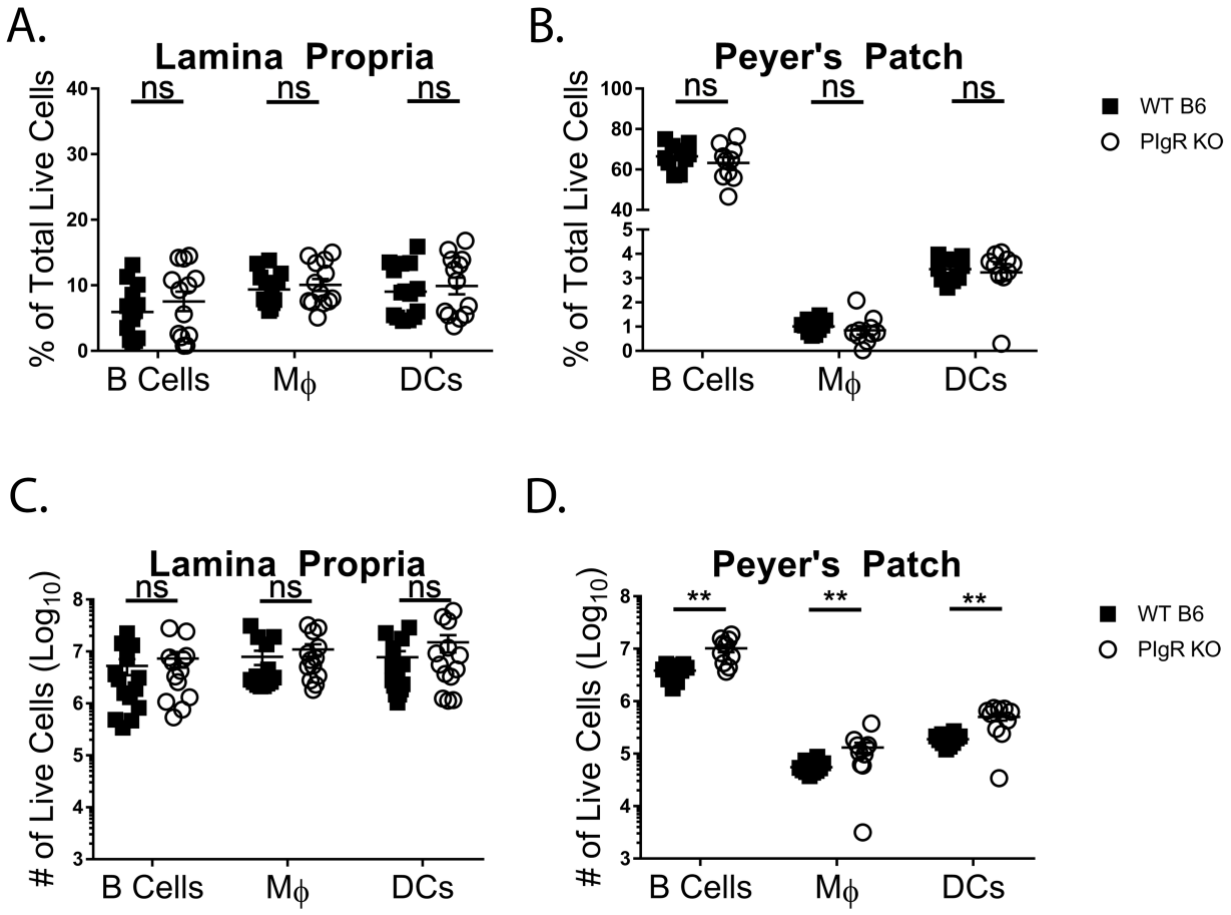

Figure 2.8: PIgR KO mice have increased small intestinal APC subsets
A-D. Peyer's Patches and small intestinal lamina propria cells were isolated from naïve pIgR KO and WT B6 mice. Live cells were analyzed via flow cytometry. The gating strategy was as follows: Antigen-presenting cells (APCs) were defined as Singlets/Live/CD45+/I-A/I-E (MHCII)+. APCs were further gated into B cells (CD19+/CD11b-), macrophages (CD19-/CD11b+/CD64+) (Mϕ), and dendritic cells (CD19-/CD11b+/CD64-/CD11c+) (DCs). **A-B.** Percentage of live lamina propria (**A**) and Peyer's patch (**B**) cells. **C-D.** Absolute number of live lamina propria (**C**) and Peyer's patch (**D**) cells. Data shown are pooled from two to three independent experiments and each symbol is a datapoint from an individual animal. The data mean is indicated for each group. Data were analyzed using Mann Whitney U test. *= P<0.05. **= P<0.01 ***= P<0.001. ****= P<0.0001. ns = not statistically significant.

I next performed further phenotyping of macrophage and DC (mononuclear phagocyte) subsets via flow cytometry to determine if differences in APC subsets may account for reduced viral replication seen in pIgR KO mice. Live cells were first gated on MHCII expression to select for all APCs, and CD19 expression was used to exclude B cells from mononuclear phagocytes. Mononuclear phagocytes were then characterized into subsets based on expression of CD11b, CD103, CX3CR1, and CD8 as previously described [43]. Percentages and absolute numbers of stationary mononuclear phagocytes ($CD11b^{-}/CD103^{+/-}/CX3CR1^{-}/CD8^{+}$) were not different between strains and represented the bulk of the mononuclear phagocyte pool (data not shown). Analysis of migratory mononuclear phagocytes, termed conventional DCs ($CD11b^{+}/CD103^{+}/CX3CR1^{-}/CD8^{-}$), revealed reduced percentages in pIgR KO villous lamina propria compared to controls, however percentages were similar in the PP (**Figure 2.9A-B**). The ability of mononuclear phagocytes to cross-present extracellular antigens to CD8 T cells is primarily undertaken by plasmacytoid dendritic cells ($CD11b^{-}/CD103^{+}/CX3CR1^{-}/CD8^{+}$), while CX3CR1 expressing mononuclear phagocyte subsets ($CD11b^{+}/CD103^{-}/CX3CR1^{+}/CD8^{-}$) comprise primarily stationary macrophages and are poor stimulators of T cells [43]. No differences in percentages of these subsets in the villous or PP lamina propria were detected (**Figure 2.9A-B**). Despite enhanced percentages of conventional DCs, the number of all mononuclear phagocyte subsets were equal in the small intestinal lamina propria of pIgR KO vs. control mice (**Figure 2.9C**). In keeping with enhanced mononuclear phagocyte numbers in the PP of pIgR KO mice compared to controls (see **Figure 2.8E**), numbers of all three mononuclear phagocyte populations assessed were enhanced in pIgR KO mice versus controls (**Figure 2.9D**). Taken together with data from **Figure 2.7**, these data suggest that access to and availability of norovirus target cells cannot account for reduced MNV-1-NR infection seen in pIgR KO mice.

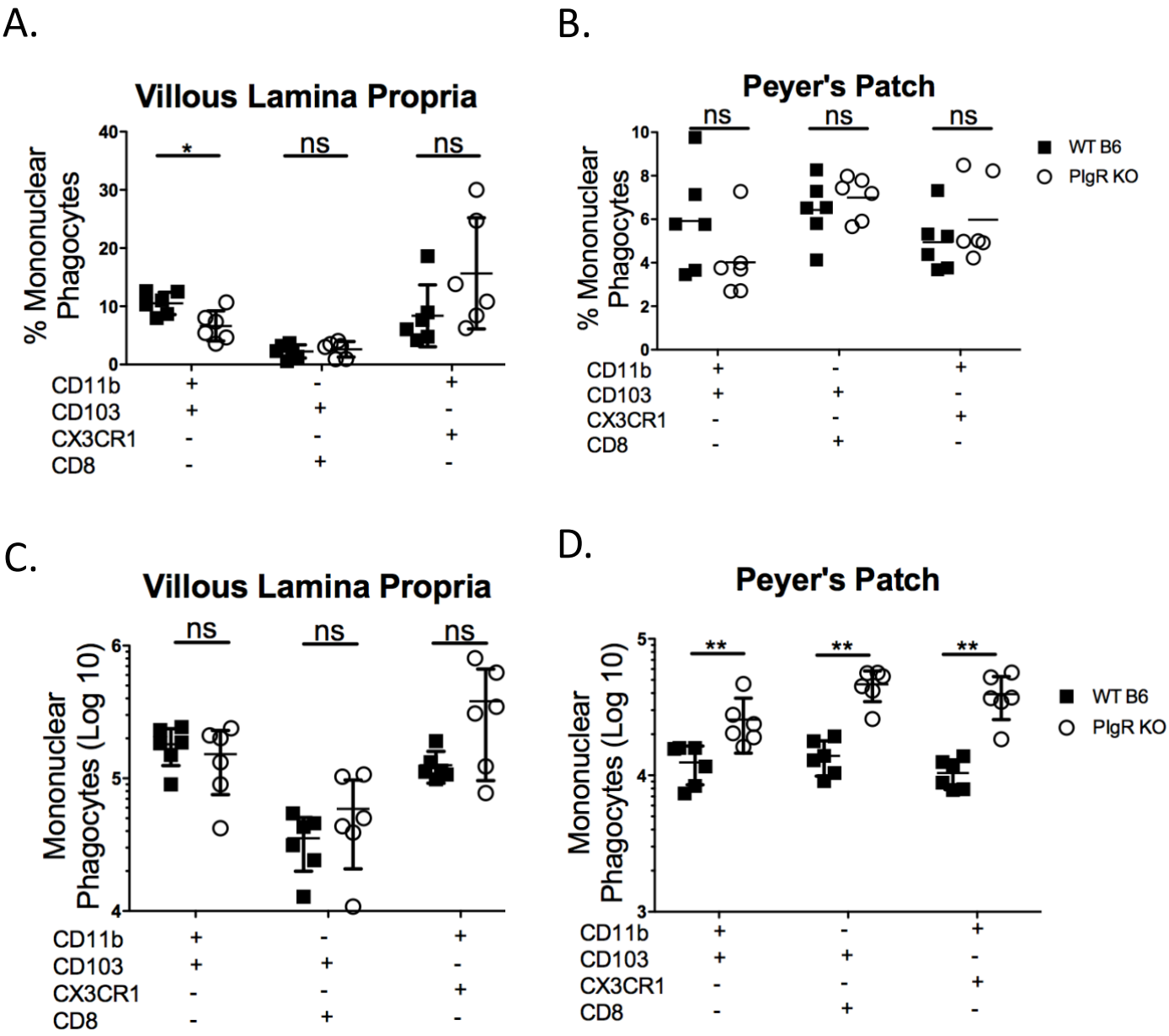

Figure 2.9: Small intestinal mononuclear phagocyte characterization
A-D. Peyer's Patches and small intestinal lamina propria cells were isolated from naïve pIgR KO and WT B6 mice. Live cells were analyzed via flow cytometry. The gating strategy was as follows: Antigen-presenting cells (APCs) were defined as Singlets/Live/CD45+/I-A/I-E (MHCII)+. Mononuclear phagocytes were further defined as CD19- and characterized based on expression of CD11b, CD103, CX3CR1 and CD8. **A-B.** Percentage of live villous lamina propria (**A**) and Peyer's patch (**B**) cells. **C-D.** Absolute number of live villous lamina propria (**C**) and Peyer's patch (**D**) cells. Data shown are pooled from two independent experiments and each symbol is a datapoint from an individual animal. The data mean is indicated for each group. Data were analyzed using Mann Whitney U test. *= $P<0.05$. **= $P<0.01$. ns = not statistically significant.

2.2E Interferon-ɣ and iNOS Levels are Enhanced in Naïve Polymeric Immunoglobulin Receptor KO Mice

It is well known that SIg complexes have immunomodulatory functions, and that when enteric bacteria are recognized in complex with SIg an anti-inflammatory response is initiated [7]. Therefore, I next explored localized mis regulation of PP immunity in pIgR KO mice as a source of reduced MNV-1 replication. Towards that end, transcript levels of a panel of cytokines and chemokines were analyzed in naïve and 9 hpi pIgR KO and compared to those from naïve and 9 hpi WT B6 mice. The ileum was chosen for assessment, as it is the initial site of MNV-1 replication and the organ in which MNV-1 titers were significantly reduced at both 9 and 18 hpi in pIgR KO mice (**Figures 2.2D**). Host mRNA was isolated from naïve and 9 hpi ilea of both groups of mice and analyzed by RT-qPCR for transcript levels of the anti-inflammatory genes TGF-β and interleukin 10, the pro-inflammatory and antiviral genes TNF-α, iNOS, IFN-ɣ, IFN-β, IFN-λ, and ISG15. IFN-ɣ transcript levels in naive pIgR KO mice were greatly enhanced over naive controls (**Figure 2.10A**). Interestingly, after 9 hours of MNV-1-NR infection IFN-ɣ transcript levels were significantly reduced in pIgR KO mice compared to uninfected controls. However, infected pIgR KO mice still exhibited enhanced IFN-ɣ transcript levels compared to infected WT B6 mice (**Figure 2.10A**).

iNOS transcript levels were significantly enhanced in naive pIgR KO mice compared to naive WT B6, however similar levels were observed in infected mice of both backgrounds (**Figure 2.10B**). In contrast, IFN-β transcript levels were significantly reduced in naive and infected pIgR KO mice compared to controls (**Figure 2.10C**). Similarly, transcript levels of the inflammatory molecules TNF-α and ISG15 were comparable in naive and infected pIgR KO mice compared to controls (**Figure 2.10D-E**), as were transcript levels of TGF-β, a cytokine

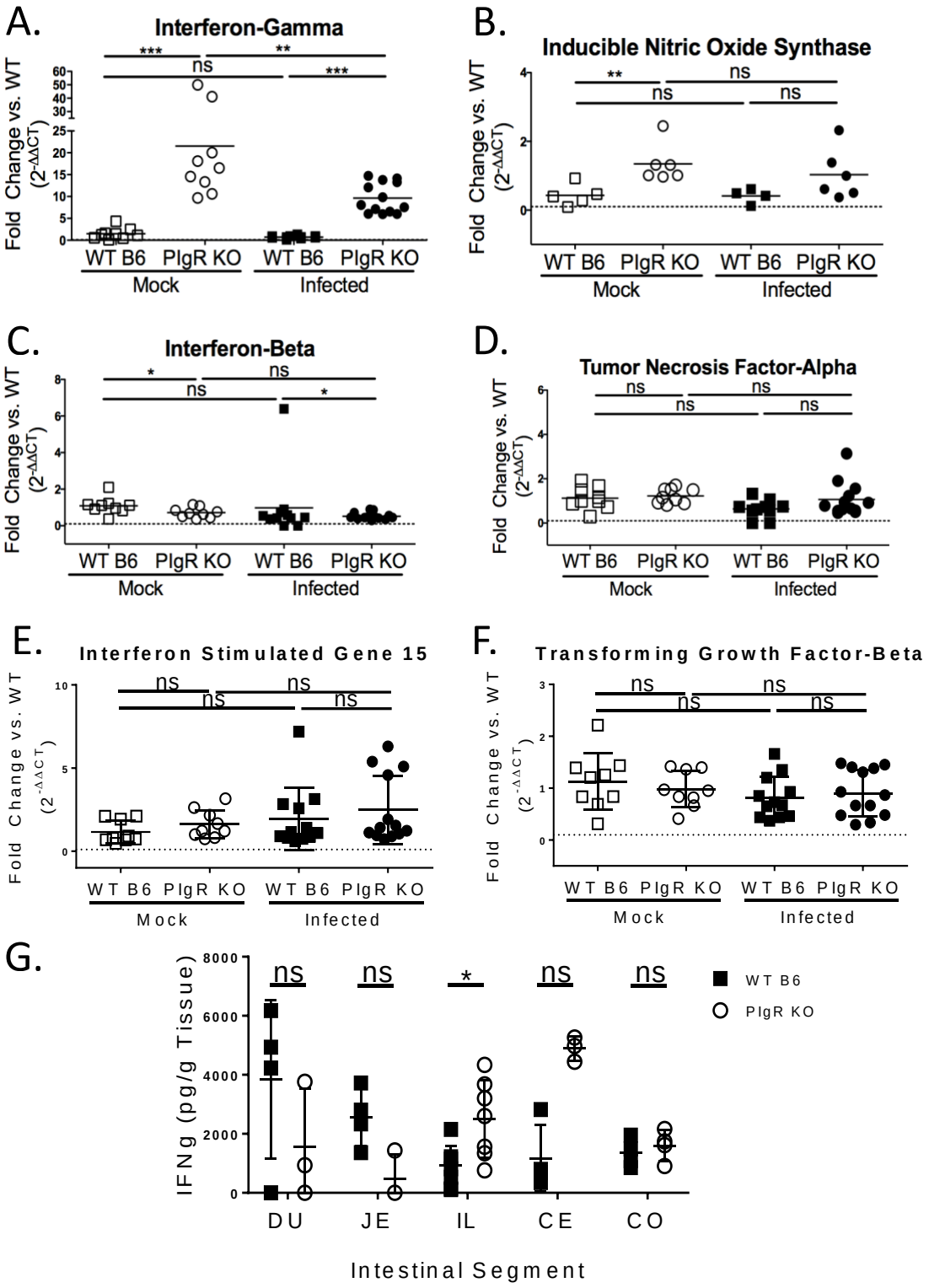

Figure 2.10: IFN-ɣ and iNOS levels are enhanced in pIgR KO mice

A-F. Total ileal RNA was isolated from naïve or 9 hpi pIgR KO and WT B6 mice to determine host gene levels in reference to *gapdh*. Data is shown in reference to WT B6 mice and displayed as 2^-(ΔΔCT). ΔCT values were analyzed for significance. **G.** Intestinal segments from naïve pIgR KO and WT B6 mice were harvested to determine host IFN-ɣ protein levels via ELISA. Each symbol is the datapoint from an individual animal. The data mean is indicated for each group. *= P<0.05. **= P<0.01 ***= P<0.001. ns = not statistically significant.

which promotes IgA class switching [44] (**Figure 2.10F**). IFN-λ and IL-10 were undetectable in either group (data not shown). Consistent with increased IFN-ɣ transcript levels, ileal IFN-ɣ protein levels were also significantly higher in pIgR KO mice versus WT B6 controls (**Figure 2.10G**). No difference in IFN-ɣ levels between strains were found in other sections of the intestinal tract (**Figure 2.10G**), suggesting site specific differences in IFN-ɣ regulation. These data demonstrate that pIgR KO mice have enhanced levels of iNOS and IFN-ɣ, consistent with previous findings that SIgA dampens inflammatory signals [7]. Both molecules have established anti-viral activities [45-48]. No significant mortality is seen in iNOS-deficient mice infected with MNV-1 [16], and MNV-1 replicates similarly in bone marrow-derived macrophages from WT B6 and iNOS-deficient mice [20]. In contrast, IFN-ɣ is a cytokine, which effectively blocks MNV infection [29-32]. Thus, these findings suggest that elevated levels of some antiviral cytokines in naïve pIgR KO mice, in particular IFN-ɣ, may limit MNV-1 replication. Furthermore, MNV-mediated downregulation of IFN-ɣ in pIgR KO mice suggests viral regulation of this antiviral cytokine.

2.2F Small Intestinal Macrophages are Resistant to Norovirus Infection

I have found that the naïve pIgR KO mice have enhanced levels of IFN-ɣ and iNOS, suggesting that they may be less susceptible to MNV infection. To determine if MNV-1 target cells, specifically macrophages, from pIgR KO mice are less susceptible to MNV-1 infection than control cells, I derived macrophages from the bone marrow of pIgR KO and WT B6 animals by culturing isolated cells at 37°C in the presence of 20% L929 supernatant [49]. After 7 days, bone marrow-derived macrophages (BMDM) were infected with MNV-1 and viral replication was assessed at 24 and 48 hpi via plaque assay. MNV-1 replication in BMDM peaked

at 24 hpi and reached equivalent levels in pIgR KO and control BMDM (**Figure 2.11A**). Small intestinal lamina propria cells were also isolated from pIgR KO and control mice as previously described [42]. Once isolated, cells were plated and allowed to adhere overnight at 37°C. Non-adherent cells were removed, and adherent cells were collected using PBS with 0.02% EDTA. Collected cells were seeded onto fresh plates and infected with MNV-1 at a MOI of 5 after attachment. Interestingly, ex vivo infection of small intestinal lamina propria macrophages was not detectable (**Figure 2.11B**).

Given that MNV-1 infection initiates in the ileum, I next sought to determine if I could detect viral infection in cells separately isolated from the lamina propria of digested duodenum, jejunum and ileum of naive pIgR KO mice and controls. These intestinal segments included both lymphoid and non-lymphoid tissue after isolation as described above [42]. A preliminary study (n=1) using an MOI of 5, showed no increase in viral genome copies by 9 hpi in adherent cells isolated from the SI segments (**Figure 2.11C-E**). However, recent data from the Karst lab demonstrated that MNV-1 replication almost exclusively occurs in the PP and not the lamina propria [19]. Therefore, I repeated the experiments above using only PP-derived immune cells. In order to determine if PP immune cells are differentially susceptible to MNV-1 infection, I harvested cells from the PP from pIgR KO mice and controls as described above. I infected both adherent and non-adherent cells (MOI of 5) and assessed cultures for MNV-1 infection by plaque assay. I detected no enhancement in MNV-1 in either the non-adherent or the adherent fractions of cells isolated from the PP of naïve mice from either strain (**Figure 2.11F-G**).

Taken together, I determined that bone-marrow derived macrophages from pIgR KO mice are equally susceptible to MNV-1 infection as cells derived from WT B6 mice. Although most of these findings are preliminary, it appears as though immune cells isolated from the small

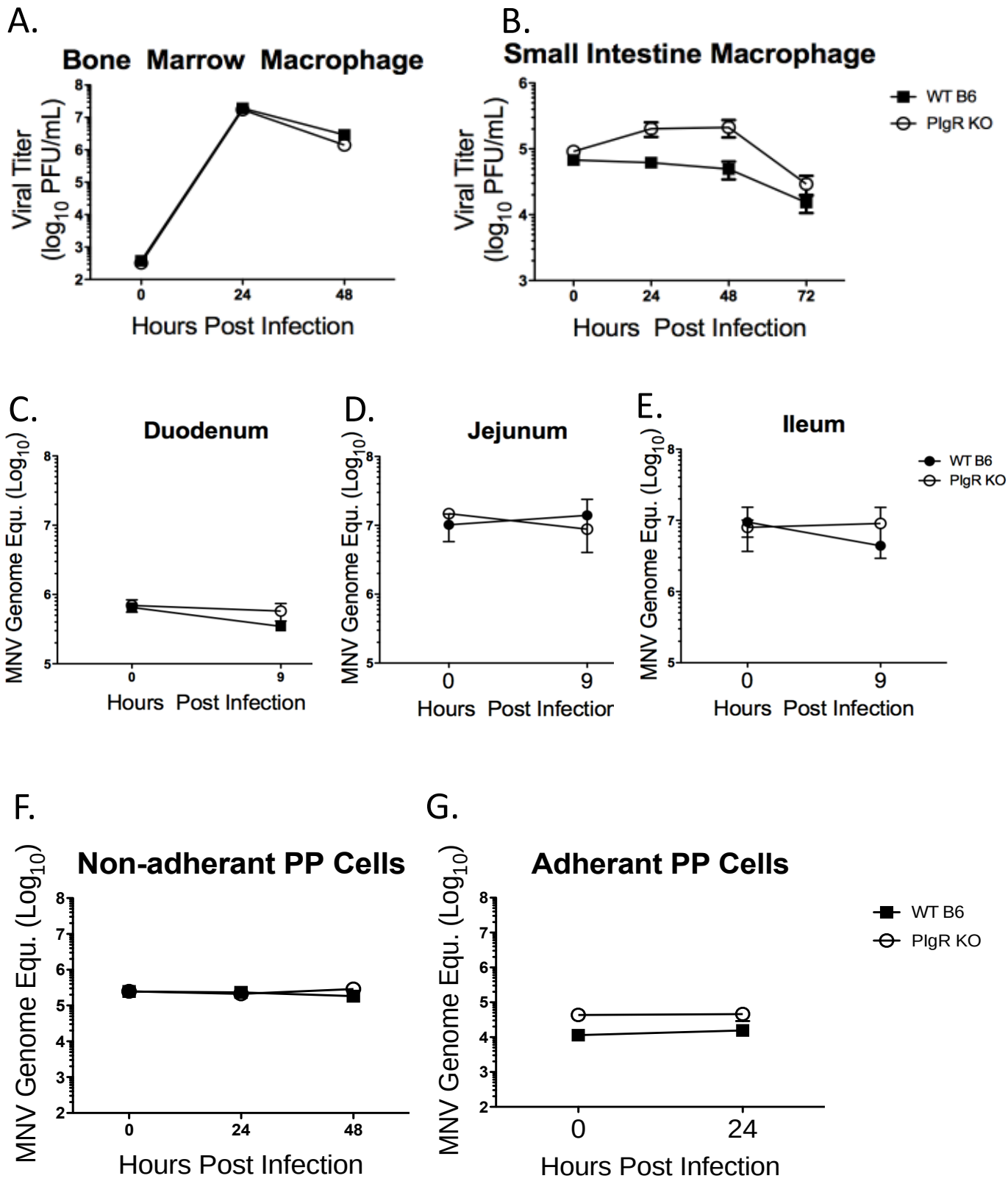
A.
Bone Marrow Macrophage
Viral Titer (log10 PFU/mL)
Hours Post Infection
B.
Small Intestine Macrophage
Viral Titer (log10 PFU/mL)
Hours Post Infection
WT B6
PIgR KO
C.
Duodenum
MNV Genome Equ. (Log10)
Hours Post Infection
D.
Jejunum
MNV Genome Equ. (Log10)
Hours Post Infection
E.
Ileum
MNV Genome Equ. (Log10)
Hours Post Infection
WT B6
PIgR KO
F.
Non-adherant PP Cells
MNV Genome Equ. (Log10)
Hours Post Infection
G.
Adherant PP Cells
MNV Genome Equ. (Log10)
Hours Post Infection
WT B6
PIgR KO

Figure 2.11: Small intestinal cells are resistant to MNV-1 infection
A. Bone marrow was harvested from naïve pIgR KO and WT B6 mice. Bone marrow derived macrophages (BMDM) were differentiated for 7 days and infected with MNV-1 at an MOI 0.05. Viral replication was assessed at indicated times post infection via plaque assay. Data are pooled from 3 independent experiments (n=8 mice). **B-G.** Small intestines were harvested from naïve pIgR KO and WT B6 mice. Small intestinal lamina propria and PP cells were isolated and incubated overnight at 37°C. Adherent cells were collected and infected with MNV-1 at an MOI 5. Viral replication was assessed at indicated times post infection via plaque assay. **B.** Data are pooled from 3 independent experiments (n= 8 mice). **C-E.** Small intestine was divided into fifths with the first section representing the duodenum, 2-4 the jejunum, and section 5 the ileum. Data are from 1 experiment (n=2 mice). **F-G.** Small intestinal PP were isolated, and cells were pooled per individual mouse. After overnight incubation, both adherent and non-adherent cells were collected and infected. Data are from 1 experiment (n=2 mice).

intestine are refractory to ex vivo MNV-1 infection regardless of mouse genotype. Despite robust infection of BMDM from pIgR KO and control mice, our findings suggest small intestinal cells are resistant to ex vivo MNV-1 infection. Numbers of PP macrophages are fairly low however and I did not verify the identity of adherent and non-adherent cell populations. Further characterization of harvested small intestinal cells is necessary to assure isolation of MNV target cell types.

2.2G Interferon-ɣ Reduces Norovirus Infection in vivo

Interferon gamma has known anti-MNV activity [29-33], and its enhancement in the ileum of pIgR KO mice compared to WT B6 controls correlates with reduction of MNV replication. To test whether enhanced levels of IFN-ɣ limit MNV-1 infection in pIgR KO mice, we neutralized intestinal IFN-ɣ in pIgR KO mice via intraperitoneal (i.p.) treatment of 500 µg anti-IFN-ɣ, or isotype control antibody 18 hours prior to MNV-1-NR infection. Viral replication was measured 18 hpi via plaque assay in intestinal segments as before. While no differences were observed in viral titers in either the ileum or the cecum of anti-IFN-ɣ or isotype control-treated pIgR KO mice (**Figure 2.12A-B**), there was a significant enhancement in MNV-1 replication in the colon of pIgR KO mice following IFN-ɣ neutralization (**Figure 2.12C**). No differences were detected in viral loads in the mesentery, duodenum, jejunum and feces between the two groups of mice (data not shown). These data suggested that the enhanced levels of IFN-ɣ in pIgR KO mice might directly inhibit MNV-1 replication. To confirm these findings, I next treated WT B6 mice i.p. with 10^4 units of IFN-ɣ 18 hours prior to MNV-1-NR infection. Viral loads were again determined 18 hpi by plaque assay. Significantly reduced titers were observed in both the ileum and the cecum of IFN-ɣ treated WT B6 mice compared to controls (**Figure**

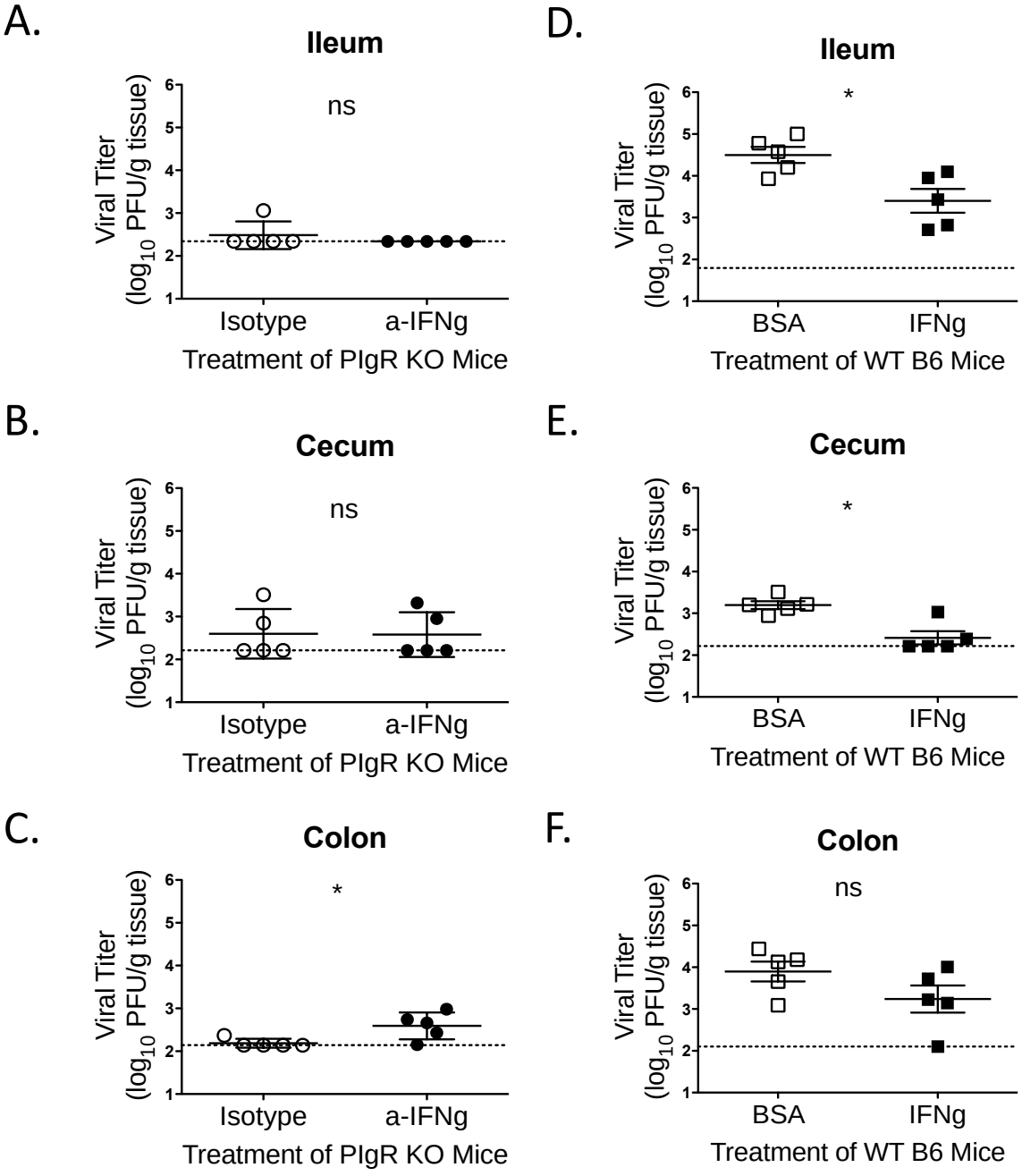

Figure 2.12: IFN-ɣ reduces MNV-1 infection in vivo

A-C. PIgR KO mice were treated with 500 µg anti-IFN-ɣ antibody or isotype control were administered intraperitoneally 18 hours before MNV-1-NR infection. **D-F.** WT B6 mice were treated with 10^4 units/animal IFN-ɣ or equivalent protein (BSA) intraperitoneally 18 hours prior to infection by oral gavage with $3.8x10^5$ PFU/animal of neutral red labeled MNV-1, and tissues were harvested at 18 hpi in a darkened room using a red photolight. The tissue homogenate was serially diluted and exposed to white light for 30 min. Replicated viral titers in the indicated tissue of WT B6 and pIgR KO mice were assessed via plaque assay. The sensitivity threshold for each graph is indicated by the dashed line and is as follows (log PFU/g tissue): **A.** 2.34 **B.** 2.21 **C.** 2.14 **D.** 1.79 **E.** 2.22 **F.** 2.1. Data are pooled from two independent experiments and each symbol is a data point from an individual animal. Error bars are standard error of the mean (SEM). Values were analyzed using Mann Whitney U test. *= 0.05 ns = not statistically significant.

2.12D-E). No difference in viral replication was seen in the colon (**Figure 2.12F**). Similar to our findings in pIgR KO mice, no differences were detected in viral loads in the mesentery, duodenum, jejunum and feces of IFN-ɣ or control-treated WT B6 mice (data not shown). These data confirm the anti-MNV properties of IFN-ɣ in vivo. Taken together, these results point to a model in which the absence of SIg results in enhanced IFN-ɣ sufficient to limit MNV-1 replication in the GI tract.

2.3 Discussion

SIg provides a first line of defense against several enteric pathogens by reducing immunogenicity of lumenal bacterial communities, mediating immune exclusion, and expulsion from the host (reviewed in [7, 50, 51]). Despite the ability of recombinant, non-MNV specific pIgA, secretory component, and SIgA to bind MNV-1, infection was not altered in vitro, and removing SIg-mediated innate intestinal defenses did not alter MNV-1 binding to the FAE, or internalization into PP. Instead, our findings demonstrated that pIgR KO mice, which lack SIg, showed reduced MNV-1 infection. This suggests natural SIg do not exclude MNV from the intestine or mediate intraepithelial expulsion of this virus. More importantly, these data indicate that natural SIg do not protect the host from norovirus infection, a finding that also extended to reovirus. This result is surprising given other enteric pathogens are controlled in this manner [3-6]. To the best or our knowledge, this represents the first example in which pIgR and natural SIg indirectly promote infection by enteric viruses.

Our current analysis of pIgR KO mice also revealed previously unrecognized features of this mouse strain. First, these mice had ~2.5 fold greater numbers of macrophages, DC and B cells in their PP, suggesting larger PP, compared to WT B6 controls. Second, key M cell

transcripts (i.e., Spi-B and GP2) were similar to controls, suggesting that M cell development is independent of SIg. Third, analysis of host mRNA levels in the small intestine revealed that IFN-ɣ and iNOS were selectively elevated in naïve pIgR KO mice compared to WT B6 controls. Previous studies have also reported enhanced inflammatory activation in pIgR KO mice, resulting in lethal systemic hyperactivity [52], spontaneous COPD [53], and enhanced susceptibility to chemically-induced colitis [54].

Analysis of pIgR KO mice revealed previously unrecognized features of this mouse strain summarized pictorially in **Figure 2.13**. First, we confirmed serum IgA protein levels were enhanced in pIgR KO mice compared to WT B6 controls (**Figure 2.13 Circle 1**). Second, I determined pIgR KO mice had ~2.5 fold greater numbers of B cells in their PP (**Figure 2.13 Circle 2**), suggesting enhanced B cell numbers detected previously in the intestinal lamina propria [34] are actually localized in the PP. Third, I determined pIgR KO mice also had ~2.5 fold greater numbers of macrophages and DC in their PP, suggesting larger PP, compared to WT B6 controls (**Figure 2.13 Circle 3**). Interestingly, subsets of the mononuclear phagocytes remained unchanged between mouse strains. Fourth, key M cell transcripts (i.e., Spi-B and GP2) were similar to controls, suggesting that M cell development is independent of SIg (**Figure 2.13 Circle 4**).

Analysis of host mRNA levels in the small intestinal ileum revealed that IFN-ɣ and iNOS were elevated in naïve and 9 hpi pIgR KO compared to WT B6 controls. Enhanced IFN-ɣ protein levels were also detected in naïve pIgR KO mice. MNV-1 infection reduced IFN-ɣ transcript levels after 9 hpi in pIgR KO mice. Previous studies have also reported enhanced inflammatory activation in conventional pIgR KO mice, resulting in lethal systemic hyperactivity [52], spontaneous COPD [53], and enhanced susceptibility to chemically-induced colitis [54].

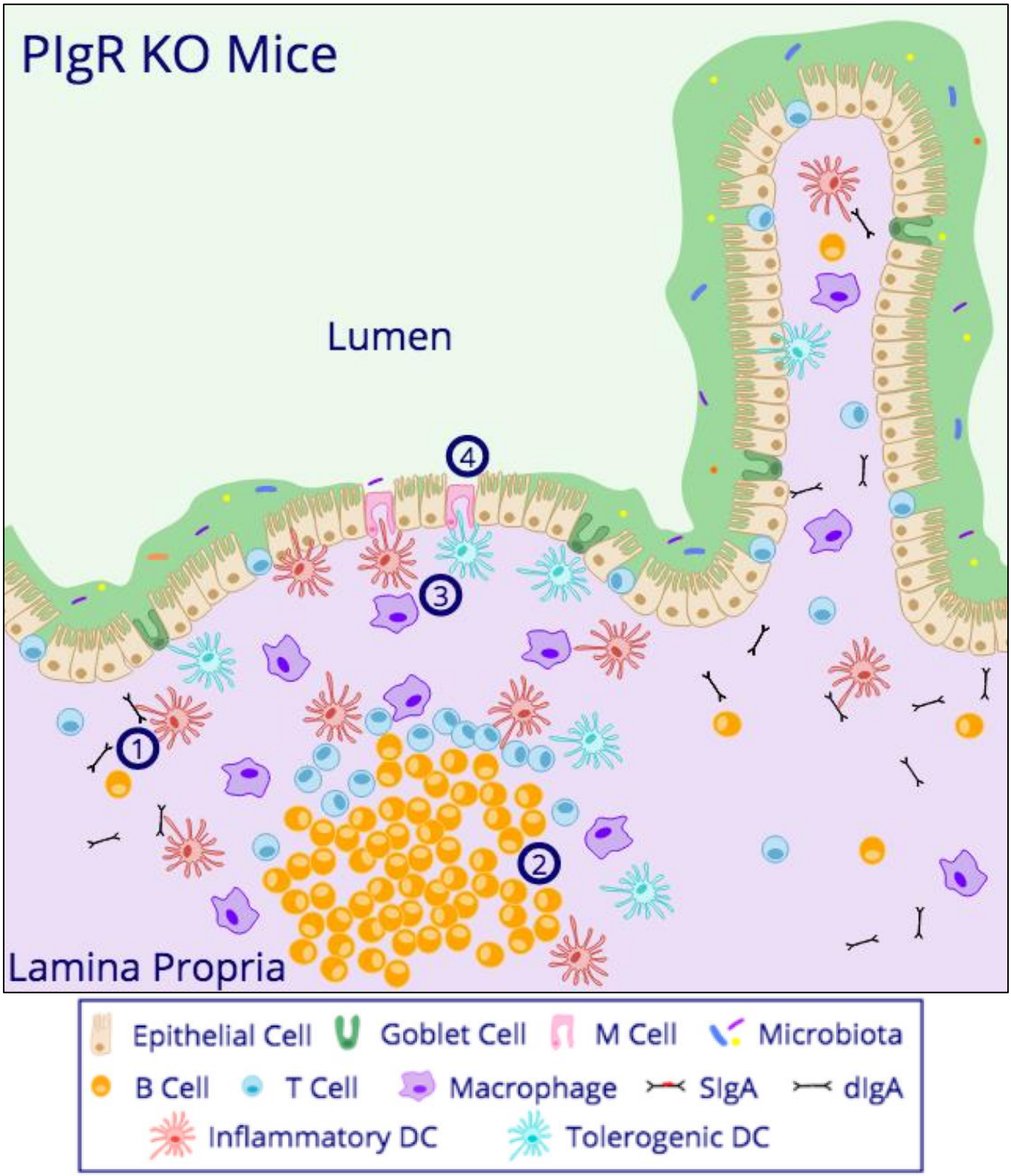

Figure 2.13: Small intestinal alterations I found in pIgR KO compared to WT B6. Diagram of small intestinal villi and PP from WT B6 (C57/Bl6) and pIgR KO mice. PIgR KO mice lack Sig in the intestinal lumen and as such exhibit enhanced serum IgA **(1)**. PIgR KO mice also have enhanced B cells **(2)**, macrophages, and dendritic cells **(3)** in the small intestine PP compared to WT B6 controls. However, M cell levels remain unchanged **(4)** in pIgR KO mice compared to controls.

These data point to a model in which reduced MNV-1 replication following oral infection is due to local immunological alterations at the FAE barrier in the absence of secretory immunoglobulins. We hypothesize pIgR KO specific enhancement of IFN-ɣ is mediated by microbial sensing, a hypothesis I will be testing in Chapter 3.

All positive-sense single stranded RNA viruses form replication complexes in the cytosol of infected cell to facilitate viral replication [23], and this process is disrupted during MNV infection by IFN-ɣ [32]. My data in addition to previously acknowledged anti-norovirus activity of IFN-ɣ [29, 32, 55], suggest that the reduced MNV-1 infection in pIgR KO mice is a direct result of enhanced levels of IFN-ɣ in the intestines of pIgR KO mice compared to WT B6 controls.

It has been shown that SIg localize in the outer mucus layer with bacteria, and that these interactions may limit bacterial access to the epithelial surface. Therefore, it is possible that without SIg, intestinal bacteria have enhanced access to the epithelial barrier contributing to the enhanced inflammatory cytokines found in conventional pIgR mice versus controls (see **Figure 2.10**). A thorough investigation of the mucus layer in the absence of SIg has been performed, and no difference in mucus thickness or bacterial localization was seen in pIgR KO compared to WT B6 mice [56]. These data suggest that the enhanced IFN-ɣ and iNOS found in naïve conventional pIgR KO mice is due to the immunomodulatory functions of SIg within the host interior.

A recent study determined that innate immune cell detection of serum IgA via the IgA receptor (FcαR1) in conjunction with pattern recognition receptor activation, resulted in a synergistic enhancement of pro-inflammatory cytokine production and release [57]. Additionally, FcαR1 engagement by CD103+ DCs has been shown to result in enhanced inflammatory cytokine release and promotion of pro-inflammatory T cell activation [58]. These

studies provide a possible explanation for the enhanced inflammatory molecules I observed in pIgR KO animals, as we (data not shown), and others [36, 37] have detected elevated serum IgA levels compared to WT B6 controls. I posit that enhanced serum IgA levels, coupled with altered bacterial communities and a lack of SIg sensing, may result in an improperly controlled immune response to enteric commensals in pIgR KO mice. Therefore, studies in Chapter 3 are aimed to dissect the role of the intestinal microbiota in the SIg-mediated enhancement of enteric virus infection.

Interestingly, the observed increase in inflammatory immune responses was not uniform, *i.e.*, elevated iNOS and IFN-ɣ levels in conventional pIgR KO mice, reduced IFN-β, and no change in transcript levels of other pro-and anti-inflammatory mediators (see **Figure 2.10**). The reason for this remains unclear. One potential explanation may come from the observed increases in the number of APC subsets (DCs, macrophages and B cells) in the PP of pIgR KO mice compared to WT B6 controls. These cell types have both FcαR1 and pathogen recognition receptors and are capable of pro-inflammatory cytokine secretion [57, 59-62]. Another potential source for the enhanced pro-inflammatory cytokines in pIgR KO mice may be intra-epithelial lymphocytes (IELs), which are enhanced in the small intestines of these mice [63, 64] and which upon activation exhibited more abundant IFN-ɣ secretion than WT B6 IELs [63]. Of note, activation of IELs via the T cell receptor in vivo resulted in significant reduction of MNV titers in the small intestine and MLN of WT B6 mice [65]. That study may point to a potential cell type that could mediate the antiviral activity in pIgR KO mice, but future studies are required to investigate this hypothesis.

Our study further highlights the importance of the intestinal cytokine milieu for optimal MNV pathogenesis. Recent findings suggest that MNV-1 induces lysis of infected cells via the

VP1 domain of the viral capsid. This inflammatory lytic cell death was found to be pro-viral as it results in recruitment of myeloid cells which in turn increases the local concentration of MNV susceptible cells[66]. However, our data demonstrates that MNV infection is reduced in pIgR KO mice (see **Figure 2.2**), despite elevated levels of inflammatory molecules (see **Figure 2.10**) and enhanced numbers of MNV target cells versus controls (see **Figure 2.8**).

IFN-ɣ has well-recognized anti-norovirus activity [29-33], and our findings provide direct evidence for IFN-ɣ mediated inhibition of MNV replication in vivo. IFN-ɣ treatment of small intestinal organoid cultures resulted in a marked increase in the inflammatory cytokines TNF-α, IL-1, and IL-6 as well as antimicrobial peptides [67]. IFN-ɣ treatment also enhanced reactive oxygen and nitrogen species [67] which is consistent with our findings in pIgR KO mice (see **Figure 2.10A-B**). Under both conditions of IFN-ɣ modulation, neutralization and addition, MNV-1 titers were altered in some regions of the intestine (see **Figure 2.12**). Interestingly, viral loads in intestinal segments were differentially affected by each treatment, which may be due to regionalization of the intestinal immune system [68]. Reovirus titers in the lower gastrointestinal tract were also reduced in pIgR KO mice compared to WT B6 controls, further emphasizing the role of pIgR in facilitation of enteric viral infection.

Taken together, these experiments demonstrate that contrary to other enteric pathogens, SIg do not protect from MNV or reovirus infection, but that instead the presence of pIgR and SIg promotes infection. Thus, both molecules are host factors that can have either anti- or pro-microbial functions depending on the pathogen. Lastly, our data further highlight that MNV and reovirus as enteric pathogens have optimized infection under conditions of intestinal homeostasis. When these conditions are perturbed, such as the absence of pIgR and SIg, virus

infection is compromised. In the future, it will be interesting to test whether this holds true for other enteric viral infections.

2.4 Materials & Methods

Animals. C57BL/6 mice were purchased from Jackson Laboratories (Bar Harbor, ME) and housed in SPF- and MNV-free conditions. A breeder pair of PIgR knockout mice on a C57BL/6 background (B6.129P2-*Pigr*^{tm1Fejo}/Mmmh, stock number: 030988-MU) was obtained from Drs. Stappenbeck and Virgin (Washington University, St. Louis, MO). All mice were bred and housed in SPF-, MNV-, and reovirus-free conditions. Age and sex matched experimental mice were used between 6 and 16 weeks of age. Mice used in the study were seronegative for anti-MNV antibodies by enzyme-linked immunosorbent assay (ELISA) as described previously [20]. Animal studies were performed in accordance with local and federal guidelines. The protocol was approved by the University of Michigan Committee on Use and Care of Animals (UCUCA number PRO00006658).

Viral Stocks. The plaque-purified MNV-1.CW3 (GV/MNV-1/2002/USA) virus stock (herein referred to as MNV-1) was generated as previously described [69]. A neutral red-labeled MNV-1 (MNV-1-NR) ($3.8x10^6$ PFU/mL), and MNV-CR3 stock (MNV-CR3-NR) ($3x10^6$ PFU/mL), were generated from MNV-1 and MNV-CR3 (GV/CR3/2005/USA) passage 6, as previously described [35]. MNV-1-NR and MNV-CR3-NR was handled in a darkened room using a red photolight (Premier OMNI) and stored in a light safe box at -80°C. To assess MNV-1-NR light inactivation, stocks of MNV-1-NR were exposed to white light or left in darkness and samples were taken

every 5 minutes to assess light mediated reduction in viral titer via plaque assay. Reovirus recombinant T1L stocks were generated with reovirus cDNAs in baby hamster kidney-T7 cells (a kind gift from Dr. Terence Dermody, University of Pittsburgh) [70, 71], followed by plaque purification, and passage in L929 cells [72].

Animal Infections. Mice were infected via oral gavage (o.g.) with 3.8 x 10^5 PFU MNV-1-NR or 2.6x10^5 PFU MNV-CR3-NR in 100 µl/mouse in a red light only room. For neutralizing antibody treatment of pIgR KO mice, 500 µg anti-IFN-ɣ antibody (rat IgG, clone XMG1.2, eBioscience), or isotype control (Rat IgG, clone HRPN, InVivoMab) were administered intraperitoneally 18 hours before MNV-1-NR infection. For IFN-ɣ treatment of B6 mice, 10^4 units IFN-ɣ (PeproTech) or equivalent weight bovine serum albumin fraction V (BSA) (Roche) was diluted in PBS, filtered with 0.22 micron filter (Fisher Scientific), and administered intraperitoneally 18 hours before MNV-1-NR infection. Mice were infected via o.g. with 3.8 x 10^5 PFU MNV-1-NR in 100 µl/mouse in a red light only room. Mice received intraperitoneal infection of 3.8 x 10^5 PFU MNV-1-NR in 100 µl/mouse in a red light only room. Tissues were harvested at 9, 18, or 48 hpi as previously described [17] with the following modifications: 2 cm of tissue was collected in pre-weighed tubes containing 1.0 mm diameter zirconia/silica beads (BioSpec), flash frozen in an ethanol/dry ice bath, weighed, and stored at -80°C. Mice were infected via o.g. with 2x10^6 PFU of reovirus T1L. Tissues were harvested at 24 hpi and processed as described for MNV, with the modification that 1 cm of tissue was collected.

Plaque Assay. Homogenized samples were exposed to white light for 30 min to inactivate input virus. Light exposure reduced MNV-1-NR titers by 3 logs. The plaque assay was performed as

previously described [73]. Reovirus viral titers of homogenized samples was determined by plaque assay as described previously using L929 cells [72]. Samples without detectable replicated virus were assigned 10 PFU/ml as the lowest detectable unit. Data were normalized to the tissue weight and expressed as PFU per gram of tissue. The sensitivity threshold was determined for each organ by averaging the PFU/gram tissue of all samples without detectable viral titers.

Intestinal Transit Assay. To measure intestinal transit time, mice were fasted for 18 h, gavaged orally with 100 ml 50 mg/ml Evans Blue solution prepared with 1% methylcellulose and euthanized 15 min later. The small intestine was divided into fifths and each piece was minced in 0.1 M sodium hydroxide, 6 mM N-acetylcysteine, sonicated, and the absorbance at 565 nm determined as previously described [74].

RNA Isolation. Total RNA was extracted from tissues using TRIzol® Reagent (ThermoFisher Scientific) following the manufacturers guidelines. Contaminating genomic DNA was removed by treating samples with Turbo DNA free DNase kit (ThermoFisher Scientific). Total RNA was quantified using a spectrophotometer (NanoDrop) and stored at -80°C.

Quantitative Real-Time PCR. To measure host cell transcripts, cDNA was generated with 100 μg of total RNA using iScript Reverse Transcription Supermix for RT-qPCR (Bio-Rad #1708841) in a thermocycler (Eppendorf Mastercycler Epgradient PCR machine) and stored at -20°C. cDNA was analyzed for levels of Gapdh [75], GP2 [75], Spi-B [75], interferon-gamma (IFN-ɣ) [76], interferon-beta (IFN-β) [76], tumor necrosis factor-alpha (TNF-α) [76], inducible

nitric oxide synthase (iNOS) [77], interferon stimulated gene 15 (ISG15) [78], transforming growth factor-beta (TGF-β) [79], interleukin-10 (IL-10) [80], interferon-lambda (IFN-λ) [78] in a Biorad CFX96 Real Time System qPCR machine using Sso Advanced Universal SYBR Green Supermix (Bio-Rad). Gene expression was normalized to transcript levels of the endogenous host gene *Gapdh*, and fold change was calculated relative to WT B6 controls using the delta delta CT method [81]. Quantification of MNV-1 genome equivalents in host tissue was performed as previously described [69].

MNV-1 Neutralization assay. MNV-1 ($2.8x10^7$ PFU) was pre-incubated with 0.25 mg/ml recombinant SIgA [82] or 0.25 mg/mL bovine serum albumin fraction V (Roche) diluted in 1x PBS for 1 hour in 37°C water bath, and neutralization was assessed via plaque assay.

Ligated Intestinal Loops and Controls. To test the effect of dithiothreitol (DTT) on virus attachment, $5x10^5$ RAW264.7 cells were plated per well in 6 well tissue culture treated plates (Corning) and incubated at 37°C. After overnight attachment, cells were exposed to MNV-1 for one hour on ice to allow virus to attach. Unbound virus was washed away, and cells were incubated for 15 min with 0, 1, or 5 mM DTT (Sigma-Aldrich) in 1x PBS (Gibco) at 37°C. Cells were frozen at -80°C after washing, RNA was isolated, and MNV-1 genome copies were determined via RT-qPCR as described above.

For ligated intestinal loop studies, mice were anesthetized and placed on a 37°C heating pad. A ~2 cm section of the ileum was tied gently on either side of a PP using silk surgical suture thread. Approximately 0.1 ml MNV-1 ($6.7x10^7$ PFU/mL) was injected as the loop was closed. The PP was excised 25 or 40 min later. Mucus was removed by a 10 min incubation with 5 mM

DTT (Sigma-Aldrich) in 1x phosphate buffered saline (PBS) (Gibco) in a 37°C water bath. The FAE was removed by shaking the PP at 250 rpm (MaxQ 600, Thermo Scientific) for 20 min in 1x PBS containing 5 mM EDTA (Fluka Analytical) and washed twice with 1x PBS. Disassociation of the FAE from the lamina propria was confirmed via flow cytometry using Ep-CAM (diluted 1:50, clone G8.8, PE, Biolegend). Ep-CAM negative cells (i.e. PP lamina propria) were washed twice with 1x PBS by gently inverting the tubes. Cells were placed in 500 μl RNALater (Sigma) and stored at -80°C.

For SIgA:MNV complex formation, MNV-1 ($2.8x10^7$ PFU) was pre-incubated with 0.25 mg/ml recombinant SIgA [82] or 0.25 mg/ml bovine serum albumin fraction V (Roche) diluted in 1x PBS for 1 hour at 37°C before adding to the loop and treated as described above.

Tissue Digestion/ Flow Cytometry. PP and small intestine lamina propria were dissected from naive PIgR KO and WT B6 mice and digested as previously described [42]. $2x10^6$ cells were then used for flow cytometric analysis. Viable cells were identified (Invitrogen Live/Dead fixable Aqua Dead Cell stain Kit) and then stained for the following surface markers: CD45 (diluted 1:200, clone 30-F11, AF700, Biolegend), I-A/I-E (diluted 1:50, clone M5/114.15.2, PE/Dazzle 594, Biolegend), CD19 (diluted 1:50, clone 6D5, PerCP/Cy5.5, Biolegend), CD11b (diluted 1:50, clone M1/70 APC/Cy7, Biolegend), CD64 (diluted 1:50, clone X54-5/7.1 FITC, Biolegend) CD11c (diluted 1:50, clone N418 PE/Cy7, Biolegend) CD103 (diluted 1:25, clone 2EZ, APC, Biolegend), CX3CR1 (diluted 1:50, clone SA011F11, PE, Biolegend), CD8 (diluted 1:100, clone 53-6.7, APC-Cy7 Biolegend). All antibodies were diluted in FACS buffer; 5% fetal bovine serum (Hyclone) and 0.1% sodium azide (Sigma) in 1x PBS, for 30 min on ice. After surface staining, cells were fixed for 10 min on ice using Cytofix/Cytoperm (BD Biosciences),

washed and fluorescence was analyzed with a BD LSRfortessa. Data was analyzed using FlowJo software (BD Biosciences) using the following gating strategy: live cells, CD45 and I-A/I-E (MHCII) positive APC were characterized into B cells (CD19+) and mononuclear phagocytes (CD19-/CD11b+), which were further delineated into macrophages (CD64+/CD11c-) and DCs (CD64-/CD11c+).

Expression and Purification of proteins. MNV-1 capsid protein protruding (P) and shell (S) domains were bacterially expressed, and recombinant proteins purified as previously described [83]. Recombinant, rotavirus-specific mouse SIgA, IgA dimer, or secretory component were expressed and purified as described [84].

Isolation, and Infection of Bone Marrow Derived Macrophages and Intestinal Cells. In a sterile biological safety cabinet, the hind legs and small intestines of pIgR KO and WT B6 mice were harvested. Hind legs were kept whole in BM20 media (10 % low endotoxin FCS (Gibco), 20 % L929-cell Supernatant harvested as described previously [49], 5 % Horse Serum (Gibco), 1 % L/glutamine (Gibco), 1 % sodium pyruvate (Gibco), 1 % Penicillin Streptomycin (Gibco), in low endotoxin DMEM (Gibco)) on ice until femurs were harvested. Femurs were isolated from the tissue of the hind leg and cut at the ends to expose the marrow. Bone marrow was flushed out using a 26 gauge needle (Fisher Scientific) attached to a 10 ml syringe (Fisher Scientific) with 5 ml BM20 media per femur. Bone marrow was collected in a 50 ml conical tube (Falcon), and after thorough mixing cells were counted and plated into non-TC treated 10 cm plates (Fisher Scientific) at a density of $1x10^7$ cells per dish in 10 ml BM20. Cells were incubated at 37°C and 10 ml BM20 was added 4 days later. After 7 days total incubation, medium was removed, and

cells are washed with 5 ml ice-cold low endotoxin PBS (Gibco). 2 ml of ice-cold low endotoxin PBS with 0.02% EDTA (Fisher Scientific) was added and the cells were incubated at 4°C for 10 minutes to aid in detachment. Cells were dislodged via gentle pipetting, pooled for each mouse, and counted. Cells were plated into 12 well TC plates (Corning) at a density of $2.5x10^6$ cells per well and were allowed to adhere incubating overnight at 37°C. Small intestines and Peyer's patches were digested as described above for flow cytometry [42]. Cells were counted and plated into non-TC treated 10 cm plates (Fisher Scientific) at a density of $1x10^7$ per dish in 10 ml intestinal macrophage media (10% FBS (Corning), 1mM HEPES (Gibco), 50mM b-mercaptoethanol (Gibco), 2mM L-glutamine (Gibco), 1mM Sodium Pyruvate (Gibco), 1% Penicillin Streptomycin (Gibco), and 1% MEM-non-essential amino acids (Gibco), In RPMI (Gibco)). Cells were allowed to adhere overnight. For infection, media was removed, and cells were infected with MNV-1 at a MOI of 5 for one hour on ice. Once virus inoculum was washed away, fresh media was added, and cells were incubated at 37°C for 0, 24, or 48 hours before being frozen at -80°C. Cells were thawed and frozen again and viral titers were determined by plaque assay.

Statistical Analysis. Unless otherwise stated, data were analyzed using Mann Whitney U test with GraphPad Prism software version 7 (GraphPad Software, La Jolla, CA). *= $P<0.05$. **= $P<0.01$ ***= $P<0.001$. ****= $P<0.0001$. ns= not significant.

2.5 Acknowledgements

I am indebted to Dr. Thaddeus Stappenbeck (Washington University, St. Louis, MO) for the generous gift of pIgR KO breeders, Dr. Blaise Corthesy for the recombinant SIgA (University

State Hospital (CHUV), Lausanne, Switzerland), and Dr. Gary Huffnagle (University of Michigan, Ann Arbor, MI) for the anti-IFN-ɣ serum.

2.6 References

1. Kaetzel, C.S., *Cooperativity among secretory IgA, the polymeric immunoglobulin receptor, and the gut microbiota promotes host-microbial mutualism.* Immunol Lett, 2014. **162**(2 Pt A): p. 10-21.
2. Corthesy, B., *Secretory immunoglobulin A: well beyond immune exclusion at mucosal surfaces.* Immunopharmacol Immunotoxicol, 2009. **31**(2): p. 174-9.
3. Gorrell, R.J., et al., *Contribution of secretory antibodies to intestinal mucosal immunity against Helicobacter pylori.* Infect Immun, 2013. **81**(10): p. 3880-93.
4. Davids, B.J., et al., *Polymeric immunoglobulin receptor in intestinal immune defense against the lumen-dwelling protozoan parasite Giardia.* J Immunol, 2006. **177**(9): p. 6281-90.
5. Wijburg, O.L., et al., *Innate secretory antibodies protect against natural Salmonella typhimurium infection.* J Exp Med, 2006. **203**(1): p. 21-6.
6. Johnston, P.F., D.N. Gerding, and K.L. Knight, *Protection from Clostridium difficile infection in CD4 T Cell- and polymeric immunoglobulin receptor-deficient mice.* Infect Immun, 2014. **82**(2): p. 522-31.
7. Corthesy, B., *Roundtrip ticket for secretory IgA: role in mucosal homeostasis?* J Immunol, 2007. **178**(1): p. 27-32.
8. Mantis, N.J., et al., *Selective adherence of IgA to murine Peyer's patch M cells: evidence for a novel IgA receptor.* J Immunol, 2002. **169**(4): p. 1844-51.
9. Rey, J., et al., *Targeting of secretory IgA to Peyer's patch dendritic and T cells after transport by intestinal M cells.* J Immunol, 2004. **172**(5): p. 3026-33.
10. Mantis, N.J., N. Rol, and B. Corthesy, *Secretory IgA's complex roles in immunity and mucosal homeostasis in the gut.* Mucosal Immunol, 2011. **4**(6): p. 603-11.
11. Bartsch, S.M., et al., *Global Economic Burden of Norovirus Gastroenteritis.* PLoS One, 2016. **11**(4): p. e0151219.
12. Hall, A.J., et al., *Norovirus disease in the United States.* Emerg Infect Dis, 2013. **19**(8): p. 1198-205.
13. Karst, S.M., et al., *Advances in norovirus biology.* Cell Host Microbe, 2014. **15**(6): p. 668-80.
14. Wobus, C.E., L.B. Thackray, and H.W.t. Virgin, *Murine norovirus: a model system to study norovirus biology and pathogenesis.* J Virol, 2006. **80**(11): p. 5104-12.
15. Karst, S.M. and C.E. Wobus, *Viruses in Rodent Colonies: Lessons Learned from Murine Noroviruses.* Annu Rev Virol, 2015. **2**(1): p. 525-48.
16. Karst, S.M., et al., *STAT1-dependent innate immunity to a Norwalk-like virus.* Science, 2003. **299**(5612): p. 1575-8.
17. Gonzalez-Hernandez, M.B., et al., *Efficient norovirus and reovirus replication in the mouse intestine requires microfold (M) cells.* J Virol, 2014. **88**(12): p. 6934-43.

18. Mumphrey, S.M., et al., *Murine norovirus 1 infection is associated with histopathological changes in immunocompetent hosts, but clinical disease is prevented by STAT1-dependent interferon responses.* J Virol, 2007. **81**(7): p. 3251-63.
19. Grau, K.R., et al., *The major targets of acute norovirus infection are immune cells in the gut-associated lymphoid tissue.* Nat Microbiol, 2017. **2**(12): p. 1586-1591.
20. Wobus, C.E., et al., *Replication of Norovirus in cell culture reveals a tropism for dendritic cells and macrophages.* PLoS Biol, 2004. **2**(12): p. e432.
21. Jones, M.K., et al., *Enteric bacteria promote human and mouse norovirus infection of B cells.* Science, 2014. **346**(6210): p. 755-9.
22. Gonzalez-Hernandez, M.B., et al., *Murine norovirus transcytosis across an in vitro polarized murine intestinal epithelial monolayer is mediated by M-like cells.* J Virol, 2013. **87**(23): p. 12685-93.
23. Karst, S.M. and C.E. Wobus, *A working model of how noroviruses infect the intestine.* PLoS Pathog, 2015. **11**(2): p. e1004626.
24. Wolf, J.L., et al., *Intestinal M cells: a pathway for entry of reovirus into the host.* Science, 1981. **212**(4493): p. 471-2.
25. Jones, M.K., et al., *Human norovirus culture in B cells.* Nat Protoc, 2015. **10**(12): p. 1939-47.
26. Baldridge, M.T., H. Turula, and C.E. Wobus, *Norovirus Regulation by Host and Microbe.* Trends Mol Med, 2016. **22**(12): p. 1047-1059.
27. Kuss, S.K., et al., *Intestinal microbiota promote enteric virus replication and systemic pathogenesis.* Science, 2011. **334**(6053): p. 249-52.
28. Schwartz-Cornil, I., et al., *Heterologous protection induced by the inner capsid proteins of rotavirus requires transcytosis of mucosal immunoglobulins.* J Virol, 2002. **76**(16): p. 8110-7.
29. Changotra, H., et al., *Type I and type II interferons inhibit the translation of murine norovirus proteins.* J Virol, 2009. **83**(11): p. 5683-92.
30. Maloney, N.S., et al., *Essential cell-autonomous role for interferon (IFN) regulatory factor 1 in IFN-gamma-mediated inhibition of norovirus replication in macrophages.* J Virol, 2012. **86**(23): p. 12655-64.
31. Biering, S.B., et al., *Viral Replication Complexes Are Targeted by LC3-Guided Interferon-Inducible GTPases.* Cell Host Microbe, 2017. **22**(1): p. 74-85 e7.
32. Hwang, S., et al., *Nondegradative role of Atg5-Atg12/ Atg16L1 autophagy protein complex in antiviral activity of interferon gamma.* Cell Host Microbe, 2012. **11**(4): p. 397-409.
33. Nice, T.J., B.A. Robinson, and J.A. Van Winkle, *The Role of Interferon in Persistent Viral Infection: Insights from Murine Norovirus.* Trends Microbiol, 2018. **26**(6): p. 510-524.
34. Uren, T.K., et al., *Role of the polymeric Ig receptor in mucosal B cell homeostasis.* J Immunol, 2003. **170**(5): p. 2531-9.
35. Gonzalez-Hernandez, M.B., J.W. Perry, and C.E. Wobus, *Neutral Red Assay for Murine Norovirus Replication and Detection in a Mouse.* Bio Protoc, 2013. **3**(7).
36. Johansen, F.E., et al., *Absence of epithelial immunoglobulin A transport, with increased mucosal leakiness, in polymeric immunoglobulin receptor/secretory component-deficient mice.* J Exp Med, 1999. **190**(7): p. 915-22.

37. Shimada, S., et al., *Generation of polymeric immunoglobulin receptor-deficient mouse with marked reduction of secretory IgA.* J Immunol, 1999. **163**(10): p. 5367-73.
38. Mabbott, N.A., et al., *Microfold (M) cells: important immunosurveillance posts in the intestinal epithelium.* Mucosal Immunol, 2013. **6**(4): p. 666-77.
39. Kolawole, A.O., et al., *Norovirus Escape from Broadly Neutralizing Antibodies Is Limited to Allostery-Like Mechanisms.* mSphere, 2017. **2**(5).
40. Li, X. and H. Chen, *Evaluation of the porcine gastric mucin binding assay for high-pressure-inactivation studies using murine norovirus and tulane virus.* Appl Environ Microbiol, 2015. **81**(2): p. 515-21.
41. Horsley, A., et al., *Reassessment of the importance of mucins in determining sputum properties in cystic fibrosis.* J Cyst Fibros, 2014. **13**(3): p. 260-6.
42. Geem, D., et al., *Isolation and characterization of dendritic cells and macrophages from the mouse intestine.* J Vis Exp, 2012(63): p. e4040.
43. Persson, E.K., et al., *Dendritic cell subsets in the intestinal lamina propria: ontogeny and function.* Eur J Immunol, 2013. **43**(12): p. 3098-107.
44. Cerutti, A., *The regulation of IgA class switching.* Nat Rev Immunol, 2008. **8**(6): p. 421-34.
45. Karupiah, G., et al., *Inhibition of viral replication by interferon-gamma-induced nitric oxide synthase.* Science, 1993. **261**(5127): p. 1445-8.
46. Saura, M., et al., *An antiviral mechanism of nitric oxide: inhibition of a viral protease.* Immunity, 1999. **10**(1): p. 21-8.
47. Persichini, T., et al., *Nitric oxide inhibits the HIV-1 reverse transcriptase activity.* Biochem Biophys Res Commun, 1999. **258**(3): p. 624-7.
48. Samuel, C.E., *Antiviral actions of interferons.* Clin Microbiol Rev, 2001. **14**(4): p. 778-809, table of contents.
49. Trouplin, V., et al., *Bone marrow-derived macrophage production.* J Vis Exp, 2013(81): p. e50966.
50. Kaetzel, C.S., *The polymeric immunoglobulin receptor: bridging innate and adaptive immune responses at mucosal surfaces.* Immunol Rev, 2005. **206**: p. 83-99.
51. Corthesy, B., et al., *Rotavirus anti-VP6 secretory immunoglobulin A contributes to protection via intracellular neutralization but not via immune exclusion.* J Virol, 2006. **80**(21): p. 10692-9.
52. Karlsson, M.R., et al., *Hypersensitivity and oral tolerance in the absence of a secretory immune system.* Allergy, 2010. **65**(5): p. 561-70.
53. Richmond, B.W., et al., *Airway bacteria drive a progressive COPD-like phenotype in mice with polymeric immunoglobulin receptor deficiency.* Nat Commun, 2016. **7**: p. e11240.
54. Murthy, A.K., et al., *Contribution of polymeric immunoglobulin receptor to regulation of intestinal inflammation in dextran sulfate sodium-induced colitis.* J Gastroenterol Hepatol, 2006. **21**(9): p. 1372-80.
55. Biering, S.B., et al., *Viral Replication Complexes Are Targeted by LC3-Guided Interferon-Inducible GTPases.* Cell Host Microbe, 2017. **22**(1): p. 74-85.e7.
56. Rogier, E.W., et al., *Secretory IgA is Concentrated in the Outer Layer of Colonic Mucus along with Gut Bacteria.* Pathogens, 2014. **3**(2): p. 390-403.

57. Hansen, I.S., et al., *Serum IgA Immune Complexes Promote Proinflammatory Cytokine Production by Human Macrophages, Monocytes, and Kupffer Cells through FcalphaRI-TLR Cross-Talk.* J Immunol, 2017. **199**(12): p. 4124-4131.
58. Hansen, I.S., et al., *FcalphaRI co-stimulation converts human intestinal CD103(+) dendritic cells into pro-inflammatory cells through glycolytic reprogramming.* Nat Commun, 2018. **9**(1): p. 863.
59. Sakamoto, N., et al., *A novel Fc receptor for IgA and IgM is expressed on both hematopoietic and non-hematopoietic tissues.* Eur J Immunol, 2001. **31**(5): p. 1310-6.
60. Otten, M.A., et al., *Inefficient antigen presentation via the IgA Fc receptor (FcalphaRI) on dendritic cells.* Immunobiology, 2006. **211**(6-8): p. 503-10.
61. Munder, M., et al., *Murine macrophages secrete interferon gamma upon combined stimulation with interleukin (IL)-12 and IL-18: A novel pathway of autocrine macrophage activation.* J Exp Med, 1998. **187**(12): p. 2103-8.
62. Cherdantseva, L.A., et al., *Association of Helicobacter pylori and iNOS production by macrophages and lymphocytes in the gastric mucosa in chronic gastritis.* J Immunol Res, 2014. **2014**: p. 762514.
63. Kato-Nagaoka, N., et al., *Enhanced differentiation of intraepithelial lymphocytes in the intestine of polymeric immunoglobulin receptor-deficient mice.* Immunology, 2015. **146**(1): p. 59-69.
64. Yamazaki, K., et al., *Accumulation of intestinal intraepithelial lymphocytes in association with lack of polymeric immunoglobulin receptor.* Eur J Immunol, 2005. **35**(4): p. 1211-9.
65. Swamy, M., et al., *Intestinal intraepithelial lymphocyte activation promotes innate antiviral resistance.* Nat Commun, 2015. **6**: p. 7090.
66. Jacob A. Van Winkle, B.A.R., A. Mack Peters, Lena Li, Ruth V. Nouboussi, Matthias Mack,vTimothy J. Nice, *Persistence of Systemic Murine Norovirus Is Maintained by Inflammatory Recruitment of Susceptible Myeloid Cells.* Cell Host & Microbe, 2018.
67. Price, A.E., et al., *A Map of Toll-like Receptor Expression in the Intestinal Epithelium Reveals Distinct Spatial, Cell Type-Specific, and Temporal Patterns.* Immunity, 2018. **49**(3): p. 560-575.e6.
68. Mowat, A.M. and W.W. Agace, *Regional specialization within the intestinal immune system.* Nat Rev Immunol, 2014. **14**(10): p. 667-85.
69. Taube, S., et al., *Murine noroviruses bind glycolipid and glycoprotein attachment receptors in a strain-dependent manner.* J Virol, 2012. **86**(10): p. 5584-93.
70. Kobayashi, T., et al., *A plasmid-based reverse genetics system for animal double-stranded RNA viruses.* Cell Host Microbe, 2007. **1**(2): p. 147-57.
71. Boehme, K.W., et al., *Reverse genetics for mammalian reovirus.* Methods, 2011. **55**(2): p. 109-13.
72. Virgin, H.W.t., et al., *Antibody protects against lethal infection with the neurally spreading reovirus type 3 (Dearing).* J Virol, 1988. **62**(12): p. 4594-604.
73. Gonzalez-Hernandez, M.B., J. Bragazzi Cunha, and C.E. Wobus, *Plaque assay for murine norovirus.* J Vis Exp, 2012(66): p. e4297.
74. Bagyanszki, M., et al., *Chronic alcohol consumption affects gastrointestinal motility and reduces the proportion of neuronal NOS-immunoreactive myenteric neurons in the murine jejunum.* Anat Rec (Hoboken), 2010. **293**(9): p. 1536-42.

75. Wood, M.B., D. Rios, and I.R. Williams, *TNF-alpha augments RANKL-dependent intestinal M cell differentiation in enteroid cultures.* Am J Physiol Cell Physiol, 2016. **311**(3): p. C498-507.
76. Mohanty, S.K., et al., *Loss of interleukin-12 modifies the pro-inflammatory response but does not prevent duct obstruction in experimental biliary atresia.* BMC Gastroenterol, 2006. **6**: p. 14.
77. Stoolman, J.S., et al., *Latent infection by gammaherpesvirus stimulates profibrotic mediator release from multiple cell types.* Am J Physiol Lung Cell Mol Physiol, 2011. **300**(2): p. L274-85.
78. Lopusna, K., et al., *Murine gammaherpesvirus targets type I IFN receptor but not type III IFN receptor early in infection.* Cytokine, 2016. **83**: p. 158-170.
79. Henderson, N.C., et al., *Galectin-3 regulates myofibroblast activation and hepatic fibrosis.* Proc Natl Acad Sci U S A, 2006. **103**(13): p. 5060-5.
80. Terashima, A., et al., *A novel subset of mouse NKT cells bearing the IL-17 receptor B responds to IL-25 and contributes to airway hyperreactivity.* J Exp Med, 2008. **205**(12): p. 2727-33.
81. Higgins, P.D., et al., *Transient or persistent norovirus infection does not alter the pathology of Salmonella typhimurium induced intestinal inflammation and fibrosis in mice.* Comp Immunol Microbiol Infect Dis, 2011. **34**(3): p. 247-57.
82. Crottet, P., et al., *Covalent homodimers of murine secretory component induced by epitope substitution unravel the capacity of the polymeric Ig receptor to dimerize noncovalently in the absence of IgA ligand.* J Biol Chem, 1999. **274**(44): p. 31445-55.
83. Taube, S., et al., *High-resolution x-ray structure and functional analysis of the murine norovirus 1 capsid protein protruding domain.* J Virol, 2010. **84**(11): p. 5695-705.
84. Crottet, P., S. Cottet, and B. Corthesy, *Expression, purification and biochemical characterization of recombinant murine secretory component: a novel tool in mucosal immunology.* Biochem J, 1999. **341 (Pt 2)**: p. 299-306.

Chapter 3: Results

Bacterial Modulation of Norovirus Infection

The text presented in this chapter was published in Viruses, Volume 10, Issue 5, Pages 237-252; 2018 and Trends in Molecular Medicine, Volume 22, Issue 12, Pages 1047-1059; 2016. Some text and figures presented in this chapter were published as a “Spotlight” article of significant interest in The Journal of Virology 92:e00826-18. https://doi.org/10.1128/JVI.00826-18

3.1 Introduction

Overlying the epithelial barrier, in the lumen of the gastrointestinal tract is a mucus layer that is continuously replenished by goblet cells [1]. The mucus layer acts as a barrier, reducing microbial access to the epithelial surface. New mucus is continually produced, and intestinal microbes get sloughed off with the old layer. Bacteria exist within the mucus layer of the

small intestine. In the large intestine they are only present in the thick, loose outer mucus layer while the thinner inner layer remains relatively sterile. Bacterial products however are capable of diffusing through the mucus layer, and epithelial cell sensing of bacterial products through microbe-associated molecular pattern receptors stimulates cells of the epithelial barrier to produce mucus and anti-microbial peptides, and to express the polymeric immunoglobulin receptor (pIgR) on the basolateral surface of the epithelial barrier [2, 3].

PIgR shuttles immunoglobulins into the intestinal lumen through epithelial cells to form secretory immunoglobulins (SIg) and secretory component (SC) [2]. SIg and SC directly bind to intestinal microbiota through receptor- and carbohydrate-mediated interactions [2]. This binding aids in regulation of bacterial species at mucosal surfaces and is an important aspect of mucosal defense [4]. Transcytotic microfold cells within the follicle-associated epithelium take up the luminal SIg:bacteria immune complexes and translocate them into the intestinal lamina propria [5]. Immediately underlying the microfold cells are dendritic cells which sample the SIg immune complexes [6] resulting in production of anti-inflammatory mediators IL-10 and TGF-β and T regulatory cell differentiation, which contribute to tolerance and intestinal homeostasis [7].

Intestinal bacteria have many beneficial functions for the host, beyond tolerance induction including digestion of insoluble fibers. Bacteria are able to process these fibers into forms in which we can digest and extract nutrients from, aiding in nutrient consumption and energy absorption [8]. Intestinal commensal bacteria can also protect the host from infection by occupying certain physical and nutritional niches within the intestinal lumen, and utilization of these nutrients prevents colonization by pathogenic bacteria [9]. Furthermore, several bacterial species produce antibiotics that may directly prevent abundant colonization of harmful species

[10]. Bacteria have also been shown to modulate viral infections [11], including norovirus [12, 13].

Both HNoVs and MNVs have been reported to bind carbohydrate moieties [14-18], including sialic acid residues which are widely expressed on bacteria [19]. One such group of carbohydrate residues, histo-blood group antigens (HBGAs), are attachment factors that facilitate binding of some caliciviruses to cells [20-22]. To date, a direct interaction of HNoV capsids with members of the microbiota is known for a few commensal (e.g., Enterobacter cloacae) and pathogenic (e.g., Clostridium difficile) bacterial species [22, 23]. However, more direct norovirus:bacteria interaction pairs are sure to be uncovered over time.

Experimentally induced bacterial dysbiosis has been shown to alter MNV infection. For instance, pretreatment of mice with an antibiotic cocktail of vancomycin, ampicillin, metronidazole, and neomycin reduces acute MNV- 1 titers [12] and reduces or prevents infection by persistent MNV strains MNV-3 and MNV-CR6, respectively [12, 13]. Importantly, MNV-CR6 viral loads are restored with a fecal transplant from untreated to antibiotic-treated animals [13]. Although antibiotic treatment reduces intestinal MNV titers, it is not an advisable treatment option for HNoV infections, given the overall beneficial impact of the microbiota on human health [24]. At the cellular level, co-infection of macrophages with MNV and various bacteria has been shown to reduce viral titers, likely stemming from bacterial triggering of innate immune responses, while at the same time fostering bacterial growth through MNV-induced inhibition of inflammatory cytokines [25-27].

Although not universally seen, both HNoV and MNV can alter host gut microbial communities under certain conditions. This dysbiosis typically results in an enhanced bacterial *Firmicutes*-to-*Bacteroidetes* (F/B) ratio, an alteration also linked to liver fibrosis and obesity [28,

29]. A subset (20%) of HNoV-infected individuals exhibited enhanced F/B ratios [30], while MNV-1 enhanced F/B ratios in C57BL/6 mice at Day 5 post infection [31]. However, longitudinal analyses of both C57BL/6 mice infected with MNV-1, or MNV-CR6, and Swiss Webster mice infected with MNV-1, or MNV-4 failed to detect MNV-induced dysbiosis of gastrointestinal bacteria at the phylum level [32]. A reduction in intestinal *Lactobacillus* strains occurred in MNV-1-infected ICR mice, with a concurrent increase in Proteobacteria delta, mirroring findings from HNoV [32].

SIg and SC are highly glycosylated [33], as such we hypothesized that MNV would associate with SIg in the intestinal lumen and this interaction would modulate MNV infection. To investigate this further, mice lacking SIg due to a deficiency in pIgR (pIgR KO) were used in studies described in Chapter 2. Briefly, I determined that MNV-1 viral loads were reduced in the gastrointestinal tract of pIgR KO mice compared to C57BL/6 controls (WT B6) (see **Figure 2.2**), despite equal access to, and enhanced numbers of MNV target cells (DCs, macrophages, and B cells) in the PP of pIgR KO mice (see **Figure 2.7** and **2.8**). Instead, I found that compared to WT B6 mice, naive pIgR KO mice had enhanced levels of interferon gamma (IFN-ɣ) (see **Figure 2.10**), a cytokine known to inhibit MNV replication [34-38]. Neutralization of IFN-ɣ in pIgR KO mice, or addition of IFN-ɣ to WT B6 mice enhanced and reduced MNV-1 viral loads respectively (see **Figure 2.12**). Taken together, my findings in Chapter 2 support a model whereby immune cell sensing of SIg downmodulates antiviral cytokine levels, thereby promoting enteric viral infection. Although it is clear that IFN-ɣ is capable of modulating MNV infection, the inducer of the enhanced IFN-ɣ in pIgR KO mice remained unexplored. Given that SIg-mediated bacterial sensing results in tolerogenic immune responses [4], I hypothesized that

altered bacterial sensing due to lack of SIg in pIgR KO mice resulted in enhanced IFN-ɣ and reduced MNV infection compared to WT B6 mice.

To determine if altered bacterial sensing resulted in enhanced IFN-ɣ levels seen in the absence of SIg, I modulated intestinal microbial communities in pIgR KO, B6, and Swiss Webster mice and determined the effect on MNV infection. I found that, in the absence of intestinal microbiota, lack of secretory immunoglobulins no longer enhance baseline IFN-ɣ levels as was seen in conventionally housed mice. Despite similar baseline levels, germ-free pIgR KO mice had enhanced anti-MNV responses; exhibiting more IFN-ɣ protein, and enhanced mRNA levels of interferon stimulated gene-15 (ISG15) after MNV-1 infection than germ-free controls. Despite the upregulated anti-MNV response germ-free pIgR KO mice, MNV-1 replication in the gastrointestinal tract was equivalent to that of germ-free controls at 18 hpi. I also determined that intestinal microbiota alter MNV-1 and MNV-CR3 intestinal regionalization, and this regionalization may not be explained by access to and availability of MNV target cells. Taken together, these data point to a model in which intestinal bacteria modulate MNV intestinal regionalization, and indirectly modulate the local microenvironment to favor MNV infection through SIg-mediated microbial sensing.

3.2 Results

3.2A Intestinal Microbial Communities Are Altered in PIgR KO Mice

Alterations in the intestinal microbiota in the absence of SIg, coupled with the lack of SIg sensing by intestinal immune cells, may skew immune activation and account for the upregulation of IFN-ɣ and iNOS seen in naive pIgR KO mice compared to controls (see **Figure 2.10**). Previous reports regarding microbial alterations in the gastrointestinal tract of pIgR KO

mice are conflicting [39, 40]. Therefore, I sterilely collected feces and luminal contents as well as intestinal mucosa tissue from the ileum and cecum of naïve pIgR KO and WT B6 mice originating from the same breeding locations as used in the infection experiments in Chapter 2. With the help of Christine Bassis and the UM Microbiome and Metabolomics Core, I determined the microbial composition of the ileal contents, ileum, cecal contents, cecum, and feces via 16S rRNA gene sequencing. Intestinal microbial community differences were assessed via analysis of molecular variance (AMOVA), and overall alpha-diversity of the microbial community was assessed via inverse Simpson analysis (invsimpson).

PIgR KO mice had equivalent diversity as compared by invsimpson analysis in their ileal contents compared to naïve WT B6 mice, but exhibited enhanced *Firmicutes* populations including *Clostridiales*, *Lactobacillus*, and *Erysipelotrichaceae* species resulting in significantly altered microbial communities by AMOVA (**Figures 3.1A-B**). The ileum lamina propria of pIgR KO mice was less diverse than the lumen by invsimpson analysis, however microbial communities were still significantly altered compared to WT B6 mice, again exhibiting enhanced *Erysipelotrichaceae* species colonization (**Figures 3.1C-D**). The microbial communities present in the cecal contents, cecum (including the cecal patch), and feces of pIgR KO mice were also significantly altered by AMOVA and more diverse by invsimpson analysis compared to WT B6 communities and showed enhancement in the *Firmicutes* species (*Clostridiales*, *Lactobacillus*, and *Erysipelotrichaceae*) also found in pIgR KO ileal contents (**Figures 3.1E-J**). The microbial community in the cecum had the highest diversity by invsimpson analysis, more than the cecal contents. Interestingly, WT B6 mice also had significant differences in microbial communities based on breeding room for all locations tested. However, differences between WT B6 and pIgR KO mice were much greater than differences among WT B6 mice. The microbial communities

A

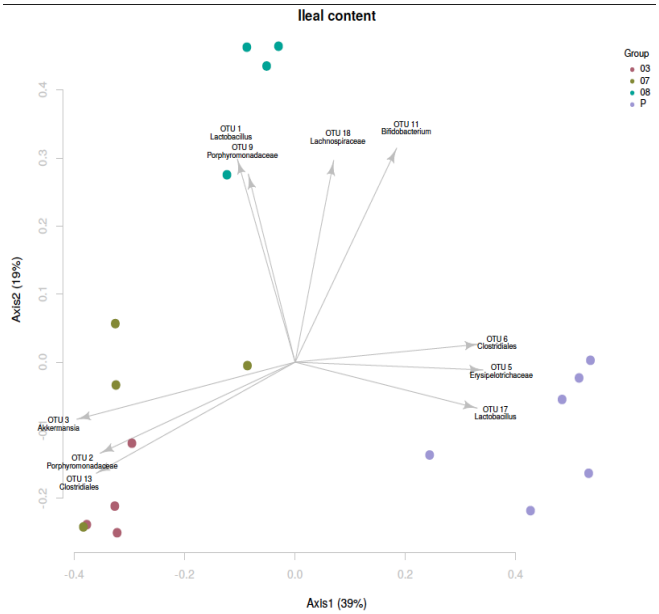

B.

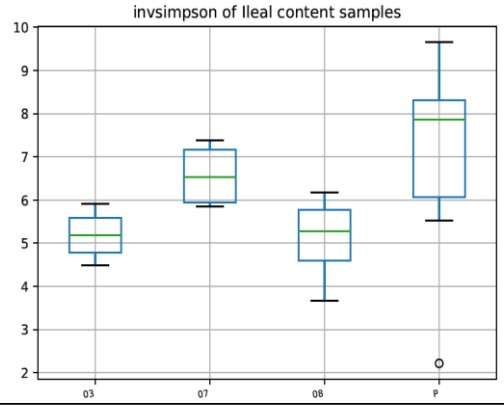

C.

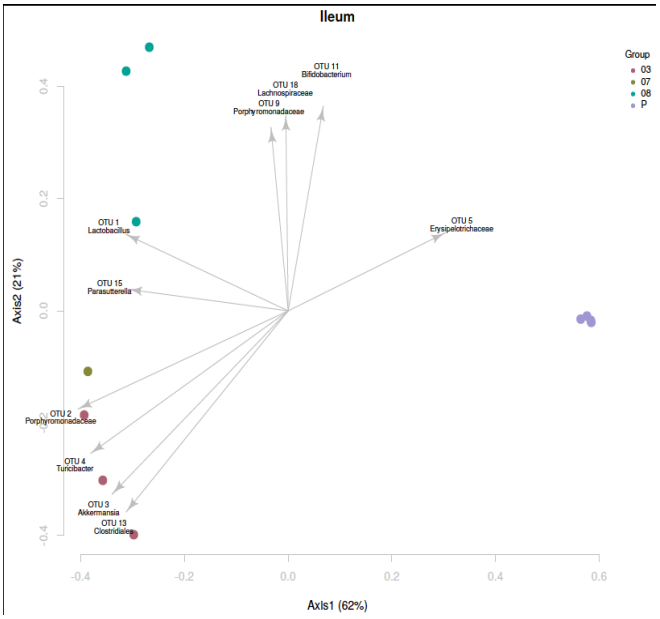

G.

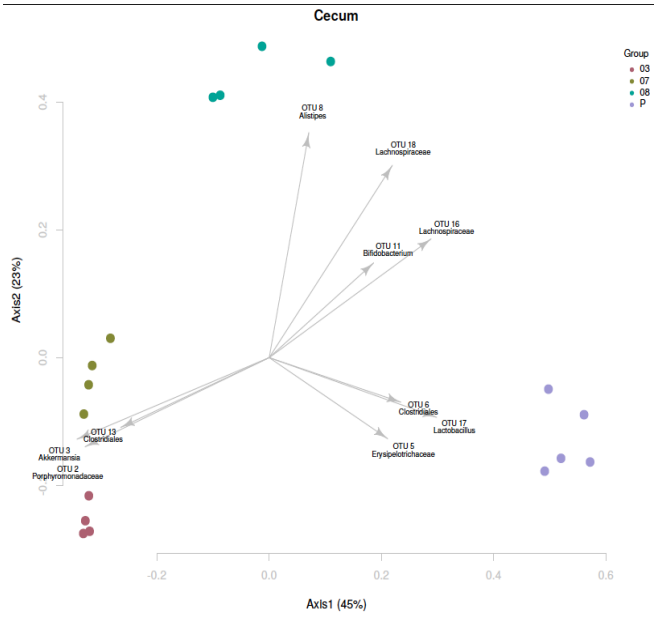

H.

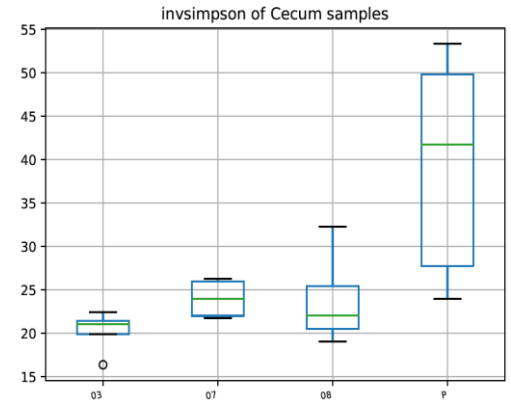

I.

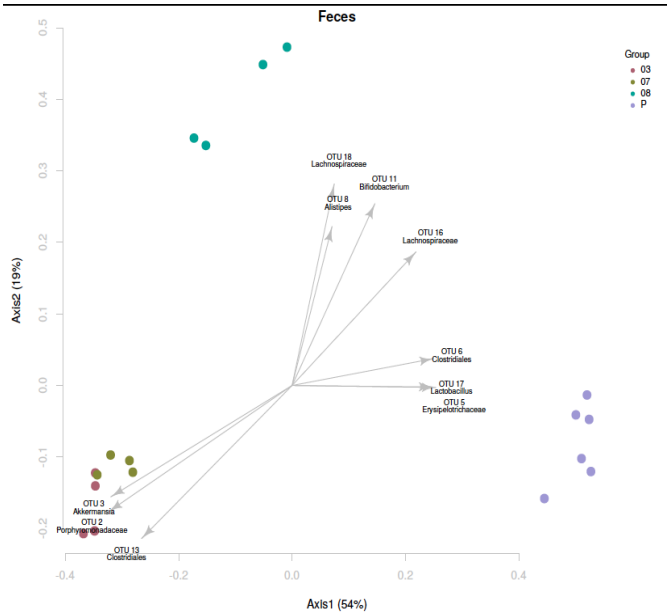

(Continued on next page)

D.

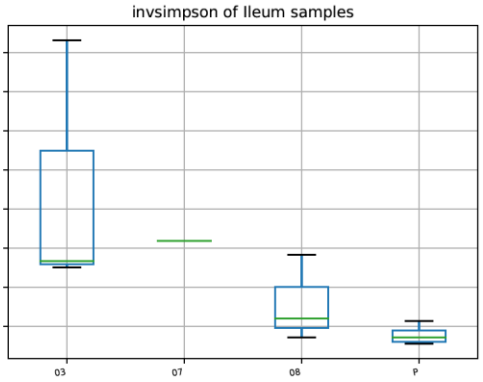
invsimpson of Ileum samples
16
14
12
10
8
6
4
2
03
07
08
P

J.

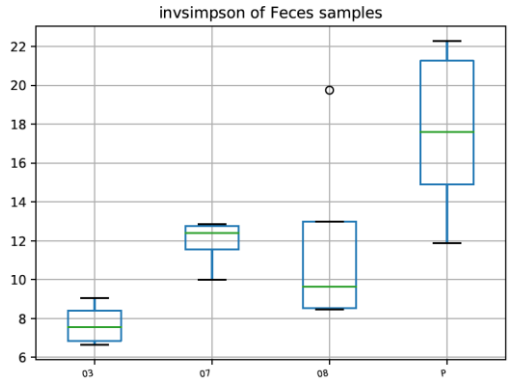
invsimpson of Feces samples
22
20
18
16
14
12
10
8
6
03
07
08
P

E.

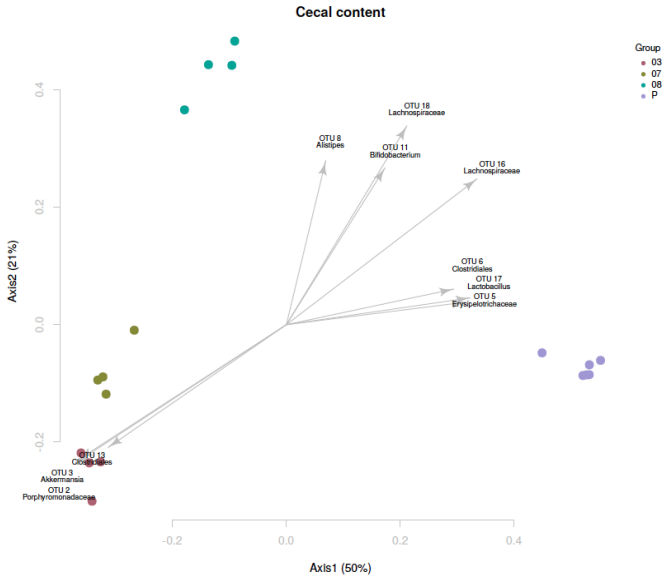
Cecal content
Group
03
07
08
P
OTU 18
Lachnospiraceae
OTU 8
Alistipes
OTU 11
Bifidobacterium
OTU 16
Lachnospiraceae
OTU 6
Clostridiales
OTU 17
Lactobacillus
OTU 5
Erysipelotrichaceae
OTU 13
OTU 3
Akkermansia
OTU 2
Axis2 (21%)
Axis1 (50%)

K.

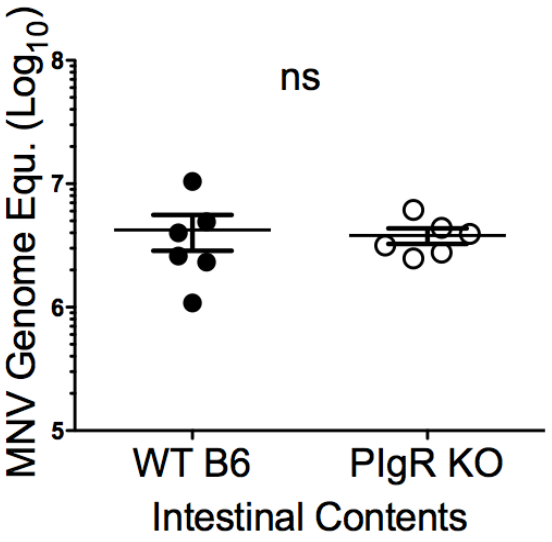
MNV Genome Equ. (Log10)
8
7
6
5
ns
WT B6
PIgR KO
Intestinal Contents

F.

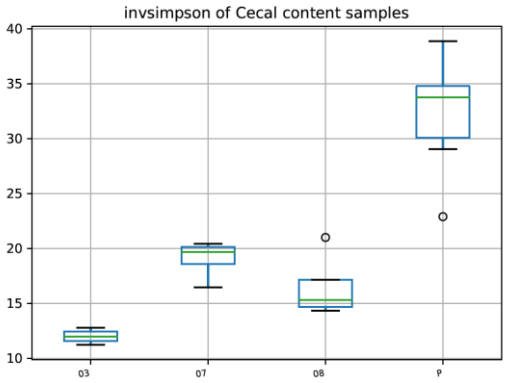
invsimpson of Cecal content samples
40
35
30
25
20
15
10
03
07
08
P

Figure 3.1: Intestinal microbial communities are altered in pIgR KO mice
A-J. Lumenal contents, and mucosal lamina propria of the ileum and cecum as well as feces were sterilely isolated from naive pIgR KO and WT B6 mice and intestinal microbial communities were anaylzed via 16S rRNA gene sequencing. **A, C, E, G, I.** Principal coordinates analysis (PCoA) plot of θ_{YC} distances between bacterial communities is shown as analyzed by analysis of molecular variance (AMOVA). Each symbol represents the bacterial community from an individual animal. Closed symbols represent WT B6 mice, and shapes distinguish between WT B6 breeding rooms. Open circles represent pIgR KO mice. **B, D, F, H, J.** Box & Whisker graphs of inverse Simpson (invsimpson) analysis of microbial diversity. Each box denotes interquartile range with line at mean. Whiskers show minimum and maximum values. Five mice per group. **K.** Ileal contents were isolated from the ileum of naïve WT B6 and pIgR KO mice. After 100 micron filter pass through, ileal contents were weighed and incubated with $1.34x10^7$ PFU MNV-1 for one hour at room temperature. Samples were then washed, RNA was isolated, and viral genome copies were assessed via RT-qPCR. Data are pooled from three independent experiments and each symbol is a data point from an individual animal. Error bars are standard error of the mean (SEM). Data were analyzed using Mann Whitney U test. ns = not statistically significant.

were significantly altered in pIgR KO mice compared to WT B6 controls in all sites analyzed by AMOVA. Our findings are consistent with the study by Reikvam *et al*. [40] and demonstrate that intestinal microbial communities are significantly altered in pIgR KO mice. These alterations may contribute to a skewed intestinal cytokine milieu.

To determine if the altered bacterial communities in pIgR KO mice altered MNV-1 bacterial binding in the lumen, I collected, filtered, and weighed ileal luminal contents and incubated contents with MNV-1. After an hour unbound virus was washed away, and viral genome copies were assessed via RT-qPCR. I found that ileal luminal contents bound MNV-1 equally well between pIgR KO and WT B6 mice (**Figure 3.1K**). These data suggest that, despite alterations in the microbiome of pIgR KO mice versus WT B6 controls, MNV can bind to ileal luminal contents equally. Taken together, these data suggest that SIg alter the microbial composition and diversity in the intestinal lumen and mucosal tissue, and these microbial alterations may be indirectly influencing MNV-1 infection in pIgR KO mice.

3.2B Antibiotic Treatment of Conventional PIgR KO Mice Reduces MNV-1 Replication

Antibiotic treatment of WT B6 mice has been shown to reduce MNV-1 infection [13, 41]. To determine if bacterial populations modulate MNV-1 infection in the absence of secretory immunoglobulins, I treated pIgR KO mice with antibiotics and infected them with MNV-1-NR. I used the antibiotic cefoperazone, a broad-spectrum antibiotic that targets both gram-positive and gram-negative bacteria [42]. Short-term antibiotic treatment will reduce the bacterial load while at the same time avoiding physiological (e.g., villus length, Peyer's patch development) and immunological (e.g. immune cell development, antibody production) differences seen in germ-free versus conventional mice [42-46]. I first determined that antibiotic treatment reduced

bacterial loads in the small intestine after MNV infection by harvesting intestinal contents. I observed that antibiotically treated pIgR KO mice had no visually detectable bacterial colony formation, whereas conventional pIgR KO mice had bacteria able to form many colonies greater than 1.2 mm in size as defined by an aCOLyte colony counter (**Figure 3.2A**).

To determine the effect of bacteria on MNV infection in the absence of SIg and SC, antibiotically treated and control pIgR KO mice were infected with 3.8 x 10^5 PFU MNV-1-NR via oral gavage and titers of replicated virus were assessed via plaque assay at 18 hpi. Determination of MNV-1 replication in these mice revealed very little detectable replication of MNV-1 in the mesentery, and small intestine (**Figure 3.2B-E**). MNV-1 replication was detectable in the cecum and colon of conventionally housed mice; however, no replication was detected in antibiotically treated pIgR KO mice (**Figure 3.2F-G**). The MNV-1 distribution in the conventionally housed pIgR KO mice was primarily detected in the cecum and colon, whereas MNV-1 was primarily detected in the ileum and cecum of WT B6 controls, the reason for this shift in tropism remains unknown. No statistically significant differences in MNV-1 shedding were detected between treatment groups (**Figure 3.2H**). These data suggest that short-term reduction in bacterial communities of pIgR KO mice significantly reduces MNV-1 viral replication, and are consistent with findings from Baldridge *et al.*, which determined that pIgR KO mice exhibited reduced fecal shedding of MNV-CR6 at 7 dpi after antibiotic treatment as compared to conventional control pIgR KO mice [13]. These data suggest bacterial species enhance MNV infection in the absence of secretory immunoglobulins. This is in contrast to data from WT B6 mice, which showed no change in MNV-1 titers after antibiotic treatment [13].

3.2C IFN-ɣ and iNOS Levels are Similar in Naive Germ-Free PIgR KO and WT B6 Mice

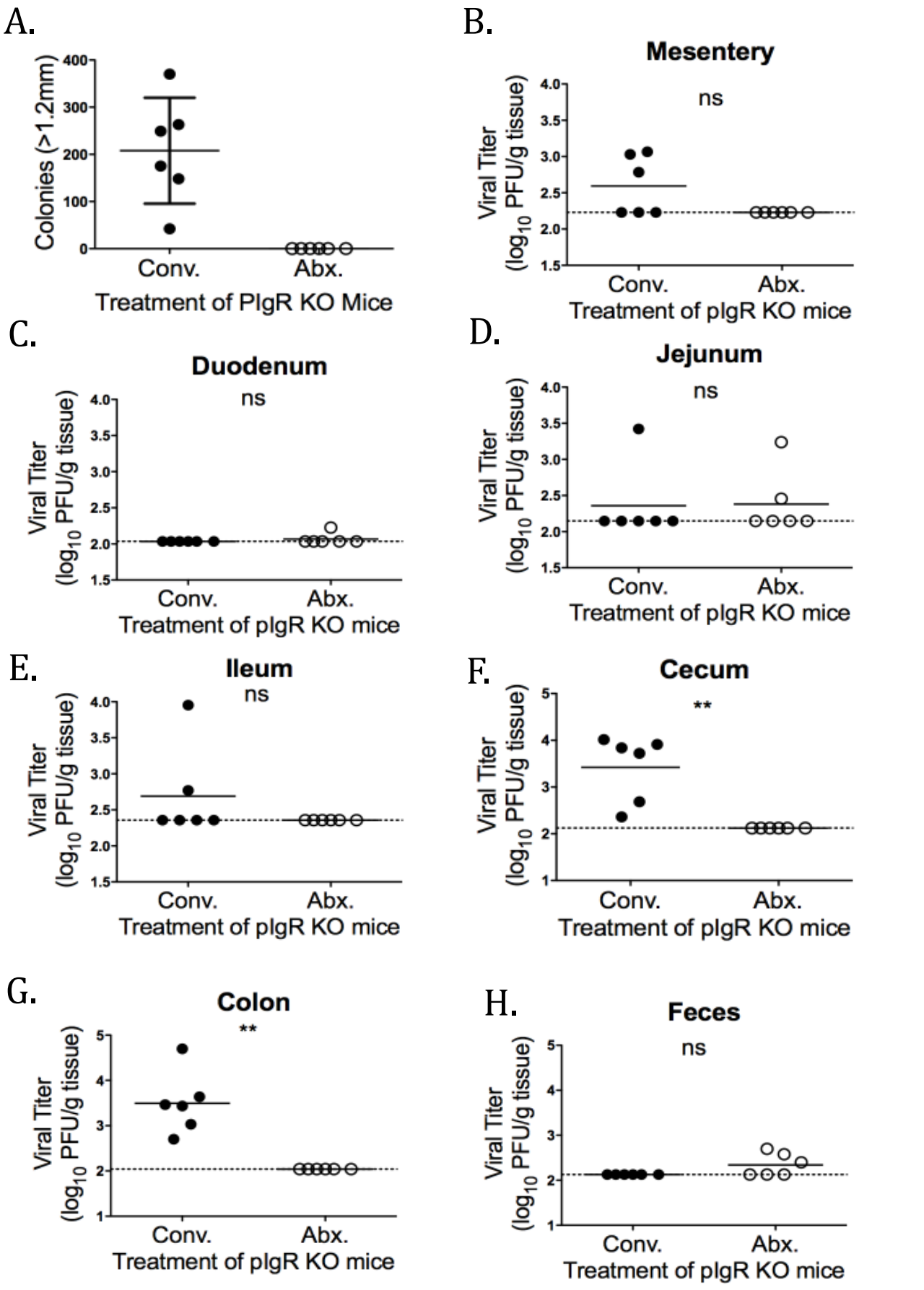
A.
Colonies (>1.2mm)
400
300
200
100
0
Conv.
Abx.
Treatment of PIgR KO Mice
B.
Mesentery
ns
Viral Titer
(log10 PFU/g tissue)
4.0
3.5
3.0
2.5
2.0
1.5
Conv.
Abx.
Treatment of pIgR KO mice
C.
Duodenum
ns
Viral Titer
(log10 PFU/g tissue)
4.0
3.5
3.0
2.5
2.0
1.5
Conv.
Abx.
Treatment of pIgR KO mice
D.
Jejunum
ns
Viral Titer
(log10 PFU/g tissue)
4.0
3.5
3.0
2.5
2.0
1.5
Conv.
Abx.
Treatment of pIgR KO mice
E.
Ileum
ns
Viral Titer
(log10 PFU/g tissue)
4.0
3.5
3.0
2.5
2.0
1.5
Conv.
Abx.
Treatment of pIgR KO mice
F.
Cecum
**
Viral Titer
(log10 PFU/g tissue)
5
4
3
2
1
Conv.
Abx.
Treatment of pIgR KO mice
G.
Colon
**
Viral Titer
(log10 PFU/g tissue)
5
4
3
2
1
Conv.
Abx.
Treatment of pIgR KO mice
H.
Feces
ns
Viral Titer
(log10 PFU/g tissue)
5
4
3
2
1
Conv.
Abx.
Treatment of pIgR KO mice

Figure 3.2: Intestinal microbiota enhance MNV-1 infection in pIgR KO mice

A-H. Conventionally housed pIgR KO mice were given untreated, or cefoperazone [0.5g/L] treated distilled water for 7 days. Mice were infected by oral gavage with $3.8x10^5$ PFU/animal of neutral red labeled MNV-1, and tissues and intestinal contents were harvested at 18 hpi in a darkened room using a red photolight. **A.** Intestinal contents were isolated and after 100 micron filter pass through, contents were weighed, and an equal amount was serially diluted in LB broth. Aliquots from each dilution was plated onto BHI plates and colonies >1.2 mm were assessed after overnight incubation at 37˚C. The -1 dilution of intestinal contents is shown. **B-H.** Intestinal tissue homogenate was serially diluted and exposed to white light for 30 min. Replicated viral titers in the indicated tissue of antibiotically treated and conventional pIgR KO mice were assessed via plaque assay. The sensitivity threshold for each graph is indicated by the dashed line and is as follows (log PFU/g tissue): **B.** 2.23 **C.** 2.035 **D.** 2.148 **E.** 2.357 **F.** 2.123 **G.** 2.041 **H.** 1.127**.** Data are pooled from two independent experiments and each symbol is a data point from an individual animal. Error bars are standard error of the mean (SEM). Values were analyzed using Mann Whitney U test. **= $P<0.01$. ns = not statistically significant.

Bacterial sensing in the absence of SIg results in inflammatory cytokine production [2], which may disrupt MNV-1 replication. To test whether enhanced levels of cytokines limit MNV-1 infection in pIgR KO mice, I first sought to identify a condition in which the levels of IFN-ɣ and iNOS were similar between pIgR KO and WT B6 mice. Since SIgA dampens the inflammatory signals of commensal bacteria [2], we hypothesized that germ-free mice of both backgrounds might represent one such condition. Thus, both pIgR KO and WT B6 mouse strains were rederived germ-free.

To determine if intestinal microbiota are necessary for the immunomodulatory functions of MNV-1 seen in conventionally housed mice, namely reduced IFN-ɣ in pIgR KO mice and reduced IFN-β and TNF-α in WT B6 mice (see **Figure 2.10**), I infected germ-free pIgR KO and WT B6 mice with 3.8 x 10^5 PFU MNV-1-NR via oral gavage and assessed host cytokine responses in comparison to naïve germ-free mice at 18 hpi via RT-qPCR.

Contrary to conventionally infected animals, ileal IFN-ɣ, iNOS IFN-β, TNF-α, and TGF-β transcript levels were comparable between naïve and infected pIgR KO mice and WT B6 controls devoid of bacterial stimulation (**Figure 3.3A-D & 3.3F**). Also contrary to conventionally housed animals, ISG15 transcript levels were enhanced after MNV-1 infection in germ-free pIgR KO mice compare to uninfected germ-free controls as well as infected germ-free WT B6 (**Figure 3.3E**). Although no change in IFN-ɣ transcripts was detected after MNV-1 infection, IFN-ɣ protein levels were significantly enhanced in pIgR KO mice compared to infected germ-free WT B6 controls (**Figure 3.3G**), this may account for the enhanced ISG15 transcript levels seen in infected germ-free pIgR KO mice.

These data demonstrate that removal of the microbiota is able to equalize small intestinal IFN-ɣ and iNOS levels in naive pIgR KO and WT B6 mice, highlighting the immunomodulatory

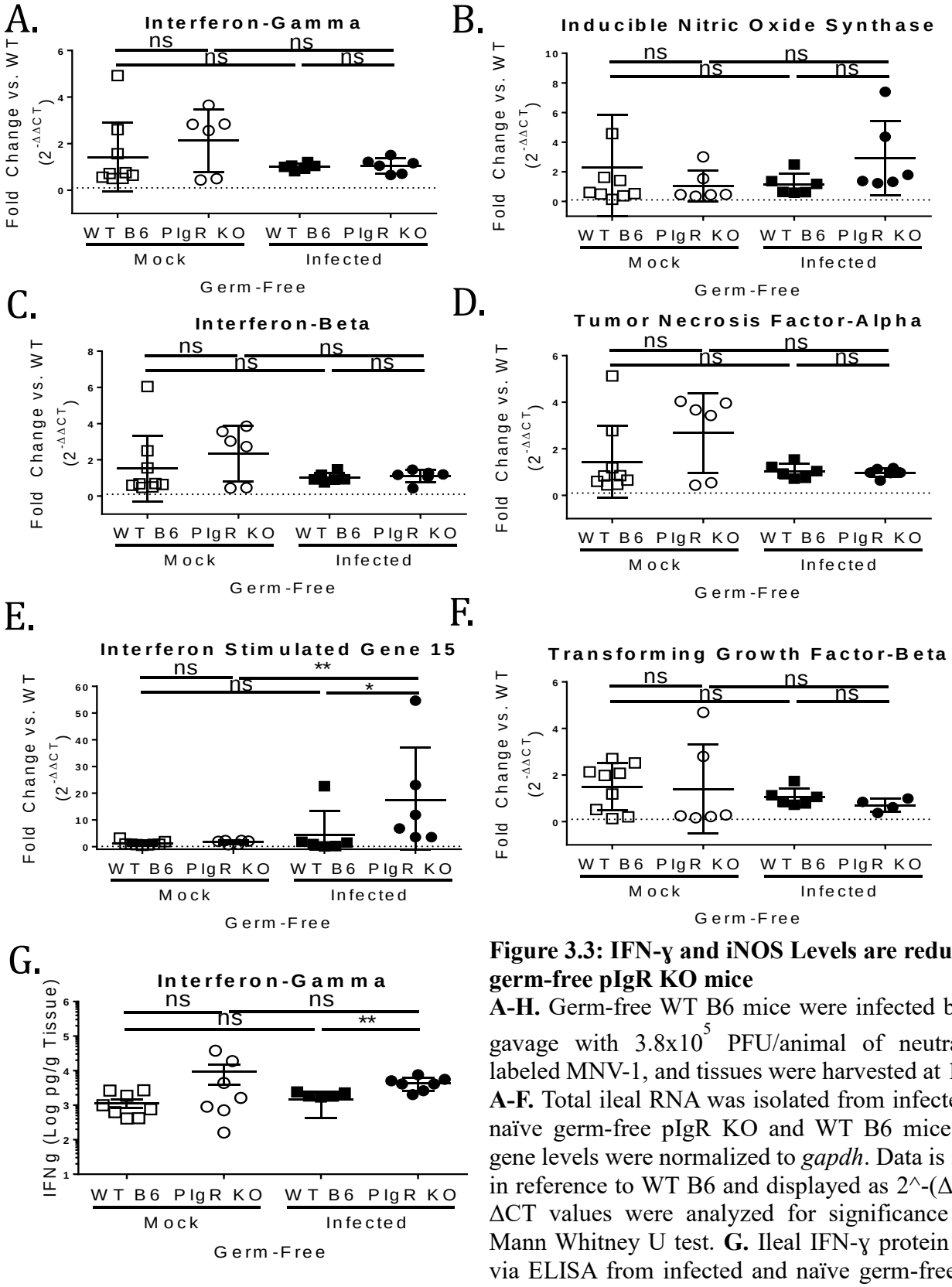

Figure 3.3: IFN-ɣ and iNOS Levels are reduced in germ-free pIgR KO mice

A-H. Germ-free WT B6 mice were infected by oral gavage with $3.8x10^5$ PFU/animal of neutral red labeled MNV-1, and tissues were harvested at 18 hpi. **A-F.** Total ileal RNA was isolated from infected and naïve germ-free pIgR KO and WT B6 mice. Host gene levels were normalized to *gapdh*. Data is shown in reference to WT B6 and displayed as 2^-(ΔΔCT). ΔCT values were analyzed for significance using Mann Whitney U test. **G.** Ileal IFN-ɣ protein levels via ELISA from infected and naïve germ-free pIgR KO and WT B6 mice. Each symbol is a data point from an individual animal. Error bars are standard error of the mean (SEM). Data were analyzed using Mann Whitney U test. *= P<0.05. **= P<0.01. ns = not statistically significant.

functions of SIg. Furthermore, these data suggest that bacteria aid in MNV-1-mediated immunomodulation.

3.2D MNV-1 Infection is Similar in Germ-Free PIgR KO and WT B6 Mice

The previous findings suggest that in the absence of pIgR and SIg (i.e. pIgR KO mice), inflammatory responses to enteric bacteria may create an inhospitable environment for MNV-1 infection. To test this hypothesis, I infected germ-free pIgR KO and WT B6 mice with 3.8×10^5 PFU MNV-1-NR via oral gavage and assessed titers of replicated virus via plaque assay at 18 hpi. Consistent with our hypothesis, germ-free pIgR KO and WT B6 had similar viral loads throughout the entire gastrointestinal tract (i.e., duodenum, jejunum, ileum, cecum, colon) and MLN as well as similar viral shedding in the feces (**Figure 3.4A-G**). In addition, it is worth noting that similar with previous studies using antibiotic-depleted WT mice [12] and data shown above (see **Figure 3.3**), overall virus loads were reduced in germ-free compared to conventional WT B6 mice. These data demonstrate that MNV-1 replicates similarly in pIgR KO and WT B6 mice under conditions where inflammatory markers such as IFN-ɣ and iNOS are equivalent.

3.2E Bacteria Alter MNV-1 Gastrointestinal Regionalization

Although direct interaction of MNV with bacteria has not yet been demonstrated, MNV binds to glycoproteins that can be found on bacterial surfaces [14, 47]. My studies have revealed that a reduction in microbial communities after antibiotic treatment of pIgR KO mice resulted in reduced MNV-1 infection compared to untreated controls. These data are consistent with previous findings [13], and suggest bacterial species enhance MNV infection in the absence of SIg. When bacteria were removed from experimental conditions, antiviral cytokine levels and

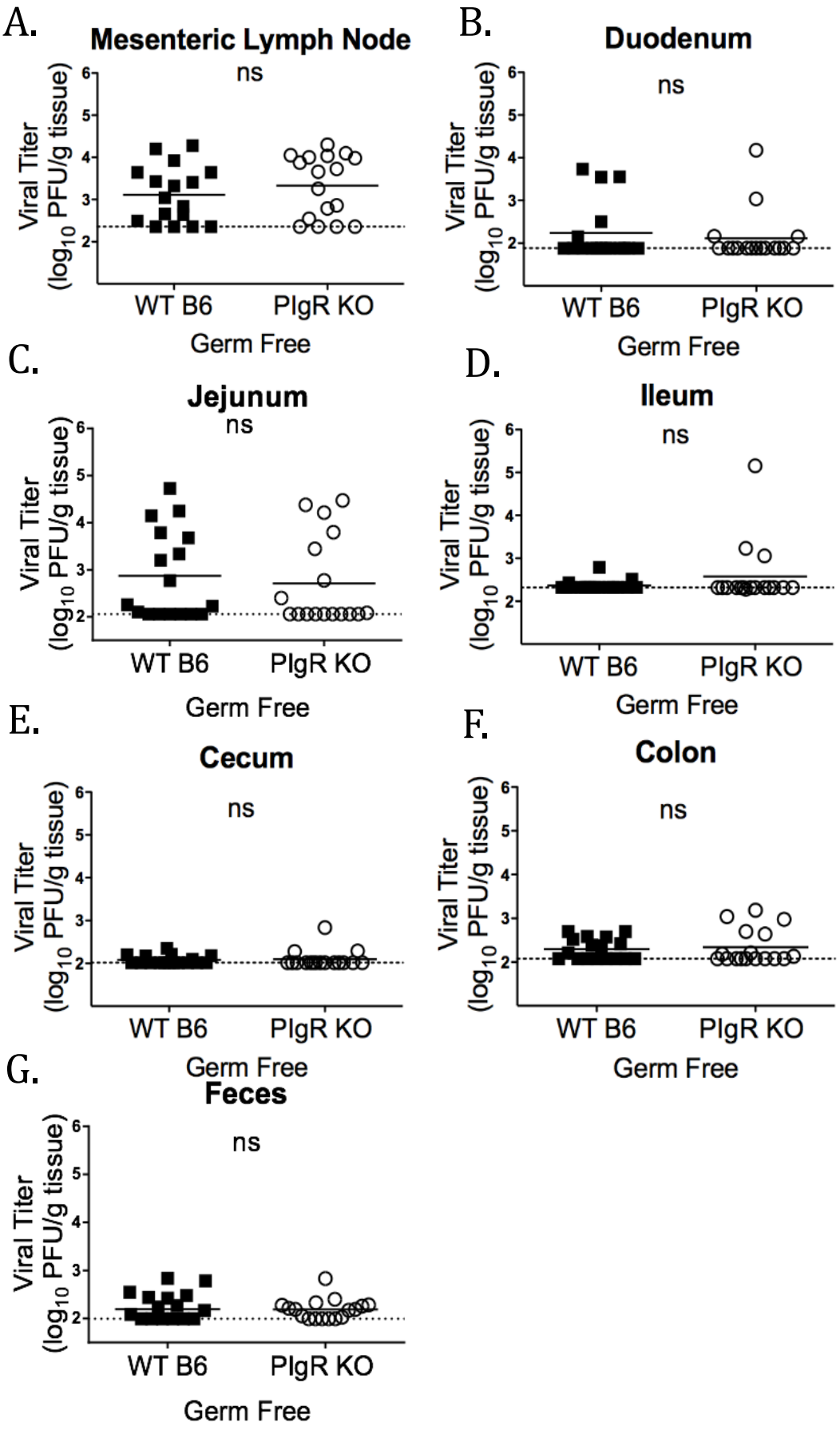
A.
Mesenteric Lymph Node
ns
Viral Titer (log10 PFU/g tissue)
WT B6
PIgR KO
Germ Free
B.
Duodenum
ns
C.
Jejunum
ns
D.
Ileum
ns
E.
Cecum
ns
F.
Colon
ns
G.
Feces
ns

Figure 3.4: MNV-1 infection is similar in germ-free pIgR KO and WT B6 mice

A-G. Germ-free pIgR KO and WT B6 mice were infected by oral gavage with $3.8x10^5$ PFU/animal of neutral red labeled MNV-1, and tissues were harvested at 18 hpi in a darkened room using a red photolight. The tissue homogenate was serially diluted and exposed to white light for 30 min. Replicated viral titers in the indicated tissue of germ-free WT B6 and pIgR KO mice were assessed via plaque assay. The sensitivity threshold for each graph is indicated by the dashed line and is as follows (log PFU/g tissue): **A.** 2.356 **B.** 2.881 **C.** 2.057 **D.** 2.317 **E.** 2.014 **F.** 2.077 **G.** 1.993**.** Data are pooled from four independent experiments and each symbol is a data point from an individual animal. Error bars are standard error of the mean (SEM). Values were analyzed using Mann Whitney U test. ns = not statistically significant.

MNV-1 replication were similar between germ-free pIgR KO and WT B6 mice (see **Figure 3.3**) but not between the conventionally housed counterparts (see **Figure 2.10**). Taken together these data support a model in which SIg modulate intestinal bacterial communities and these bacterial communities in turn modulate MNV infection.

To study these trans-kingdom interactions in more detail, I infected conventional and germ-free C57/Bl6 mice with 3.8 x 10^5 PFU MNV-1-NR via oral gavage and assessed viral replication at 9 hpi via plaque assay. I found that there was little MNV-1 replication in the mesentery of either conventional or germ-free mice (**Figure 3.5A**). In the duodenum, germ-free mice exhibited detectable viral replication in 10/15 mice, while only 2/14 conventional mice had detectable viral replication (**Figure 3.5B**). Thus, MNV-1 replication was significantly increased in the duodenum of germ-free mice. Viral replication in the jejunum was not altered between conventionally housed and germ-free housed mice (**Figure 3.5C**). In contrast, conventionally housed mice had significantly more MNV viral replication and more mice (9/14) in the ileum than germ-free housed animals (1/15) (**Figure 3.5D**). Although more conventionally housed mice had detectable viral replication in the cecum (6/14 conv. vs. 1/15 germ-free), it failed to reach statistical significance (**Figure 3.5E**). No differences in MNV replication were detected in the colon (**Figure 3.5F**). Taken together these results suggest that the small intestinal region where MNV-1 infection is initiated is altered in germ-free animals versus conventionally housed controls, which is surprising given intestinal bacteria are primarily located in the colon [1].

Reduced viral replication in the ileum at this early time post infection could suggest that MNV-1-NR access to the distal small intestine is altered in germ-free mice versus conventional controls. To determine if the enhanced MNV-1 replication in the proximal small intestine, and the reduced MNV-1 replication in distal small intestine is due to intestinal trafficking differences

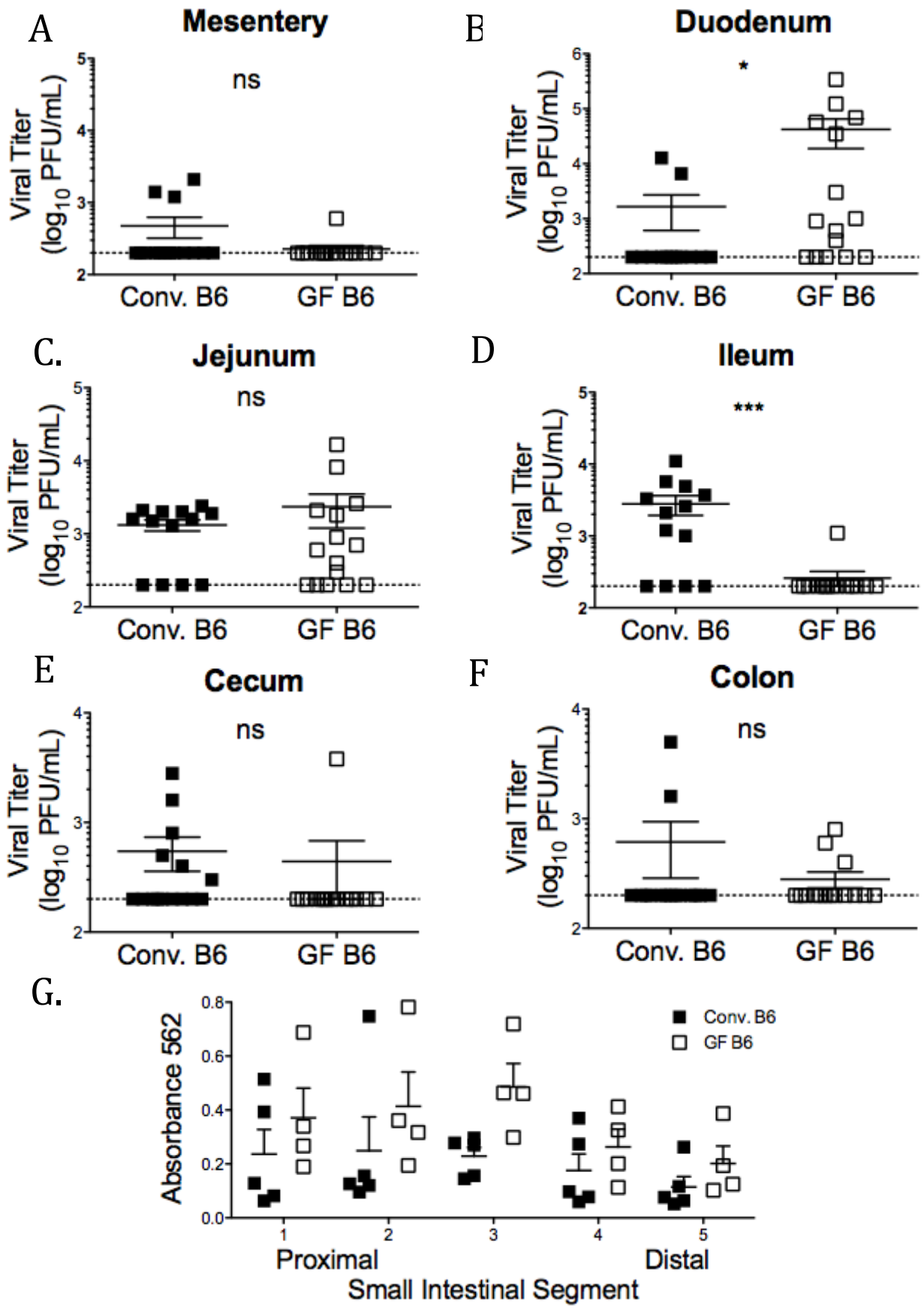
A
Mesentery
ns
Viral Titer (log10 PFU/mL)
Conv. B6
GF B6
B
Duodenum
*
C.
Jejunum
ns
D
Ileum
***
E
Cecum
ns
F
Colon
ns
G.
Absorbance 562
Conv. B6
GF B6
Proximal
Distal
Small Intestinal Segment

Figure 3.5: Intestinal regionalization of MNV-1 is altered in the absence of the microbiome

A-F. Germ-free or conventionally housed WT B6 mice were infected by oral gavage with $3.8x10^5$ PFU/animal of neutral red labeled MNV-1, and tissues were harvested at 9 hpi in a darkened room using a red photolight. The tissue homogenate was serially diluted and exposed to white light for 30 min. Replicated viral titers in the indicated tissue of germ-free WT B6 and pIgR KO mice were assessed via plaque assay. The sensitivity threshold for each graph is indicated by the dashed line and is set to 200. Viral titers are shown as log PFU/mL tissue. Data are pooled from four independent experiments. Values were analyzed using Mann Whitney U test. *= $P<0.05$. ***= $P<0.001$. ns = not statistically significant. **G.** Evans blue dye was administered to fasting conventional and germ-free B6 mice. After 15 minutes the stomach and small intestine were harvested. The small intestine was divided into fifths and transit of the dye was measured by absorbance at 562 nm. Data are pooled from two independent experiments. Data was analyzed using 2-way ANOVA. Each symbol is a data point from an individual animal. Error bars are standard error of the mean (SEM).

in conventionally housed versus germ-free housed mice, I performed an intestinal transit assay. Conventional and germ-free B6 mice were fasted for 18 hours. Evan's blue dye was diluted into 1x PBS with 1% methylcellulose and administered via oral gavage. 15 minutes after administration, the stomach and small intestinal segments were harvested and processed, and absorbance of Evans blue dye was assessed in each segment as a readout of peristalsis rate. I determined that there was no difference in intestinal transit rate as Evans blue dye was distributed similarly in conventional and germ-free housed B6 mice (**Figure 3.5G**). These data suggest that MNV-1-NR can reach the distal small intestine equally well in germ-free and conventional controls and cannot account for the altered regionalization in MNV-1 infection seen in germ-free mice. Taken together, these data demonstrate that MNV-1 infection of the small intestine is altered in the absence of the intestinal microbiota and suggest that intestinal bacteria modulate the regionalization of the MNV-1 replication site.

3.2F Bacteria Alter MNV-CR3 Gastrointestinal Regionalization

Bacterial facilitation of MNV infection was shown for MNV-1 [11, 12], however the effect of bacteria on other MNV strains has not been explored. To determine the effects of bacteria on MNV-CR3 infection, I infected germ-free and conventionally housed mice with $2.6x10^5$ PFU MNV-CR3-NR via oral gavage and assessed viral replication at 12 hpi via plaque assay. These preliminary (n=1) findings showed that after the first round of viral replication, very little virus was detectable in the mesentery (**Figure 3.6A**). Similar to MNV-1 replication, MNV-CR3-NR replication also exhibited altered small intestinal distribution. Detection of viral replication was highest in the proximal small intestine in germ-free housed animals, with less virus detected in the more distal small intestine whereas viral replication in conventionally

housed animals was opposite (**Figure 3.6B-D**). Little replicated virus was detected in the colon and feces at this early time point for either group (**Figure 3.6E-F**). These data show that MNV-CR3 intestinal distribution is altered in the absence of intestinal microbiota. Taken together with **Figures 3.2** and **3.5**, these data demonstrate that the intestinal location of MNV infection is reduced in an MNV strain-independent manner when the intestinal microbiota is reduced or absent.

3.2G Distribution of Small Intestinal Immune Cells is Not Altered Under Germ-Free Housing Conditions

Germ-free animals have several abnormalities including less vascularized intestinal villi, thinner mucus layer, and an underdeveloped immune system, SIg production, and lymphoid follicle maturation versus conventionally housed animals [46]. MNV-1 has been shown to infect T and B cells [12], dendritic cells and macrophages [48], therefore, alterations in these populations could account for the altered intestinal distribution in germ-free housed mice versus controls. In order to determine if the immune cell distribution in our naive germ-free housed mice was dysregulated compared to naive conventionally housed control mice, I assessed the distribution of the small intestinal immune cells via flow cytometry in different intestinal segments. Intestinal segments were harvested and digested as previously described to create single cell suspensions [49]. Immune cell subsets were defined as B and T cells, NK cells, neutrophils, macrophages, dendritic cells, and eosinophils and were distinguished using cell markers outlined in **Table 3.1**.

These preliminary studies (n=1, 3 mice/group) show no differences in B cell populations across the small intestine for either group, and no differences between germ-free and

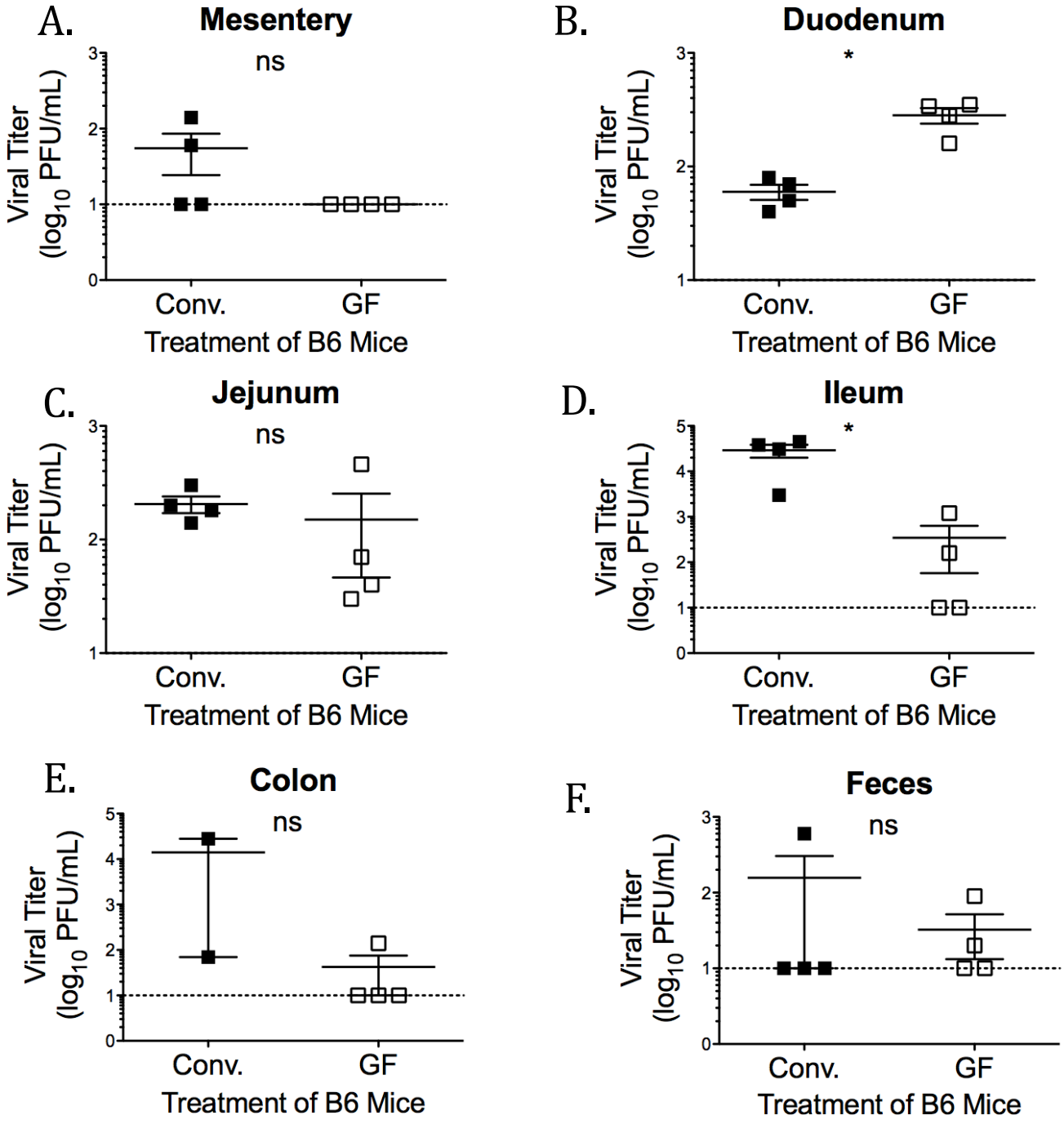

Figure 3.6: Intestinal regionalization of MNV-CR3 is altered in the absence of the microbiome

A-F. Germ-free and conventional WT B6 mice were infected by oral gavage with $2.6x10^5$ PFU/animal of neutral red labeled MNV-CR3, and tissues were harvested at 12 hpi in a darkened room using a red photolight. The tissue homogenate was serially diluted and exposed to white light for 30 min. Replicated viral titers in the indicated tissue of germ-free WT B6 and pIgR KO mice were assessed via plaque assay. The sensitivity threshold for each graph is indicated by the dashed line and is set at 10. Viral titers are displayed as log PFU/mL tissue**.** Data are from one experiment and each symbol is a data point from an individual animal. Error bars are standard error of the mean (SEM). Values were analyzed using Mann Whitney U test. ns = not statistically significant.

	CD11b	CD11c	CD19	CD49b	Ly6C	Ly6G	TCRb	SSCA
B Cells	-		+					
T Cells	-			-			+	
NK Cells				+			-	
Neutrophils	High	-	-	-	-	+		
Macrophages	+	-	-	-	+	-		Low
Dendritic Cells	+	+	-	-				
Eosinophils	+	-	-	-	-	+		High

Table 3.1: Characterization of Small Intestinal Immune Cells
Immune cell subsets characterized in **Figure 3.7** were defined as B and T cells, Natural Killer (NK) cells, neutrophils, macrophages, dendritic cells, and eosinophils and were distinguished using cell surface markers outlined above using flow cytometry. SSCA= side scatter area.

conventional animals were evident throughout the small intestine (**Figure 3.7A-B**). There is a trend toward fewer percentages of T cells across the small intestine in germ-free housed mice versus controls, however these preliminary data (n=1, 3 mice/group) are not significantly different, nor is the absolute number of T cells (**Figure 3.7C-D**). No differences were notable in natural killer cells either across the small intestine or between housing conditions (**Figure 3.7E-F**). Similar to natural killer cells, no differences were notable in the neutrophil compartment either across the small intestine or between housing conditions (**Figure 3.8A-B**). Macrophage, dendritic cell (DC) and eosinophil populations were reduced in percentage distally throughout the small intestine in both housing conditions, however absolute numbers appear constant throughout the SI segments (**Figure 3.8C-H**). These preliminary results suggest that the percentage and number of immune cell subsets across the small intestine may be comparable in germ-free and conventionally housed mice, and that access to MNV target cells cannot account for the altered intestinal distribution of MNV in germ-free housed mice versus controls. However, additional repeats are needed to confirm these findings.

3.2H *Bacteroides thetaiotaomicron* Colonization of Germ-Free Mice Does Not Enhance MNV-1 Infection

Secretory immunoglobulins, intestinal transit, and MNV target cell distribution cannot explain the altered intestinal distribution MNV in bacteria-deplete conditions. Further exploration of the mechanism behind this altered tissue tropism led us to explore norovirus-bacterial interactions. It is clear that optimal MNV infection occurs in the context of a robust microbiome. To more readily delineate a mechanism in the future, I next sought to determine if

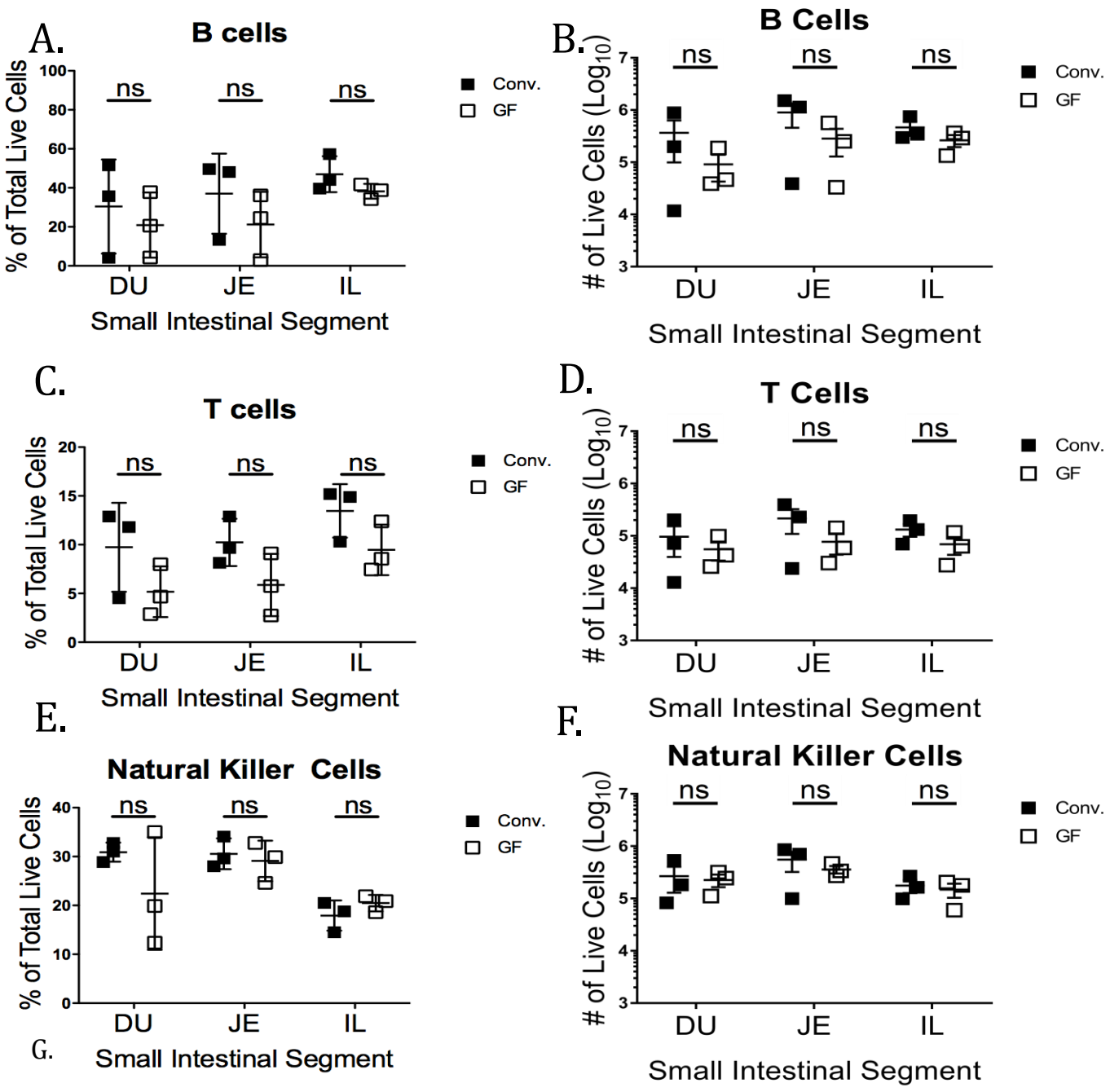

Figure 3.7: Distribution of small intestinal adaptive immune cells are not altered under germ-free housing conditions

A-F. Small intestinal segments were isolated from naïve germ-free (GF) and conventional WT B6 mice (Conv.) and lamina propria cells were isolated. Live single cells were analyzed via flow cytometry, and B, T and natural killer cells were defined as outlined in **Table 3.1**. **A**, **C, E**. (left column) Percentage of live cells indicated on graph. **B, D, F.** (right column) Absolute number of live cells indicated on graph. Data shown are from one experiment and each symbol is a data point from an individual animal. Error bars are standard error of the mean (SEM). Data were analyzed using Mann Whitney U test. ns = not statistically significant.

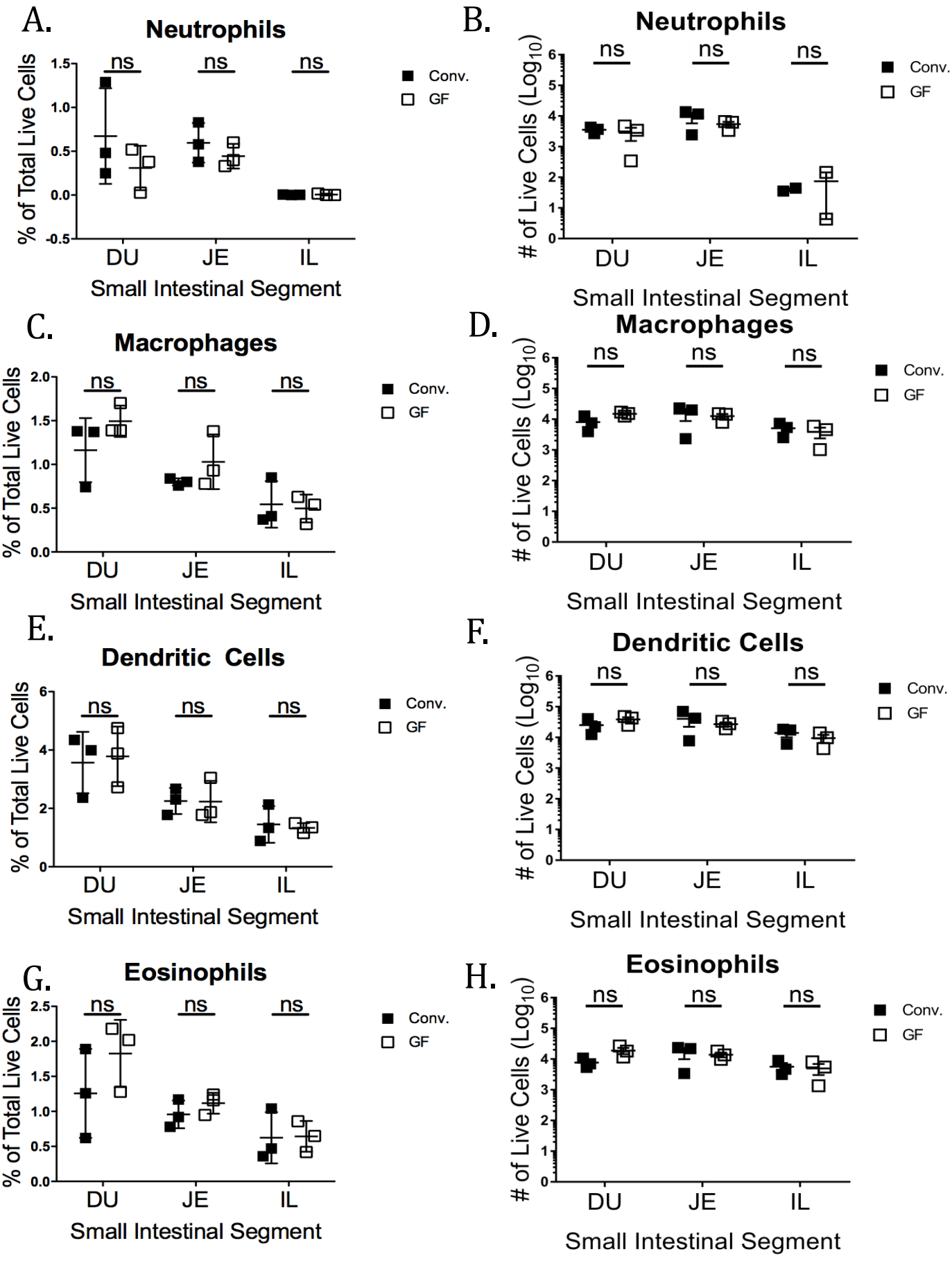
A.
Neutrophils
% of Total Live Cells
ns
Conv.
GF
DU
JE
IL
Small Intestinal Segment
B.
Neutrophils
# of Live Cells (Log10)
C.
Macrophages
D.
Macrophages
E.
Dendritic Cells
F.
Dendritic Cells
G.
Eosinophils
H.
Eosinophils

Figure 3.8: Distribution of small intestinal innate immune cells are not altered under germ-free housing conditions (on following page)
A-H. Small intestinal segments were isolated from naïve germ-free (GF) and conventional WT B6 mice (Conv.) and lamina propria cells were isolated. Live single cells were analyzed via flow cytometry, and neutrophils, macrophages, dendritic cells and eosinophils were defined as outlined in **Table 3.1**. **A**, **C, E, G**. (left column) Percentage of live cells indicated on graph. **B, D, F, H.** (right column) Absolute number of live cells indicated on graph. Data shown are from one experiment and each symbol is a data point from an individual animal. Error bars are standard error of the mean (SEM). Data were analyzed using Mann Whitney U test. ns = not statistically significant.

the beneficial nature of bacteria-replete conditions in MNV infection could be recapitulated with a single bacterial species. Previous work by Dr. Juliana Bragazzi-Cunha in the Wobus lab determined that the MNV-1 P-domain of the viral capsid is capable of binding to *Bacteroides thetaiotaomicron* **(***B. theta***)** via the SusD protein (not shown). The binding of *B. theta* SusD recombinant protein to the P-domain of the MNV-1 capsid led us to hypothesize that *B. theta* SusD binding aids in MNV-1 attachment to target cells as was shown with the H-antigen of *Enterobacter cloacae* and human norovirus [12]. Furthermore, we hypothesized that *B. theta* colonization and interaction with MNV may be able to restore MNV tissue tropism in germ-free animals to that of conventional controls.

To determine if *B. theta* colonization of germ-free mice can restore the shift in intestinal regional tropism observed in the germ-free mice in comparison to conventionally housed mice, we monocolonized germ-free Swiss Webster mice with *B. theta* by orally gavaging a one-time dose of 10^8 bacteria. After two weeks of colonization, I infected *B. theta* monocolonized and germ-free Swiss Webster mice with 3.8 x 10^5 PFU MNV-1-NR via oral gavage and assessed viral replication at 9 hpi via plaque assay. To determine if monocolonization of *B. theta* was successful, I first analyzed the small intestinal contents of MNV-1-NR infected mice for 16S DNA levels. Unfortunately, only 2 of the 5 *B. theta* monocolonized mice had detectable 16S DNA bands after PCR amplification (**Figure 3.9A**).

Furthermore, I found that colonization with *B. theta* did not alter MNV-1 regionalization seen in germ-free housed mice versus conventionally housed controls (see **Figure 3.5**) as MNV-1 replication was primarily detected in the duodenum in both germ-free and *B. theta* colonized cohorts (**Figure 3.9C**). There was no significant difference in MNV-1 viral loads between germ-free and *B. theta* colonized mice in any organ, and mice with detectable 16S DNA in their small

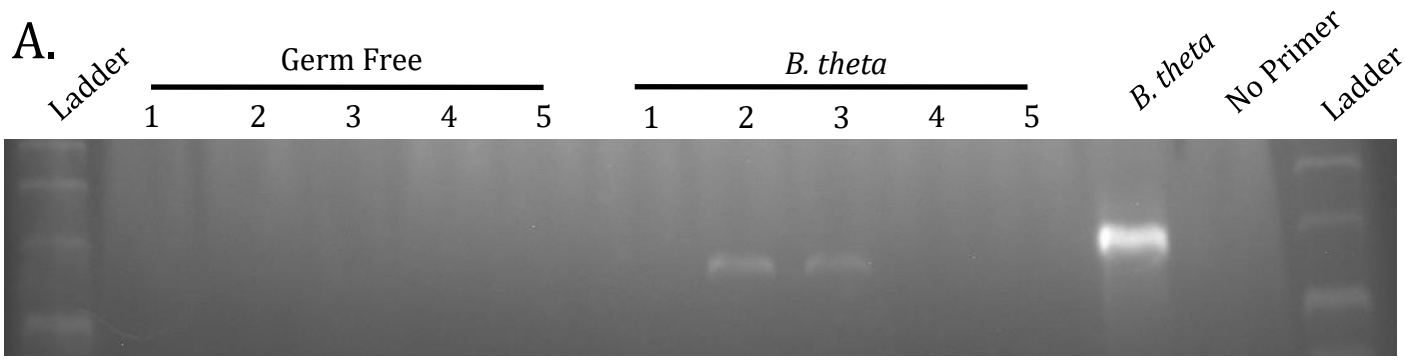
A.
Ladder
Germ Free
1
2
3
4
5
B. theta
1
2
3
4
5
B. theta
No Primer
Ladder

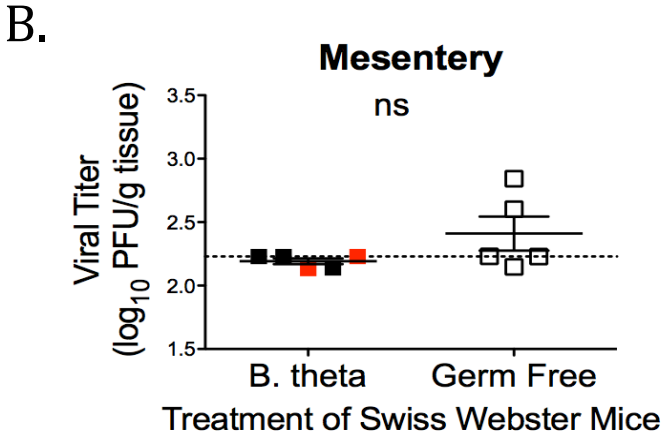
B.
Mesentery
ns
Viral Titer (log10 PFU/g tissue)
3.5
3.0
2.5
2.0
1.5
B. theta
Germ Free
Treatment of Swiss Webster Mice

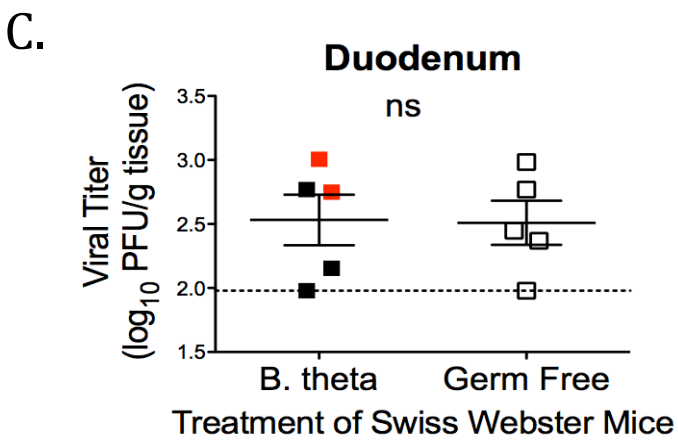
C.
Duodenum
ns
Viral Titer (log10 PFU/g tissue)
3.5
3.0
2.5
2.0
1.5
B. theta
Germ Free
Treatment of Swiss Webster Mice

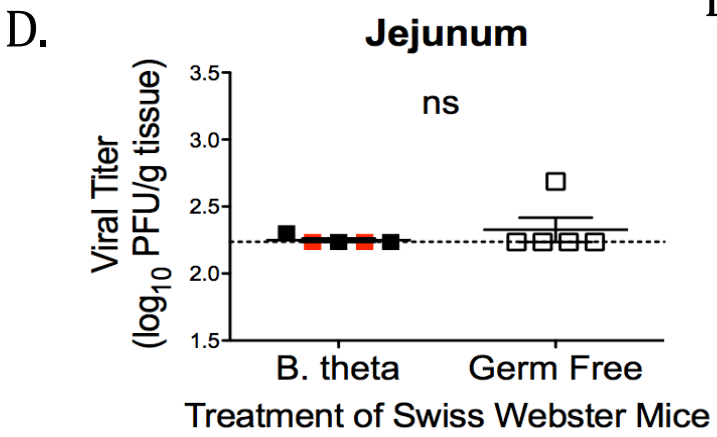
D.
Jejunum
ns
Viral Titer (log10 PFU/g tissue)
3.5
3.0
2.5
2.0
1.5
B. theta
Germ Free
Treatment of Swiss Webster Mice

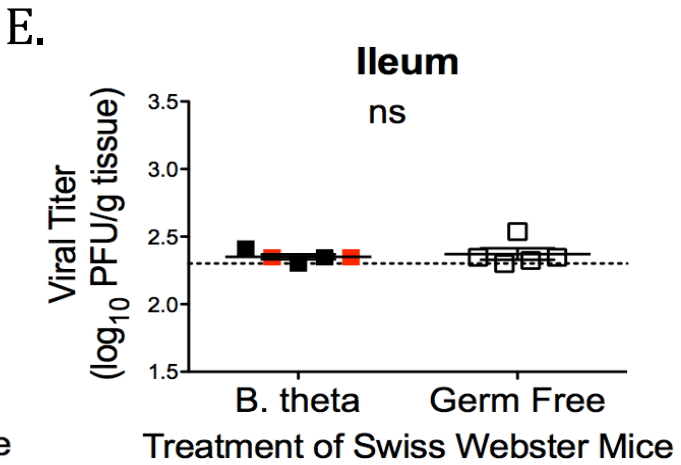
E.
Ileum
ns
Viral Titer (log10 PFU/g tissue)
3.5
3.0
2.5
2.0
1.5
B. theta
Germ Free
Treatment of Swiss Webster Mice

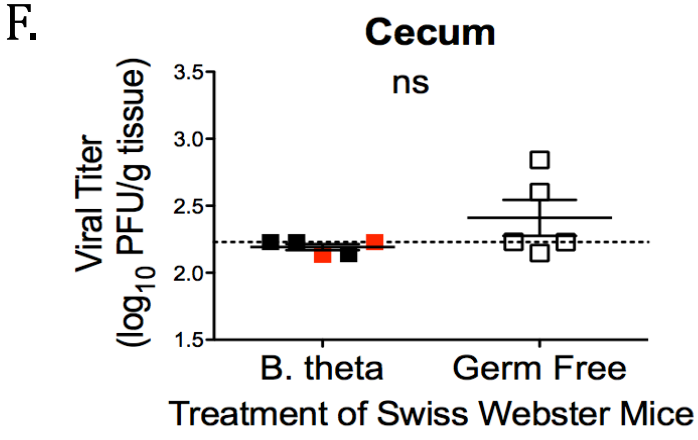
F.
Cecum
ns
Viral Titer (log10 PFU/g tissue)
3.5
3.0
2.5
2.0
1.5
B. theta
Germ Free
Treatment of Swiss Webster Mice

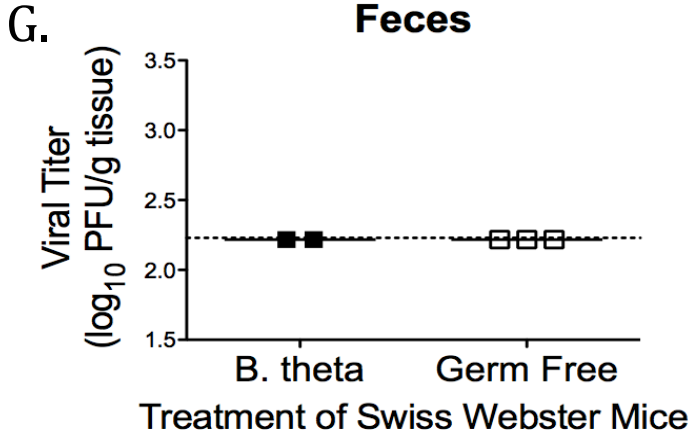
G.
Feces
Viral Titer (log10 PFU/g tissue)
3.5
3.0
2.5
2.0
1.5
B. theta
Germ Free
Treatment of Swiss Webster Mice

Figure 3.9: Monocolonization with *Bacteroides thetaiotaomicron* may not alter MNV-1 regionalization

A-G. Germ-free Swiss Webster mice were either untreated or colonized via oral gavage with $1x10^9$ colony forming units of *Bacteroides thetaiotaomicron* (*B. theta*) for 2 weeks before infection by oral gavage with $3.8x10^5$ PFU/animal of neutral red labeled MNV-1. Tissues and intestinal contents were harvested at 9 hpi in a darkened room using a red photolight. **A.** DNA was isolated from intestinal contents and a culture of *B. theta* grown overnight in LB broth at 37˚C. 16S rDNA was amplified via PCR and visualized using gel electrophoresis. **B-G.** The tissue homogenate was serially diluted and exposed to white light for 30 min. Replicated viral titers in the indicated tissue of germ-free and *B. theta* colonized Swiss Webster mice were assessed via plaque assay. The sensitivity threshold for each graph is indicated by the dashed line and is set at 10. Viral titers are displayed as log PFU/mL tissue**.** Data are from two independent experiments and each symbol is a data point from an individual animal. Error bars are standard error of the mean (SEM). Values were analyzed using Mann Whitney U test. ns = not statistically significant.

intestinal lumen (red squares) showed no obvious differences from their 16S undetectable *B. theta* colonized cohort (black squares), or germ-free mice (**Figure 3.9B-G**). These data suggest the MNV-1 binding to intestinal commensal *B. theta* was not capable of altering the intestinal regionalization of MNV-1 infection of germ-free mice, and thus the physical interaction may not be the main driver of the regionalization differences. However, future studies are needed to confirm these findings in additional animals.

3.3 Discussion

In this study I sought to determine if enhanced IFN-ɣ levels seen in the absence of SIg and SC were due to differences in immune sensing of bacterial communities in pIgR KO mice vs B6 Controls. I found that intestinal microbial communities are altered in the absence of SIg and the immune response to bacteria in the absence of SIg is skewed toward inflammation, as no enhancement in IFN-ɣ and iNOS transcripts were seen in naïve germ-free pIgR KO compared to germ-free B6. I also determined that MNV-1 was able to replicate to similar levels in germ-free mice regardless of SIg in contrast to conventionally housed pIgR KO mice which showed reduced MNV-1 replication in multiple organs throughout infection compared to controls, suggesting bacterial sensing in the presence of SIg is beneficial for MNV infection. Furthermore, antibiotic treatment of pIgR KO mice suggests that intestinal bacteria can modulate MNV infection in the absence of SIg sensing. These data, and findings outlined in Chapter 2, point to a model in which SIg indirectly promote norovirus infection through immune sensing of microbial communities. In this study I also sought to directly examine the role of bacteria in MNV pathogenesis. My findings revealed an altered intestinal distribution of MNV-1 and MNV-CR3 in germ-free mice compared to conventional WT B6 controls. This shift in regionalization could

not be explained by intestinal transit differences or MNV target cell availability or recapitulated with *B. theta*. Collectively, these data and published studies [12, 50] demonstrate that intestinal bacteria both directly and indirectly modulate norovirus infection.

In the case of MNV, infection of antibiotic-treated mice results in decreased MNV loads in the ileum [12, 50], and commensal bacteria promote MNV persistence in the intestine via modulation of type III interferon responses [13]. Our microbiome analysis revealed that different bacterial communities could support optimal MNV infection as no difference was seen in MNV-1 viral replication between WT B6 breeding facilities despite significant microbiome differences (see **Figure 3.1** and **Figure 2.2**). However, MNV infection was inhibited in pIgR KO mice when the intestines were inflamed, and a different microbial community was present compared to WT B6 controls. Direct assessment of microbial communities in naïve pIgR KO and WT B6 mice revealed enhanced *Firmicutes* species were present throughout the pIgR KO intestinal tract compared to WT B6 controls (see **Figure 3.1**), and these mice consistently exhibited decreased MNV-1 infection (see **Figure 2.2**). Interestingly, HNoV [30] and MNV [31] infection can both result in enhanced *Firmicutes* species contributing to intestinal microbial dysbiosis, however whether enhancement in *Firmicutes* species is detrimental to norovirus infection remains untested.

I found that, after initial detection at 9 hpi, MNV-1 viral titers increased throughout the time course in the ileum of WT B6 mice. However, there was no detectable MNV-1 infection in the ileum after the initial round of replication in pIgR KO mice compared to WT B6 mice (see **Figure 2.2**). MNV-1 infection appears to favor the cecum and colon at later times post infection (see **Figure 2.2** and **Figure 3.2**), perhaps due to the lower levels of IFN-ɣ found in those tissues compared to the ileum (see **Figure 2.10G**).

Norovirus infections are modulated directly and indirectly by the presence of commensal bacteria [11]. In case of MNV, infection of antibiotic-treated mice results in decreased MNV loads in the ileum [12, 50], and commensal bacteria promote MNV persistence in the intestine via modulation of type III interferon responses [13]. My preliminary (n=1, 4 mice/group) findings in antibiotically treated pIgR KO mice show reduced infection compared to conventional pIgR KO controls (see **Figure 3.2**). Furthermore, I determined that MNV infects germ-free pIgR KO and WT B6 mice similarly regardless of SIg and SC (see **Figure 3.5**). Together these data suggest that bacterial modulation of MNV infection is not dependent on SIg or SC.

In combination with results from Chapter 2 (see **Figure 2.2**), MNV-1 infection was reduced only in conventional pIgR KO mice, which exhibited elevated levels of intestinal iNOS and IFN-ɣ, but not in their germ-free counterpart, when naïve cytokine levels were similar to WT B6 mice. Since IFN-ɣ has well-recognized anti-norovirus activity [34-37], these data suggest that the immune response generated towards the enteric microbiota in the absence of SIg was capable of inhibiting norovirus replication. Enhanced ISG15 transcript levels were detected after MNV-1 infection of germ-free pIgR KO animals, but not germ-free WT B6 controls. These data suggest that, in the absence of tolerizing secretory immunoglobulins, at least parts of the immune response to MNV-1 infection may be enhanced. This enhancement in ISG15 transcripts in infected germ-free pIgR KO mice was not seen in conventionally housed pIgR KO animals (compare **Figure 2.10E** to **3.3E**) and could suggest bacterially-mediated immune suppression. Reduction in IFN-β and TNF-α levels seen in naive and infected conventional pIgR KO mice compared to WT B6 controls was not recapitulated in germ-free conditions (compare **Figure 2.10C-D** to **3.3C-D**), again suggesting that reduction in immune mediators is driven by the

intestinal microbiota. Together these results suggest that intestinal bacteria not only modulate MNV-1 infection but may also impact the resulting anti-viral immune response.

However, my data is not the first example of bacterially-mediated alterations in viral immunity. Similar observations have been demonstrated in rotavirus infection, with reduced bacterial species resulting in enhanced anti-rotaviral immunity regardless of viral burden [51]. Intestinal bacterial species can also modulate enteric viral infection directly. Similar to human norovirus [11, 12], both reovirus [52] and rotavirus [51] target cell entry is enhanced by the presence of intestinal bacteria, as is viral replication. Additionally, mouse mammary tumor virus (MMTV) utilizes bacterially-derived lipopolysaccharide to engage host pathogen recognition receptor toll-like receptor-4 (TLR-4) which promotes immune responses that are favorable for MMTV infection and host immune evasion [53, 54].

Under germ-free conditions, the intestinal distribution of MNV-1 is similar in both pIgR KO and WT B6 mice and is skewed (more virus in proximal intestine) compared to conventional WT B6 mice (compare **Figure 2.2** & **Figure 3.4**). However, in conventionally housed pIgR KO and WT B6 mice the intestinal distribution of MNV-1 is different between mouse strains (see **Figure 2.2**). These data suggest that intestinal distribution of MNV is dependent on bacteria regardless of the presence of SIg and SC. Previous studies regarding virus bacterial interactions have revealed that bacterial components can help to stabilize the poliovirus viral capsid resulting in increased infection and transmission [52, 55], however whether bacterial components stabilize MNV remains unexplored. It is possible that as MNV progresses through the harsh intestinal luminal environment virions become increasingly unstable without bacterial products to stabilize the capsid, resulting in reduced infection of the distal small intestine observed in germ-free animals.

My preliminary (n=1) studies of naive germ-free versus conventionally housed mice showed no differences in intestinal immune cell distribution throughout the small intestine. However, additional experimentation is needed before conclusions can be drawn as these findings are contrary to previous studies which show bacteria stimulate B and T cell populations [45].One potential reason for the lack of expansion in immune cell subsets in conventionally housed animals compared to germ-free housed animals may be attributed to the cleanliness of our animal facility. Since MNV is endemic in animal facilities across the country [56], great precaution is taken to minimize potential pre-exposure to MNV in our facility. Another potential reason could be the collection and digestion method used for analysis. I analyzed both lymphoid and non-lymphoid tissue together, however perhaps if I had analyzed them separately minor differences would be revealed. Although more work must be done, the current studies into these trans-kingdom interactions suggest that intestinal bacteria modulate MNV infection and distribution throughout the gastrointestinal tract.

Investigation into the mechanism of altered intestinal distribution of MNV in germ-free mice led us to hypothesize that altered intestinal motility might account for the reduced MNV-1 infection in the distal small intestine (see **Figure 3.2**). Previous studies investigating intestinal motility under germ-free conditions measured transit of yttrium 91, which was significantly delayed in germ-free mice after intragastric administration compared to conventional controls [43]. Twelve week antibiotic (ampicillin and neomycin) treatment of conventional C3H/HeOuJ mice resulted in increased stool retention and reduced defecation compared to untreated controls suggesting bacterial modulation of intestinal motility [57]. Despite these previously seen differences in gastrointestinal transit, I did not find any differences between germ-free and

conventional control animals. There may be several reasons for this discrepancy including varied detection methods, mouse strains, and bacterial colonization status.

Several studies have suggested bacterial interactions aid in norovirus infection [11-13]. However, preliminary results from Swiss Webster mice after confirmed monocolonization of *B. theta* (**d**, red squares) suggest that MNV-1 binding to intestinal bacteria may not always facilitate MNV-1 infection. *B.* theta used in this study were grown under conditions shown to stimulate SusD expression [58] and therefore mediate MNV binding. However, the presence of SusD was not confirmed, and could account for the lack of change in MNV-1 distribution after *B. theta* colonization compared to germ-free controls. In the future, it would be interesting to determine if *B. theta* binding to MNV-1 will enhance target cell attachment, and if robust *B. theta* colonization is sufficient to correct intestinal distribution of MNV-1 viral replication seen in germ-free mice compared to conventional controls.

Taken together, my work suggests intestinal commensal bacteria are capable of modulating: 1. MNV distribution throughout the gastrointestinal tract, 2. MNV viral loads, and 3. anti-MNV host immunity through secretory immunoglobulins. These studies highlight the need for further trans-kingdom studies to understand the complex intestinal threesome between host, bacteria, and norovirus.

3.4 Materials & Methods

Animals. C57BL/6 mice were purchased from Jackson Laboratories (Bar Harbor, ME) and housed in SPF- and MNV-free conditions. A breeder pair of PIgR knockout mice on a C57BL/6 background (B6.129P2-*Pigr*^{tm1Fejo}/Mmmh, stock number: 030988-MU) was obtained from Drs.

Stappenbeck and Virgin (Washington University, St. Louis, MO). All mice were bred and housed in SPF- and MNV-free conditions. Germ-free C57/BL6, Swiss Webster, and pIgR KO mice were derived and housed in University of Michigan Germ-Free and Gnotobiotic facilities. Germ-free status was verified regularly through fecal analysis and necropsy. Age and sex matched experimental mice were used between 6 and 16 weeks of age. Mice used in the study were seronegative for anti-MNV antibodies by enzyme-linked immunosorbent assay (ELISA) as described previously [48]. Animal studies were performed in accordance with local and federal guidelines. The protocol was approved by the University of Michigan Committee on Use and Care of Animals (UCUCA number PRO00006658).

16S rRNA gene Sequencing. The Microbial Systems Molecular Biology Laboratory at the University of Michigan provided 16S rRNA gene sequencing and analysis of samples. DNA was isolated with a MagAttract PowerMicrobiome DNA/RNA Kit (Qiagen) using an epMotion 5075 liquid handling system. The V4 region of the 16S rRNA gene was amplified and sequenced as described previously except using a MiSeq Reagent Nano Kit v2 (500-cycles)[59]. The 16S rRNA gene sequence data was processed and analyzed using the software package mothur (v.1.40.2) and the most recent MiSeq SOP [60, 61]. After sequence processing and alignment to the SILVA reference alignment (release 128) [62], sequences were binned into operational taxonomic units (OTUs) based on 97% sequence similarity using the OptiClust method [63]. A total of 2212 sequences per sample were subsampled and samples with fewer than 2212 sequences were not included in the analysis. By calculating θ_{YC} distances (a metric that takes relative abundances of both shared and non-shared OTUs into account) [64] between communities and using analysis of molecular variance (AMOVA) [65] it was possible to

determine if there were statistically significant differences between the microbiota of different groups. Principal coordinates analysis (PCoA) was used to visualize the θ_{YC} distances between samples by plotting in R (version 3.5.1). We also investigated the microbial diversity via Inverse Simpson (invsimpson) analysis as well as taxonomic composition of the bacterial communities by classifying sequences within mothur using a modified version of the Ribosomal Database Project (RDP) training set (version 16) [66, 67].

Viral Stocks. The plaque-purified MNV-1.CW3 (GV/MNV-1/2002/USA) virus stock (herein referred to as MNV-1) was generated as previously described [14]. A neutral red-labeled MNV-1 (MNV-1-NR) ($3.8x10^6$ PFU/mL), and MNV-CR3 stock (MNV-CR3-NR) ($3x10^6$ PFU/mL), were generated from MNV-1 and MNV-CR3 (GV/CR3/2005/USA) passage 6, as previously described [68]. MNV-1-NR and MNV-CR3-NR was handled in a darkened room using a red photolight (Premier OMNI) and stored in a light safe box at -80°C. To assess MNV-1-NR light inactivation, stocks of MNV-1-NR were exposed to white light or left in darkness and samples were taken every 5 minutes to assess light mediated reduction in viral titer via plaque assay.

MNV-1 Ileal Contents Binding Assay. Ileal contents were removed from naïve pIgR KO and WT B6 mice and contents were allowed to pass through a 100 micron strainer by flushing with 10 mLs of cold 1x PBS. PBS was removed, and pass-through contents were collected after centrifugation (10,000 rpm 5 min). Contents were weighed and resuspended in 500 μl PBS and equal weight of ileal contents was added to wells of a 96 well U bottom plate (Fisher Scientific). Contents were spun down (10,000 rpm 1 min) to remove 1xPBS and were resuspend in 200 μl ($1.34x10^7$ PFU) MNV-1. After an hour incubation at room temperature, contents were washed

with 1 ml 1x PBS, spun down (10,000 rpm 1 min), and supernatant was discarded. This process was repeated twice to remove unbound MNV-1 and contents were stored in RNALater at -80˚C until RNA isolation as described below.

RNA Isolation. Total RNA was extracted from tissues using TRIzol® Reagent (ThermoFisher Scientific) following the manufacturers guidelines. Contaminating genomic DNA was removed by treating samples with Turbo DNA free DNase kit (ThermoFisher Scientific). Total RNA was quantified using a spectrophotometer (NanoDrop) and stored at -80°C.

Quantitative Real-Time PCR. To measure host cell transcripts, cDNA was generated with 100 μg of total RNA using iScript Reverse Transcription Supermix for RT-qPCR (Bio-Rad #1708841) in a thermocycler (Eppendorf Mastercycler Epgradient PCR machine) and stored at -20°C. cDNA was analyzed for levels of Gapdh [69], GP2 [69], Spi-B [69], interferon-gamma (IFN-ɣ) [70], interferon-beta (IFN-β) [70], tumor necrosis factor-alpha (TNF-α) [70], inducible nitric oxide synthase (iNOS) [71], interferon stimulated gene 15 (ISG15) [72], transforming growth factor-beta (TGF-β) [73], interleukin-10 (IL-10) [74], interferon-lambda (IFN-λ) [72] in a Biorad CFX96 Real Time System qPCR machine using Sso Advanced Universal SYBR Green Supermix (Bio-Rad). Gene expression was normalized to transcript levels of the endogenous host gene *Gapdh*, and fold change was calculated relative to WT B6 controls using the delta delta CT method [75]. Quantification of MNV-1 genome equivalents in host tissue was performed as previously described [14].

Animal Infections. Mice were infected via oral gavage (o.g.) with 3.8 x 10^5 PFU MNV-1-NR or 2.6x10^5 PFU MNV-CR3-NR in 100 μl/mouse in a red light only room. Mice received intraperitoneal infection of 3.8 x 10^5 PFU MNV-1-NR in 100 μl/mouse in a red light only room. Tissues were harvested at 9, 18, or 48 hours post infection (hpi) as previously described [76] with the following modifications: 2 cm of tissue was collected in pre-weighed tubes containing 1.0 mm diameter zirconia/silica beads (BioSpec), flash frozen in an ethanol/dry ice bath, weighed, and stored at -80°C. Mice were infected via o.g. with 2x10^6 PFU of reovirus T1L. Tissues were harvested at 24 hpi and processed as described for MNV, with the modification that 1 cm of tissue was collected.

Plaque Assay. Homogenized samples were exposed to white light for 30 min to inactivate input virus. Light exposure reduced MNV-1-NR titers by 3 logs. The plaque assay was performed as previously described [77]. Samples without detectable replicated virus were assigned 10 PFU/ml as the lowest detectable unit. Data were normalized to the tissue weight and expressed as PFU per gram of tissue. The sensitivity threshold was determined for each organ by averaging the PFU/gram tissue of all samples without detectable viral titers.

Antibiotic Treatment of PIgR KO Mice. Cefoperazone (MP biomedicals #199695) was diluted to [0.5g/L] in distilled water and kept protected from light using brown bottles and administered to conventionally housed pIgR KO mice via drinking water. Antibiotic treated, or regular distilled water as a control was changed every other day for 7 days. Mice were then infected with 3.8 x 10^5 PFU MNV-1-NR via oral gavage and tissues and intestinal contents were collected at 9 hpi under red light only conditions. Antibiotic treatment efficacy was assessed by collecting

intestinal contents from antibiotically treated and control pIgR KO mice at 18 hpi. Intestinal contents were allowed to pass through a 100-micron strainer by flushing with 10 mLs of cold 1x PBS. PBS was removed, and pass-through contents were collected after centrifugation (10,000 rpm 5 min). Contents were weighed and resuspended in 500 μl LB broth (Fisher Scientific) and equal weight of ileal contents was serially diluted in 500ul LB broth. 100 ul aliquots from each dilution was plated onto BHI plates and colonies >1.2mm were counted using an aCOLyte colony counter (Synbiosis) after overnight incubation at 37˚C.

Intestinal Transit Assay. To measure intestinal transit time, mice were fasted for 18 h, gavaged orally with 100 ml 50 mg/ml Evans Blue solution in 1x PBS (Gibco) prepared with 1% methylcellulose and euthanized 15 min later. The small intestine was divided into fifths and each piece was minced in 1x PBS containing 0.1 M sodium hydroxide, 6 mM N-acetylcysteine, sonicated, and the absorbance at 565 nm determined as previously described [78].

Tissue Digestion/ Flow Cytometry. PP and small intestine lamina propria were dissected from naive PIgR KO and WT B6 mice and digested as previously described [49]. $2x10^6$ cells were then used for flow cytometric analysis. Viable cells were identified (Invitrogen Live/Dead fixable Aqua Dead Cell stain Kit) and then stained for the following surface markers: CD45 (diluted 1:200, clone 30-F11, AF700, Biolegend), I-A/I-E (diluted 1:50, clone M5/114.15.2, PE/Dazzle 594, Biolegend), CD19 (diluted 1:50, clone 6D5, PerCP/Cy5.5, Biolegend), CD11b (diluted 1:50, clone M1/70 APC/Cy7, Biolegend), CD64 (diluted 1:50, clone X54-5/7.1 FITC, Biolegend) CD11c (diluted 1:50, clone N418 PE/Cy7, Biolegend) CD103 (diluted 1:25, clone 2EZ, APC, Biolegend), CX3CR1 (diluted 1:50, clone SA011F11, PE, Biolegend), CD8 (diluted

1:100, clone 53-6.7, APC-Cy7 Biolegend). All antibodies were diluted in FACS buffer; 5% fetal bovine serum (Hyclone) and 0.1% sodium azide (Sigma) in 1x PBS, for 30 min on ice. After surface staining, cells were fixed for 10 min on ice using Cytofix/Cytoperm (BD Biosciences), washed and fluorescence was analyzed with a BD LSR Fortessa. Data was analyzed using FlowJo software (BD Biosciences) using the gating strategy outlined in **Table 3.1**.

***Bacteroides thetaiotaomicron* (*B. theta*) Monocolonization of Swiss Webster Mice.**

Germ-free Swiss Webster mice were either media treated or colonized via oral gavage with $1x10^9$ colony forming units of *Bacteroides thetaiotaomicron* (*B. theta*), for 2 weeks before infection with $3.8x10^5$ MNV-1-NR via oral gavage. Small intestinal contents and the gastrointestinal tract was harvested at 9 hpi as described above. To assess colonization efficiency, DNA was isolated from intestinal contents using Promega Wizard genomic DNA purification kit Protocol 3.G. "Isolating Genomic DNA from Gram-Positive and Gram-Negative Bacteria" following the manufacturers protocols. The 16S DNA [79] was amplified in 5 ng total DNA using Taq polymerase (Invitrogen) and dNTPs (Invitrogen) and the following PCR reaction: 95˚C for 5 min, 95 ˚C for 30 sec, 50˚C for 30 sec, 72 ˚C for 1.5 min 72 ˚C for 5 min. PCR products were separated on a 2% agarose gel, stained with ethidium bromide (Fisher Scientific), and DNA was visualized via ultraviolet light.

Statistical Analysis. Unless otherwise stated, data were analyzed using Mann Whitney U test with GraphPad Prism software version 7 (GraphPad Software, La Jolla, CA). *= $P<0.05$. **= $P<0.01$ ***= $P<0.001$. ****= $P<0.0001$. ns= not significant.

3.5 Acknowledgements

I would like to thank Dr. Kate Eaton and her team at the University of Michigan Germ-Free and Gnotobiotic facilities for their continued diligence. I would also like to thank Joel Whitfield at the University of Michigan Cancer Center Immunology ELISA core, and Clarisse Betancourt Román, and Christine Bassis at the University of Michigan Host Microbiome Initiative for making extreme exceptions so that I could have my data in time for resubmission.

3.6 References

1. Mowat, A.M. and W.W. Agace, *Regional specialization within the intestinal immune system.* Nat Rev Immunol, 2014. **14**(10): p. 667-85.
2. Corthesy, B., *Roundtrip ticket for secretory IgA: role in mucosal homeostasis?* J Immunol, 2007. **178**(1): p. 27-32.
3. Sakamoto, N., et al., *A novel Fc receptor for IgA and IgM is expressed on both hematopoietic and non-hematopoietic tissues.* Eur J Immunol, 2001. **31**(5): p. 1310-6.
4. Kaetzel, C.S., *Cooperativity among secretory IgA, the polymeric immunoglobulin receptor, and the gut microbiota promotes host-microbial mutualism.* Immunol Lett, 2014. **162**(2 Pt A): p. 10-21.
5. Mantis, N.J., et al., *Selective adherence of IgA to murine Peyer's patch M cells: evidence for a novel IgA receptor.* J Immunol, 2002. **169**(4): p. 1844-51.
6. Baumann, J., C.G. Park, and N.J. Mantis, *Recognition of secretory IgA by DC-SIGN: implications for immune surveillance in the intestine.* Immunol Lett, 2010. **131**(1): p. 59-66.
7. Mantis, N.J., N. Rol, and B. Corthesy, *Secretory IgA's complex roles in immunity and mucosal homeostasis in the gut.* Mucosal Immunol, 2011. **4**(6): p. 603-11.
8. Krajmalnik-Brown, R., et al., *Effects of gut microbes on nutrient absorption and energy regulation.* Nutr Clin Pract, 2012. **27**(2): p. 201-14.
9. Pereira, F.C. and D. Berry, *Microbial nutrient niches in the gut.* Environ Microbiol, 2017. **19**(4): p. 1366-1378.
10. Vogt, S.L. and B.B. Finlay, *Gut microbiota-mediated protection against diarrheal infections.* J Travel Med, 2017. **24**(suppl_1): p. S39-s43.
11. Karst, S.M., *The influence of commensal bacteria on infection with enteric viruses.* Nat Rev Microbiol, 2016. **14**(4): p. 197-204.
12. Jones, M.K., et al., *Enteric bacteria promote human and mouse norovirus infection of B cells.* Science, 2014. **346**(6210): p. 755-9.

13. Baldridge, M.T., et al., *Commensal microbes and interferon-lambda determine persistence of enteric murine norovirus infection.* Science, 2015. **347**(6219): p. 266-9.
14. Taube, S., et al., *Murine noroviruses bind glycolipid and glycoprotein attachment receptors in a strain-dependent manner.* J Virol, 2012. **86**(10): p. 5584-93.
15. Taube, S., et al., *Ganglioside-linked terminal sialic acid moieties on murine macrophages function as attachment receptors for murine noroviruses.* J Virol, 2009. **83**(9): p. 4092-101.
16. Bally, M., et al., *Norovirus GII.4 virus-like particles recognize galactosylceramides in domains of planar supported lipid bilayers.* Angew Chem Int Ed Engl, 2012. **51**(48): p. 12020-4.
17. Rydell, G.E., et al., *Human noroviruses recognize sialyl Lewis x neoglycoprotein.* Glycobiology, 2009. **19**(3): p. 309-20.
18. Tamura, M., et al., *Genogroup II noroviruses efficiently bind to heparan sulfate proteoglycan associated with the cellular membrane.* J Virol, 2004. **78**(8): p. 3817-26.
19. Almagro-Moreno, S. and E.F. Boyd, *Bacterial catabolism of nonulosonic (sialic) acid and fitness in the gut.* Gut Microbes, 2010. **1**(1): p. 45-50.
20. Tan, M. and X. Jiang, *Histo-blood group antigens: a common niche for norovirus and rotavirus.* Expert Rev Mol Med, 2014. **16**: p. e5.
21. Sestak, K., *Role of histo-blood group antigens in primate enteric calicivirus infections.* World J Virol, 2014. **3**(3): p. 18-21.
22. Miura, T., et al., *Histo-blood group antigen-like substances of human enteric bacteria as specific adsorbents for human noroviruses.* J Virol, 2013. **87**(17): p. 9441-51.
23. Li, D., et al., *Binding to histo-blood group antigen-expressing bacteria protects human norovirus from acute heat stress.* Front Microbiol, 2015. **6**: p. 659.
24. Pettigrew, M.M., J.K. Johnson, and A.D. Harris, *The human microbiota: novel targets for hospital-acquired infections and antibiotic resistance.* Ann Epidemiol, 2016. **26**(5): p. 342-7.
25. Agnihothram, S.S., et al., *Infection of Murine Macrophages by Salmonella enterica Serovar Heidelberg Blocks Murine Norovirus Infectivity and Virus-induced Apoptosis.* PLoS One, 2015. **10**(12): p. e0144911.
26. Li, D., et al., *Anti-viral Effect of Bifidobacterium adolescentis against Noroviruses.* Front Microbiol, 2016. **7**: p. 864.
27. Lee, H. and G. Ko, *Antiviral effect of vitamin A on norovirus infection via modulation of the gut microbiome.* Sci Rep, 2016. **6**: p. 25835.
28. De Minicis, S., et al., *Dysbiosis contributes to fibrogenesis in the course of chronic liver injury in mice.* Hepatology, 2014. **59**(5): p. 1738-49.
29. Compare, D., et al., *The Gut Bacteria-Driven Obesity Development.* Dig Dis, 2016. **34**(3): p. 221-9.
30. Nelson, A.M., et al., *Disruption of the human gut microbiota following Norovirus infection.* PLoS One, 2012. **7**(10): p. e48224.
31. Hickman, D., et al., *The effect of malnutrition on norovirus infection.* MBio, 2014. **5**(2): p. e01032-13.

32. Nelson, A.M., et al., *Murine norovirus infection does not cause major disruptions in the murine intestinal microbiota.* Microbiome, 2013. **1**(1): p. 7.
33. Huang, J., et al., *Site-specific glycosylation of secretory immunoglobulin A from human colostrum.* J Proteome Res, 2015. **14**(3): p. 1335-49.
34. Changotra, H., et al., *Type I and type II interferons inhibit the translation of murine norovirus proteins.* J Virol, 2009. **83**(11): p. 5683-92.
35. Maloney, N.S., et al., *Essential cell-autonomous role for interferon (IFN) regulatory factor 1 in IFN-gamma-mediated inhibition of norovirus replication in macrophages.* J Virol, 2012. **86**(23): p. 12655-64.
36. Hwang, S., et al., *Nondegradative role of Atg5-Atg12/ Atg16L1 autophagy protein complex in antiviral activity of interferon gamma.* Cell Host Microbe, 2012. **11**(4): p. 397-409.
37. Biering, S.B., et al., *Viral Replication Complexes Are Targeted by LC3-Guided Interferon-Inducible GTPases.* Cell Host Microbe, 2017. **22**(1): p. 74-85 e7.
38. Rubin, B.Y., et al., *The anticellular and protein-inducing activities of human gamma interferon preparations are mediated by the interferon.* J Immunol, 1983. **130**(3): p. 1019-20.
39. Sait, L., et al., *Secretory antibodies do not affect the composition of the bacterial microbiota in the terminal ileum of 10-week-old mice.* Appl Environ Microbiol, 2003. **69**(4): p. 2100-9.
40. Reikvam, D.H., et al., *Epithelial-microbial crosstalk in polymeric Ig receptor deficient mice.* Eur J Immunol, 2012. **42**(11): p. 2959-70.
41. Baldridge, M.T., H. Turula, and C.E. Wobus, *Norovirus Regulation by Host and Microbe.* Trends Mol Med, 2016. **22**(12): p. 1047-1059.
42. Lyon, J.A., *Cefoperazone (Cefobid, Pfizer).* Drug Intell Clin Pharm, 1983. **17**(1): p. 7-11.
43. Abrams, G.D. and J.E. Bishop, *Effect of the normal microbial flora on gastrointestinal motility.* Proc Soc Exp Biol Med, 1967. **126**(1): p. 301-4.
44. Johansson, M.E., et al., *Normalization of Host Intestinal Mucus Layers Requires Long-Term Microbial Colonization.* Cell Host Microbe, 2015. **18**(5): p. 582-92.
45. Min, Y.W. and P.L. Rhee, *The Role of Microbiota on the Gut Immunology.* Clin Ther, 2015. **37**(5): p. 968-75.
46. Parker, A., et al., *Host-microbe interaction in the gastrointestinal tract.* Environ Microbiol, 2018. **20**(7): p. 2337-2353.
47. Nothaft, H. and C.M. Szymanski, *Protein glycosylation in bacteria: sweeter than ever.* Nat Rev Microbiol, 2010. **8**(11): p. 765-78.
48. Wobus, C.E., et al., *Replication of Norovirus in cell culture reveals a tropism for dendritic cells and macrophages.* PLoS Biol, 2004. **2**(12): p. e432.
49. Geem, D., et al., *Isolation and characterization of dendritic cells and macrophages from the mouse intestine.* J Vis Exp, 2012(63): p. e4040.
50. Kernbauer, E., Y. Ding, and K. Cadwell, *An enteric virus can replace the beneficial function of commensal bacteria.* Nature, 2014. **516**(7529): p. 94-8.
51. Uchiyama, R., et al., *Antibiotic treatment suppresses rotavirus infection and enhances specific humoral immunity.* J Infect Dis, 2014. **210**(2): p. 171-82.
52. Kuss, S.K., et al., *Intestinal microbiota promote enteric virus replication and systemic pathogenesis.* Science, 2011. **334**(6053): p. 249-52.

53. Wilks, J., et al., *Mammalian Lipopolysaccharide Receptors Incorporated into the Retroviral Envelope Augment Virus Transmission.* Cell Host Microbe, 2015. **18**(4): p. 456-62.
54. Kane, M., et al., *Successful transmission of a retrovirus depends on the commensal microbiota.* Science, 2011. **334**(6053): p. 245-9.
55. Robinson, C.M., P.R. Jesudhasan, and J.K. Pfeiffer, *Bacterial lipopolysaccharide binding enhances virion stability and promotes environmental fitness of an enteric virus.* Cell Host Microbe, 2014. **15**(1): p. 36-46.
56. Ohsugi, T., et al., *Natural infection of murine norovirus in conventional and specific pathogen-free laboratory mice.* Front Microbiol, 2013. **4**: p. 12.
57. Iwai, H., et al., *Effects of bacterial flora on cecal size and transit rate of intestinal contents in mice.* Jpn J Exp Med, 1973. **43**(4): p. 297-305.
58. Foley, M.H., E.C. Martens, and N.M. Koropatkin, *SusE facilitates starch uptake independent of starch binding in B. thetaiotaomicron.* Mol Microbiol, 2018. **108**(5): p. 551-566.
59. Seekatz, A.M., et al., *Fecal Microbiota Transplantation Eliminates Clostridium difficile in a Murine Model of Relapsing Disease.* Infection and Immunity, 2015. **83**(10): p. 3838-3846.
60. Kozich, J.J., et al., *Development of a Dual-Index Sequencing Strategy and Curation Pipeline for Analyzing Amplicon Sequence Data on the MiSeq Illumina Sequencing Platform.* Applied and Environmental Microbiology, 2013. **79**(17): p. 5112-5120.
61. Schloss, P.D., et al., *Introducing mothur: Open-Source, Platform-Independent, Community-Supported Software for Describing and Comparing Microbial Communities.* Appl. Environ. Microbiol., 2009. **75**(23): p. 7537-7541.
62. Schloss, P.D., *A High-Throughput DNA Sequence Aligner for Microbial Ecology Studies.* PLoS ONE, 2009. **4**(12): p. e8230.
63. Westcott, S.L. and P.D. Schloss, *OptiClust, an Improved Method for Assigning Amplicon-Based Sequence Data to Operational Taxonomic Units.* mSphere, 2017. **2**(2).
64. Yue, J.C. and M.K. Clayton, *A similarity measure based on species proportions.* Communications in Statistics-Theory and Methods, 2005. **34**(11): p. 2123-2131.
65. Anderson, M.J., *A new method for non-parametric multivariate analysis of variance.* Austral Ecology, 2001. **26**(1): p. 32-46.
66. Wang, Q., et al., *Naive Bayesian Classifier for Rapid Assignment of rRNA Sequences into the New Bacterial Taxonomy.* Appl. Environ. Microbiol., 2007. **73**(16): p. 5261-5267.
67. Cole, J.R., et al., *Ribosomal Database Project: data and tools for high throughput rRNA analysis.* Nucleic Acids Research (Online), 2014. **42**(Database issue): p. D633-42.
68. Gonzalez-Hernandez, M.B., J.W. Perry, and C.E. Wobus, *Neutral Red Assay for Murine Norovirus Replication and Detection in a Mouse.* Bio Protoc, 2013. **3**(7).
69. Wood, M.B., D. Rios, and I.R. Williams, *TNF-alpha augments RANKL-dependent intestinal M cell differentiation in enteroid cultures.* Am J Physiol Cell Physiol, 2016. **311**(3): p. C498-507.

70. Mohanty, S.K., et al., *Loss of interleukin-12 modifies the pro-inflammatory response but does not prevent duct obstruction in experimental biliary atresia.* BMC Gastroenterol, 2006. **6**: p. 14.
71. Stoolman, J.S., et al., *Latent infection by gammaherpesvirus stimulates profibrotic mediator release from multiple cell types.* Am J Physiol Lung Cell Mol Physiol, 2011. **300**(2): p. L274-85.
72. Lopusna, K., et al., *Murine gammaherpesvirus targets type I IFN receptor but not type III IFN receptor early in infection.* Cytokine, 2016. **83**: p. 158-170.
73. Henderson, N.C., et al., *Galectin-3 regulates myofibroblast activation and hepatic fibrosis.* Proc Natl Acad Sci U S A, 2006. **103**(13): p. 5060-5.
74. Terashima, A., et al., *A novel subset of mouse NKT cells bearing the IL-17 receptor B responds to IL-25 and contributes to airway hyperreactivity.* J Exp Med, 2008. **205**(12): p. 2727-33.
75. Higgins, P.D., et al., *Transient or persistent norovirus infection does not alter the pathology of Salmonella typhimurium induced intestinal inflammation and fibrosis in mice.* Comp Immunol Microbiol Infect Dis, 2011. **34**(3): p. 247-57.
76. Gonzalez-Hernandez, M.B., et al., *Efficient norovirus and reovirus replication in the mouse intestine requires microfold (M) cells.* J Virol, 2014. **88**(12): p. 6934-43.
77. Gonzalez-Hernandez, M.B., J. Bragazzi Cunha, and C.E. Wobus, *Plaque assay for murine norovirus.* J Vis Exp, 2012(66): p. e4297.
78. Bagyanszki, M., et al., *Chronic alcohol consumption affects gastrointestinal motility and reduces the proportion of neuronal NOS-immunoreactive myenteric neurons in the murine jejunum.* Anat Rec (Hoboken), 2010. **293**(9): p. 1536-42.
79. Klindworth, A., et al., *Evaluation of general 16S ribosomal RNA gene PCR primers for classical and next-generation sequencing-based diversity studies.* Nucleic Acids Res, 2013. **41**(1): p. e1.

Chapter 4: Discussion & Future Directions

4.1 Summary of Results

Enteric virus infections, such as norovirus, cause significant morbidity and mortality worldwide. However, direct antiviral infection prevention strategies are limited. Herein, I investigated the role of the polymeric immunoglobulin receptor (pIgR) – secretory immunoglobulin (SIg) cycle and enteric bacteria during enteric virus infections. The classical innate immune functions of SIg (agglutination, immune exclusion, neutralization, and expulsion) were not required during control of acute murine norovirus (MNV) infection. Specifically, data in **Figure 2.7D** showed MNV epithelial binding was not altered, suggesting natural SIg-mediated agglutination and immune exclusion are not sufficient to limit MNV access to the epithelial barrier. SIg-mediated intraepithelial expulsion is also not sufficient to limit MNV epithelial crossing as **Figure 2.7E** shows no difference in MNV barrier crossing. Furthermore, data in **Figure 2.2** showed reduced titers of MNV in intestinal tissues after the first and second round of viral replication suggesting that despite MNV binding to IgA and SC (data not shown) SIg is not mediating MNV neutralization in the lumen, or expulsion from the lamina propria. Instead, lack of pIgR resulted in increased IFN-ɣ levels in conventionally housed mice (see **Figure 2.10A**), This in turn contributed to reduced MNV titers (see **Figure 2.12**). Another enteric virus, reovirus, also showed decreased infection in pIgR KO mice (see **Figure 2.4**).

Investigation into the signals resulting in enhanced IFN-ɣ and iNOS stimulus in pIgR KO mice revealed altered intestinal microbial communities in pIgR KO mice (see **Figure 3.1**). When mice were rederived under germ-free conditions, IFN-ɣ and iNOS levels were equivalent between strains (see **Figure 3.3A-B**) as was MNV-1 viral replication (see **Figure 3.4**). Probing the role of intestinal bacteria on MNV infection, I found that bacteria alter MNV-1 and MNV-CR3 gastrointestinal regionalization despite equivalent gastrointestinal motility (see **Figure 3.5G**) and MNV target cell distribution (see **Figure 3.7**). Collectively, my data point to a model in which SIg-mediated microbial sensing promotes norovirus and reovirus infection (**Figure 4.1**). These data provide the first evidence of the pro-viral role of natural SIg during enteric virus infections and provide another example of how intestinal bacterial communities indirectly influence MNV pathogenesis. These findings highlight the need to further study complex, trans-kingdom interactions and their effects on the host. Below, I will discuss potential future studies into SIg and bacterial interactions with two enteric viruses; norovirus and reovirus.

4.2 Determine Whether Natural Secretory Immunoglobulins and Polymeric Immunoglobulin Receptor Aid in Murine Norovirus Shedding

There are several immune defense functions of SIg that may limit MNV access to the host interior and reduce infection, however the SIg:MNV interaction may also be beneficial for MNV. We hypothesized that MNV interaction with SIg may provide selective uptake of SIg:MNV complexes across the epithelial barrier by M cells. However, I was unable to detect any enhanced epithelial crossing of MNV in the presence of SIg. This suggests that SIg are neither helping nor hindering MNV to cross the epithelial barrier.

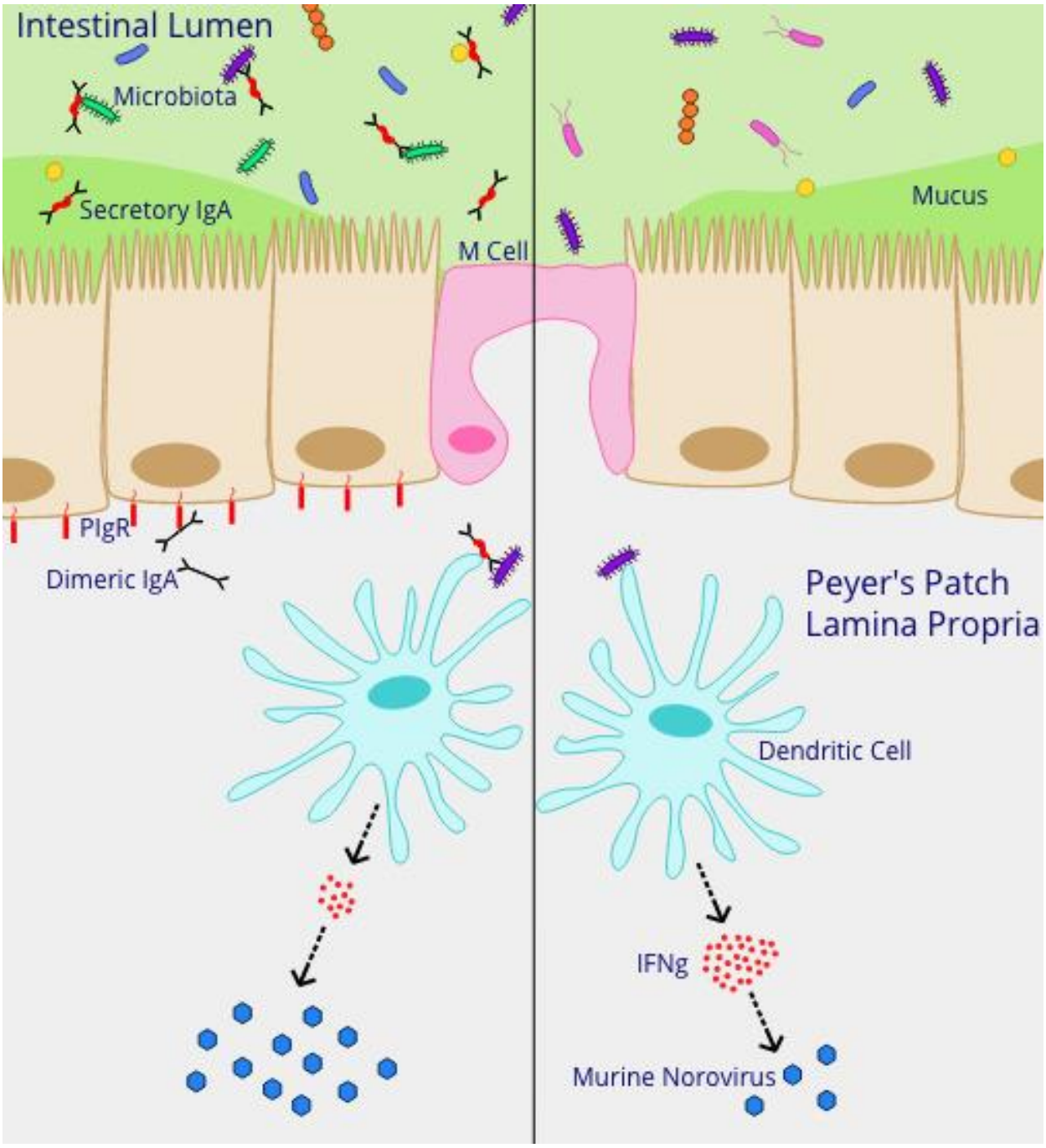
Intestinal Lumen
Microbiota
Secretory IgA
M Cell
Mucus
PIgR
Dimeric IgA
Peyer's Patch
Lamina Propria
Dendritic Cell
IFNg
Murine Norovirus

Figure 4.1: Model of natural secretory immunoglobulin enhancement of norovirus infection.
Dimeric IgA are transcytosed across the mucosal epithelial barrier into the intestinal lumen via the polymeric immunoglobulin receptor (pIgR), forming secretory IgA (SIgA). In the lumen, SIgA binds to microbes via antigen-binding domains or carbohydrate residues. Specialized cells in the follicle-associated epithelium (FAE), called microfold (M) cells, transport SIgA-immune complexes and microbes into the PP lamina propria to be sampled by underlying dendritic cells (DC), which mediates immune responses. DC:immune complex sensing is tolerogenic and indirectly lowers levels of the anti-viral cytokine interferon gamma (IFNg), thus creating an environment which favors murine norovirus replication.

Dr. Mariam Gonzalez-Hernandez, a former graduate student of the Wobus lab, found that MNV-1 binds to dimeric IgA (dIgA) and secretory component (SC), the soluble form of pIgR (data not shown) [1]. Despite this interaction, no direct role for SIg in MNV infection could be determined. One possible unexplored outcome of the SIg:MNV interaction is that virus within the host interior can interact with newly synthesized dIgA and/or epithelial cell pIgR, and that the association would result in expulsion of the virus through the pIgR secretion pathway aiding in viral spread. Investigation into the role of pIgR and secretion of SIg in the excretion of MNV-1, was unsuccessful as despite viral replication in multiple organs including the colon, replicated virus was undetectable in the feces of both pIgR KO or WT B6 mice at 9, 18 and 48 hpi (see **Figure 2.2**). Non-uniform MNV-1 shedding was only detected at 18 hpi (data not shown), however, infection with the persistent MNV-CR3 strain results in detectable viral shedding [2] allowing investigation into the role of SIg in MNV shedding.

To assess the role of pIgR in MNV shedding I would infect mice orally with concentrated, high titer persistent MNV-CR3 to encourage robust infection and viral shedding. I would then assess shedding by sampling feces longitudinally at 0, 18, 24, 36, 48, and 60 hpi. Gastrointestinal tissues and feces would be harvested at 72 hpi and viral titers in tissues and feces would be determined via plaque assay. Virus detected in the feces at indicated time points would be compared to viral titers in the tissues at 72 hpi to determine percent viral shedding in pIgR KO compared to WT B6 mice. This comparison would allow us to control for any reduced infection seen in pIgR KO mice and more directly assess the role of SIg in MNV shedding. If SIg does enhance MNV shedding, further studies into SIg-mediated transmission of norovirus would be enlightening.

4.3 Determine Whether Natural Secretory Immunoglobulins Mediate Murine Norovirus Recombination

SIg complexes allow for direct sampling by MNV susceptible antigen-presenting cells (APCs), which may facilitate MNV infection. When complexed with SIg, MNV-1 infection of the macrophage like cell line (RAW264.7) was not enhanced, although further experiments using primary APCs would be necessary to rule out enhanced MNV uptake in the presence of SIg. Norovirus binding to multivalent SIg complexes may also promote co-infections of APCs, which in turn can increase viral fitness via complementation or recombination (e.g., [3-5]). However, additional work is needed to test these hypotheses.

4.4 Determine Whether Interferon-ɣ Limits Acute Reovirus Infection in Polymeric Immunoglobulin Receptor KO Mice

My data showed reduced reovirus infection of pIgR KO mice (see **Figure 2.4**), but I did not investigate the mechanism of reduced infection. Similar to MNV, reovirus replication is sensitive to IFN-ɣ [6, 7]. Thus, I hypothesize that enhanced levels of this cytokine may also be directly responsible for reduced viral loads seen in pIgR KO mice compared to WT B6 controls. To determine if the enhanced baseline IFN-ɣ levels seen in pIgR KO mice account for reduced reovirus replication in pIgR KO mice, I would repeat the experiments in **Figure 2.12** described for MNV with reovirus T1L. Briefly, I would treat pIgR KO mice with 500 μg isotype control or IFN-ɣ neutralizing antibody 18 hours prior to reovirus infection. Additionally, control or IFN-ɣ treated B6 mice would be infected with reovirus 24 hours after treatment. After 24 hours, tissues would be harvested, and viral titers would be assessed via plaque assay. I hypothesize that

reovirus viral loads would be reduced in the presence of enhanced IFN-ɣ (isotype treated pIgR KO and IFN-ɣ treated B6) regardless of mouse genetic background.

It would also be interesting to investigate if the reduction of reovirus infection in pIgR KO mice is due to immune cell sensing of the intestinal microbiota as is seen in norovirus infection. To this aim, germ-free pIgR KO and WT B6 would be infected with reovirus and viral replication would be assessed 24 hpi via plaque assay. Concurrent infection of conventionally housed mice would provide insight into the role of intestinal microbiota in the facilitation of reovirus infection. Successful completion of these experiments would provide further evidence of the antiviral role of IFN-ɣ in enteric viral infection and may provide potential avenues for treatment in other double-stranded RNA viral infections such as rotavirus or blue tongue virus.

4.5 Determine Whether Natural Secretory Immunoglobulins Alter M Cell Patterning Within Peyer's Patches

M cells rely on immune cues for development, which could be altered in the absence of SIg. To assess M cells levels in the absence of SIg, I analyzed M cell-related transcripts (Spi-B and GP2) and found no differences between strains (see **Figure 2.6B**). This data suggests similar levels of functional M cells, which is further supported by the finding that MNV-1, which utilizes M cells [8, 9], crosses the epithelial barrier similarly between strains (see **Figure 2.7**). However, analysis of the distribution of M cells within the Peyer's patch (PP) via immunofluorescence would be necessary to make a final conclusion regarding M cell levels in the absence of SIg. The absence of SIg, and altered microbiota (see **Figure 3.1**), might also result in other intestinal abnormalities. To fully investigate the role of SIg in shaping the intestinal

tissue, naïve intestines would need to be processed, sectioned, and stained for specialized cells in the epithelial barrier such as enteroendocrine cells, Paneth cells, and tuft cells, the latter of which are known MNV target cells [10]. M cells are attractive therapeutic targets for drug delivery in mucosal diseases [11, 12], and enhancing the proportion of M cells within the PP may aid in uptake of therapeutics.

4.6 Determine the Molecular Basis of Murine Norovirus Binding to Natural Secretory Immunoglobulins

MNV has been shown to bind to N- and O-linked carbohydrate residues on host cells [13] and these same glycosylations are also found on pIgA, SIgA, and SC [14-19]. Therefore, we hypothesize that MNV capsid protein P-domain binding to SIg is likely mediated by N- and O-linked glycosylations. However, these carbohydrate residues are necessary for proper protein folding, making assessment of the interaction by removal of these residues difficult. One potential approach to determine if MNV is binding to N- and O-linked glycosylations present on SIg,is to perform a competition experiment. Pre-incubation of MNV with N- and O-linked carbohydrate residues should inhibit MNV:SIg interactions. If MNV P-domain does mediate SIg binding via N- and O-linked glycosylations, future assessment of MNV P-domain binding to other immunoglobulins such as secretory IgM, which is also present in the intestinal lumen and lamina propria, would be enlightening. Human norovirus (HuNoV) also interacts with carbohydrate structures, including histo-blood group antigens [20-24], as well as fucose and sialic acid carbohydrate residues [25]. Fucosylated and sialydated carbohydrate residues are present on human SIgA [16, 26], therefore it is possible that HuNoV may also interact with SIg.

Using a capture ELISA to determine binding, HuNoV virus-like particles could be screened against human immunoglobulins and secretory component. I hypothesize that HuNoV is capable of interacting with human immunoglobulins and secretory component. These findings would allow for a greater understanding of the complex luminal environment and provide potential therapeutic and prevention avenues.

4.7 Determine Whether Natural Secretory Immunoglobulins Inhibit Murine Norovirus Mucosal Barrier Crossing

A major caveat to the intestinal loop assays is the injection of 100 μl of fluid into a small (~2 cm) closed off section of the intestine. This mass injection of fluid may wash away SIg containing mucus from the epithelial surface, thereby removing any ability for the mucus bound SIg to exert its effector functions. MNV pre-incubation with SIg prior to injection into the intestinal loop failed to alter MNV binding to the epithelium or MNV epithelial crossing (see **Figure 2.7D-E**). However, SIg may mediate its innate effector functions to prevent virus crossing through the mucus layer, and removal of the mucus layer may make SIg innate immune functions such as immune exclusion ineffective.

To assess the role of SIg in MNV crossing without disrupting mucosal barriers, MNV-1 would be administered to pIgR KO or WT B6 mice via oral gavage and intestinal tissues and Peyer's patches would be harvested shortly after viral administration. Based on intestinal transit data, traces of a one percent methylcellulose solution can already be detected in the distal small intestine 15 minutes after administration (see **Figure 2.10G**). M cells have been shown to transcytose particles in as few as 15 minutes [8], and given that the virus inoculum is

considerably less viscous than one percent methylcellulose, I hypothesize it would move through the gastrointestinal system at an accelerated rate. Therefore, I would harvest tissues at 30 minutes after administration of virus. After harvest of intestinal contents, Peyer's patches, and remaining intestinal tissue, samples would be processed to assess viral loads via RT-qPCR. The epithelial barrier would be digested from the lamina propria using DTT as to assess binding to and crossing of the epithelial barrier.

Given that MNV uses M cells to aid in barrier crossing [8, 9] and MNV target cells are concentrated within the follicle associated epithelium [12], it is no surprise that MNV-1 replication has been shown to be concentrated in Peyer's patches [27]. I hypothesize that MNV primarily crosses the intestinal epithelial barrier at lymphoid structures, and collection and assessment of non-lymphoid tissue as well as Peyer's patches from WT B6 mice would allow me to determine the proportion of virus crossing the barrier at lymphoid structures and pIgR KO tissues would allow assessment of the contribution of SIg in physiologic MNV crossing.

4.8 Determine Whether Natural Secretory Immunoglobulins Alter Small Intestinal Immune Subsets

At the time of characterization of MNV target cells in pIgR KO and WT B6 mice (see **Figure 2.8**), T cells [27] and tuft cells [10] were not known MNV target cells. No one to date has investigated tuft cell levels in pIgR KO compared to control mice. Thus, an investigation would be warranted to determine whether the lack of pIgR affects tuft cell levels. Furthermore, previous studies have shown that T cells expand to similar levels in response to pathogens in pIgR KO compared to control mice [28], and that pIgR KO mice have enhanced numbers of intraepithelial

lymphocytes (IELs) [29, 30]. This data suggests naïve T cells are enhanced in pIgR KO mice, but more direct analysis of T cell populations in naïve animals is needed.

Given that there are enhanced numbers of APCs and enhanced inflammatory molecules IFN-ɣ and iNOS, it is possible that MNV target cells in pIgR KO mice are activated to a greater degree [31]. Interestingly, despite enhanced IFN-ɣ levels, phenotypic analysis of mononuclear phagocytes (macrophages and dendritic cells) in the intestines of pIgR KO and control mice revealed no major differences (see **Figure 2.9**). Further characterization and functional analysis of intestinal immune cells should be carried out to determine the role of SIg in immune cell programming. Previous investigations into the role of SIg in immune cell activation and programming suggest that SIg sampling initiates non-inflammatory activation of dendritic cells and results in alterations in intestinal immune cell subsets, specifically enhancement of T regulatory cells [32-36]. Therefore, our finding that mononuclear phagocyte subsets are not altered in the absence of SIg would suggest that other unknown factors may aid in establishment of mucosal tolerance.

4.9 Determine Whether Interaction of Murine Norovirus with Natural Secretory Immunoglobulin Complexes Skews Viral Immunity to Promote Infection

To address immunomodulatory functions of both SIg and MNV-1, I would treat isolated intestinal immune cells with MNV-1, natural, non-MNV specific, SIg, and both MNV-1 and natural SIg together for 0, 18, 24, or 48 hpi. Examination of immune cell responses (cytokines, pattern recognition receptors, activation markers, etc.) via RT-qPCR and flow cytometry would allow for further investigation into the tolerogenic properties of SIg, as well as innate immune

responses to MNV. To address the role of bacteria in MNV-mediated immunomodulation in a more comprehensive manner, a gene array of common host cytokine responses would be analyzed in ileal Peyer's patches of infected germ-free versus conventional WT B6 mice as compared to naïve controls. In addition to assessment of host cytokine responses to MNV infection, analysis of pIgR expression changes would be interesting given other pathogens modulate pIgR expression [37].

In addition to SIg-mediated immune modulation, intestinal bacteria can also influence intestinal immunity. In MNV-infected conventional WT B6 mice, transcript levels of IFN-γ and TNF-α were reduced compared to naïve conventional controls (see **Figure 2.10C-D**), and in infected conventional pIgR KO mice IFN-ɣ transcript levels were reduced (see **Figure 2.10A**). Interestingly, the immunomodulatory functions of MNV seem to be dependent on enteric microbiota as transcript reductions are not observed in germ-free WT B6 or pIgR KO animals (see **Figure 3.3A & 3.3C-D**). MNV-mediated reduction of IFN-ɣ in conventional mice was not recapitulated in germ-free mice, where IFN-ɣ protein increased after infection of PIgR KO vs naive controls (see **Figure 3.3G**). Future work is required to test whether interaction of enteric viruses with SIg:bacterial complexes could skew the inflammatory viral immune response promoting tolerogenic responses and intestinal homeostasis. Such a response may account for the weak inflammatory response and poor lasting immunity observed in norovirus infections [38].

4.10 Determine Whether Small Intestinal Macrophages are Resistant to Murine Norovirus Infection

Immune cells stimulated with IFN-ɣ have been shown to be resistant to MNV-1 viral replication in vitro [39-41]. Therefore, I sought to determine if in vivo IFN-ɣ levels influence ex vivo infectivity of intestinal immune cells from pIgR KO and WT B6 animals. To that end, I isolated intestinal immune cells from the villous and PP lamina propria and infected them with MNV-1. Unfortunately, I was not able to detect productive MNV-1 infection in ex vivo small intestinal cells from either mouse strain (see **Figure 2.11**). In addition, my investigation into MNV-1 in vivo target cells from infected ilea and PP's of highly MNV susceptible STAT1-/- mice [42] using a flow cytometry-based in situ hybridization assay to detect viral RNA were unsuccessful (n=3 experiments, 4 infected, 3 mock; data not shown). While these findings are preliminary, it appears as though lamina propria cells isolated from the small intestine are refractory to ex vivo MNV-1 infection regardless of mouse genotype. Since MNV successfully infects cells in vivo, I would want to confirm these ex vivo findings.

It is unclear how long intestinal immune cells survive ex vivo, therefore phenotypic and viability analysis of isolated cell types should be performed via flow cytometry to assure viable MNV target cells are present in the culture. In addition, although I saw no enhancement of genome copies at 9 hpi that may be too soon to detect replication (see **Figure 2.11C-E**). In the future, MNV viral genome copies should be assessed at 24 hpi to allow for detection of enhanced genome copies, while minimizing the amount of ex vivo cell death. If productive replication of immune cells from the small intestine can be achieved ex vivo, one can begin to ask questions regarding their immune responses to MNV as antigen-presenting cells in the presence and absence of SIg, as well as assess their susceptibility to MNV infection. Additionally, cultivation of an ex vivo system for assessment of MNV infection would allow for more physiologically relevant assessments of host responses to norovirus infection.

4.11 Determine Whether MNV-CR3 is Sensitive to Interferon-ɣ Mediated Control of Viral Replication

Interestingly, MNV-CR3 infection was not altered in pIgR KO mice, despite enhanced IFN-ɣ levels in target organs (see **Figure 2.3D** & **Figure 2.10G**). To date, all published studies regarding MNV susceptibility to IFN-ɣ use the MNV-1 strain only, therefore it would be interesting to determine if MNV-CR3 is also susceptible to IFN-ɣ mediated control of viral replication. To determine if IFN-ɣ alters MNV-CR3 infection, I would infect the macrophage-like cell line (RAW264.7), as well as primary bone marrow derived macrophages with MNV-CR3 in the presence of increasing concentrations (0 to 1000 units/ml) of murine IFN-ɣ at a multiplicity of infection (MOI) of 0.05 and 5 and viral titers would be assessed at 0, 18, 24 and 48 hours post infection (hpi) via plaque assay.

Given that MNV-CR3 also utilizes replication complexes, and IFN- ɣ mediates disruption of these complexes, it would be very interesting to find that it was insensitive to IFN-ɣ mediated replication complexes disruption. To determine if IFN-ɣ mediates disruption of MNV-CR3 replication complex, increases in the IFN-ɣ-inducible immunity-related GTPase IRGA6 would also be assessed [39]. Several other positive-sense, single-stranded RNA viruses have been shown to be controlled by IFN-ɣ during the replication phase [43-45]. Identification of IFN-ɣ-mediated disruption of the viral replication complex in MNV-CR3 and other positive-sense, single-stranded RNA virus infections would enhance our understanding of IFN-ɣ-mediated antiviral immunity.

4.12 Determine Which Intestinal Microbial Communities Enhance Interferon-ɣ in Polymeric Immunoglobulin Receptor KO Mice

The finding that intestinal microbial communities are altered throughout the intestinal tract in the absence of SIg (see **Figure 3.1A-F**) is hardly surprising given the overwhelming evidence regarding the role of SIg in shaping intestinal microbial communities [15, 18, 33, 35-37, 46]. To determine which bacteria induce IFN-ɣ in pIgR KO mice, I would select bacterial species from our 16S rRNA analysis found in the intestinal lumen of pIgR KO mice known to induce inflammatory immune responses. For example, *Erysipelotrichaceae* species were found to be increased in the intestinal lumen and mucosal tissues of pIgR KO mice versus WT B6 controls (see **Figure 3.1**) and are highly immunogenic [47]. Monocolonization of germ-free pIgR KO mice with *Erysipelotrichaceae* species and subsequent IFN-ɣ transcript and protein analysis in intestinal tissues would determine their immunogenicity in the absence of SIg. Aberrant inflammation caused by alterations in microbial communities can result in irritable bowel syndrome, Crohn's disease and ulcerative colitis and the intestinal microbiota have been linked to many seemingly unrelated maladies including depression, obesity and autism [48-52]. Identification of specific bacterial species that enhance intestinal inflammation would allow for avenues of treatment of the above maladies through modulation of harmful bacterial species in disease states.

4.13 Determine the Mechanism of Bacterially-Mediated MNV-1 & MNV-CR3 Gastrointestinal Regionalization

4.13A Determine if Loss of Mucosal Barrier Integrity Results in Altered Murine Norovirus Gastrointestinal Regionalization

MNV infection in the absence of the microbiota results in altered intestinal regionalization of MNV infection with more virus produced in the proximal versus distal small intestine in the absence of the microbiota (see **Figures 3.5** & **3.6**). The intestinal mucus layer has been shown to be more permeable in germ-free housed mice than in conventionally housed controls [50, 53]. Perhaps the reduction in mucus facilitates enhanced access of MNV to the first intestinal epithelial surface it encounters, the duodenum. Additionally, intestinal epithelial barrier integrity could be compromised in mice housed under germ-free conditions [54], resulting in leakier intestines and greater absorption of MNV in the proximal small intestine. These factors may explain the altered intestinal distribution of MNV in the absence of the intestinal microbiota (see **Figure 3.5**) and are potential avenues of further exploration.

To determine if our germ-free mice have altered intestinal permeability, small and large intestines from naïve germ-free and conventional WT B6 mice would be harvested and processed for histological examination and immunofluorescence imaging of the mucus layer and tight junctional proteins. Permeability of intestines would be directly measured using penetration of FITC-dextran into the intestinal lamina propria of conventional and germ-free WT B6 mice [55]. To directly test MNV permeability across the intestinal barrier, I would inoculate conventional and germ-free WT B6 mice with MNV-1 and harvest intestines less than one hour after viral administration. MNV genome copies in the lamina propria of the duodenum, jejunum, and ileum would be assessed via RT-qPCR allowing us to determine if enhanced access to the lamina propria of the proximal small intestine in germ-free mice can account for the altered viral distribution compared to conventional controls.

Loss of barrier integrity in germ-free mice may also affect viral shedding. If we determine germ-free mice have altered intestinal barrier integrity, conventional and germ free WT B6 mice would be infected with high titer MNV-CR3 as this MNV strain has been shown to cause viral shedding [56]. Feces would be collected daily for one week and MNV genome copies would be assessed via RT-qPCR to determine the role of bacteria in MNV viral shedding. Determination of the mechanism of bacterially-mediated norovirus gastrointestinal regionalization would provide insights into the complex role of intestinal bacteria during MNV infection, which may also extend to HuNoV and other enteric viral infections.

4.13B Determine Whether Bacterial Colonization of Germ-Free Mice Alter Murine Norovirus Gastrointestinal Regionalization

Discovery of specific bacterial species capable of correcting MNV gastrointestinal regionalization in germ-free animals to that of conventional mice would allow for mechanistic studies regarding MNV intestinal distribution. My pilot studies tested *Bacteroides thetaiotaomicron* (*B. theta)* as a modulator of MNV infection (see **Figure 3.9A**). Since the *B. theta* colonization was not robust enough in germ-free animals more experiments are needed to determine whether the intestinal distribution of MNV infection is modulated by this bacterial species. Longer colonization, and multiple inoculations of *B. theta* may enhance colonization and allow for a more accurate examination of the role of *B. theta* in MNV infection. It is likely however that several species of bacteria are capable of interacting with MNV and indirectly or directly modulating MNV infection. Therefore, it may be necessary to inoculate germ-free mice

with a cocktail of several bacterial species to see robust colonization and a reversal of the germ-free phenotype.

In addition to identifying specific bacterial species that modulate MNV regionalization of infection, another unresolved question is the molecular determinant of MNV binding on the bacteria. To determine what bacterial factor(s) mediate MNV binding to bacteria, we would assess bacterial characteristics such as LPS, Flagella, HBGA, sialic acids, and SIg binding. This analysis would offer the first evidence of MNV:bacterial interactions and may provide clues regarding the mechanism of this interaction. Direct MNV binding of bacterial factors of interest would be demonstrated using ELISA. To determine the role of specific bacterial factor(s) in MNV infection, we would engineer bacteria deficient in the protein(s) of interest in collaboration with Dr. Nicole Koropatkin's lab. Reconstitution of germ-free mice with WT or deficient bacteria prior to MNV infection and MNV viral loads would be assessed via plaque assay. If the bacterial factor is important for MNV infection, I would likely see reduced viral infection in mice colonized with bacterial factor-deficient versus WT bacteria. If differences in viral loads were detected, analysis of in vivo MNV:bacterial interactions as well as viral crossing of intestinal barriers would be assessed to determine the function of the bacterial factor of interest in MNV infection. It is conceivable that through these studies we could discover specific bacterial species that modulate norovirus infection, providing potential avenues for norovirus treatment.

4.14 Concluding Remarks

No organism exists in isolation. Likewise, people are teeming with bacteria and other microbes, and it is highly likely that unrecognized trans-kingdom interactions exist within the human gastrointestinal tract. These interactions may have unrecognized effects on both host and pathogen. Studying pathogen:pathogen and pathogen:commensal interactions within the host allows for a more complex and thorough understanding of infection. Investigation of SIg-mediated modulation of immunity in the context of these trans-kingdom interactions are severely limited, or entirely lacking. Completion of the proposed experiments would allow for a broader understanding of the complex interactions of secretory immunoglobulins, norovirus, and bacteria and may provide avenues of exploration for other enteric viral infections as well as norovirus treatment options.

4.15 References

1. Turula, H., et al., *Natural Secretory Immunoglobulins Promote Enteric Viral Infections.* J Virol, 2018.
2. Taube, S., et al., *Murine noroviruses bind glycolipid and glycoprotein attachment receptors in a strain-dependent manner.* J Virol, 2012. **86**(10): p. 5584-93.
3. Erickson, A.K., et al., *Bacteria Facilitate Enteric Virus Co-infection of Mammalian Cells and Promote Genetic Recombination.* Cell Host Microbe, 2017.
4. Allison, R., C. Thompson, and P. Ahlquist, *Regeneration of a functional RNA virus genome by recombination between deletion mutants and requirement for cowpea chlorotic mottle virus 3a and coat genes for systemic infection.* Proc Natl Acad Sci U S A, 1990. **87**(5): p. 1820-4.
5. Chen, Y.H., et al., *Phosphatidylserine vesicles enable efficient en bloc transmission of enteroviruses.* Cell, 2015. **160**(4): p. 619-30.
6. L. A. Schiff, M.L.N.a.K.L.T., *Orthoreoviruses and Their Replication.* Fields Virology, 2007. **5th Edition**: p. pp. 1853-1915. .
7. Rubin, B.Y., et al., *The anticellular and protein-inducing activities of human gamma interferon preparations are mediated by the interferon.* J Immunol, 1983. **130**(3): p. 1019-20.
8. Gonzalez-Hernandez, M.B., et al., *Murine norovirus transcytosis across an in vitro polarized murine intestinal epithelial monolayer is mediated by M-like cells.* J Virol, 2013. **87**(23): p. 12685-93.
9. Gonzalez-Hernandez, M.B., et al., *Efficient norovirus and reovirus replication in the mouse intestine requires microfold (M) cells.* J Virol, 2014. **88**(12): p. 6934-43.

10. Wilen, C.B., et al., *Tropism for tuft cells determines immune promotion of norovirus pathogenesis.* Science, 2018. **360**(6385): p. 204-208.
11. Mabbott, N.A., et al., *Microfold (M) cells: important immunosurveillance posts in the intestinal epithelium.* Mucosal Immunol, 2013. **6**(4): p. 666-77.
12. Mowat, A.M. and W.W. Agace, *Regional specialization within the intestinal immune system.* Nat Rev Immunol, 2014. **14**(10): p. 667-85.
13. Taube, S., et al., *Murine noroviruses bind glycolipid and glycoprotein attachment receptors in a strain-dependent manner.* J Virol, 2012. **86**(10): p. 5584-93.
14. Huang, J., et al., *Site-specific glycosylation of secretory immunoglobulin A from human colostrum.* J Proteome Res, 2015. **14**(3): p. 1335-49.
15. Phalipon, A., et al., *Secretory component: a new role in secretory IgA-mediated immune exclusion in vivo.* Immunity, 2002. **17**(1): p. 107-15.
16. Royle, L., et al., *Secretory IgA N- and O-glycans provide a link between the innate and adaptive immune systems.* J Biol Chem, 2003. **278**(22): p. 20140-53.
17. Crottet, P., S. Cottet, and B. Corthesy, *Expression, purification and biochemical characterization of recombinant murine secretory component: a novel tool in mucosal immunology.* Biochem J, 1999. **341 (Pt 2)**: p. 299-306.
18. Perrier, C., N. Sprenger, and B. Corthesy, *Glycans on secretory component participate in innate protection against mucosal pathogens.* J Biol Chem, 2006. **281**(20): p. 14280-7.
19. Stadtmueller, B.M., et al., *The structure and dynamics of secretory component and its interactions with polymeric immunoglobulins.* Elife, 2016. **5**: p. e10640.
20. Jones, M.K., et al., *Enteric bacteria promote human and mouse norovirus infection of B cells.* Science, 2014. **346**(6210): p. 755-9.
21. Li, D., et al., *Binding to histo-blood group antigen-expressing bacteria protects human norovirus from acute heat stress.* Front Microbiol, 2015. **6**: p. 659.
22. Miura, T., et al., *Histo-blood group antigen-like substances of human enteric bacteria as specific adsorbents for human noroviruses.* J Virol, 2013. **87**(17): p. 9441-51.
23. Sestak, K., *Role of histo-blood group antigens in primate enteric calicivirus infections.* World J Virol, 2014. **3**(3): p. 18-21.
24. Tan, M. and X. Jiang, *Histo-blood group antigens: a common niche for norovirus and rotavirus.* Expert Rev Mol Med, 2014. **16**: p. e5.
25. Wegener, H., et al., *Human norovirus GII.4(MI001) P dimer binds fucosylated and sialylated carbohydrates.* Glycobiology, 2017. **27**(11): p. 1027-1037.
26. Orczyk-Pawilowicz, M., et al., *Lectin-based analysis of fucose and sialic acid expressions on human amniotic IgA during normal pregnancy.* Glycoconj J, 2013. **30**(6): p. 599-608.
27. Grau, K.R., et al., *The major targets of acute norovirus infection are immune cells in the gut-associated lymphoid tissue.* Nat Microbiol, 2017. **2**(12): p. 1586-1591.
28. Uren, T.K., et al., *Role of the polymeric Ig receptor in mucosal B cell homeostasis.* J Immunol, 2003. **170**(5): p. 2531-9.
29. Yamazaki, K., et al., *Accumulation of intestinal intraepithelial lymphocytes in association with lack of polymeric immunoglobulin receptor.* Eur J Immunol, 2005. **35**(4): p. 1211-9.
30. Kato-Nagaoka, N., et al., *Enhanced differentiation of intraepithelial lymphocytes in the intestine of polymeric immunoglobulin receptor-deficient mice.* Immunology, 2015. **146**(1): p. 59-69.

31. Sidman, C.L., et al., *Gamma-interferon is one of several direct B cell-maturing lymphokines.* Nature, 1984. **309**(5971): p. 801-4.
32. Baumann, J., C.G. Park, and N.J. Mantis, *Recognition of secretory IgA by DC-SIGN: implications for immune surveillance in the intestine.* Immunol Lett, 2010. **131**(1): p. 59-66.
33. Corthesy, B., *Secretory immunoglobulin A: well beyond immune exclusion at mucosal surfaces.* Immunopharmacol Immunotoxicol, 2009. **31**(2): p. 174-9.
34. Diana, J., et al., *Secretory IgA induces tolerogenic dendritic cells through SIGNR1 dampening autoimmunity in mice.* J Immunol, 2013. **191**(5): p. 2335-43.
35. Mantis, N.J., N. Rol, and B. Corthesy, *Secretory IgA's complex roles in immunity and mucosal homeostasis in the gut.* Mucosal Immunol, 2011. **4**(6): p. 603-11.
36. Pabst, O., V. Cerovic, and M. Hornef, *Secretory IgA in the Coordination of Establishment and Maintenance of the Microbiota.* Trends in Immunology, 2016. **37**(5): p. 287-296.
37. Turula, H. and C.E. Wobus, *The Role of the Polymeric Immunoglobulin Receptor and Secretory Immunoglobulins during Mucosal Infection and Immunity.* Viruses, 2018. **10**(5).
38. Newman, K.L. and J.S. Leon, *Norovirus immunology: Of mice and mechanisms.* Eur J Immunol, 2015. **45**(10): p. 2742-57.
39. Biering, S.B., et al., *Viral Replication Complexes Are Targeted by LC3-Guided Interferon-Inducible GTPases.* Cell Host Microbe, 2017. **22**(1): p. 74-85.e7.
40. Changotra, H., et al., *Type I and type II interferons inhibit the translation of murine norovirus proteins.* J Virol, 2009. **83**(11): p. 5683-92.
41. Hwang, S., et al., *Nondegradative role of Atg5-Atg12/ Atg16L1 autophagy protein complex in antiviral activity of interferon gamma.* Cell Host Microbe, 2012. **11**(4): p. 397-409.
42. Karst, S.M., et al., *STAT1-dependent innate immunity to a Norwalk-like virus.* Science, 2003. **299**(5612): p. 1575-8.
43. Burdeinick-Kerr, R. and D.E. Griffin, *Gamma interferon-dependent, noncytolytic clearance of sindbis virus infection from neurons in vitro.* J Virol, 2005. **79**(9): p. 5374-85.
44. Rowland, R.R., et al., *Inhibition of porcine reproductive and respiratory syndrome virus by interferon-gamma and recovery of virus replication with 2-aminopurine.* Arch Virol, 2001. **146**(3): p. 539-55.
45. Grunvogel, O., et al., *DDX60L Is an Interferon-Stimulated Gene Product Restricting Hepatitis C Virus Replication in Cell Culture.* J Virol, 2015. **89**(20): p. 10548-68.
46. Kaetzel, C.S., *Cooperativity among secretory IgA, the polymeric immunoglobulin receptor, and the gut microbiota promotes host-microbial mutualism.* Immunol Lett, 2014. **162**(2 Pt A): p. 10-21.
47. Kaakoush, N.O., *Insights into the Role of Erysipelotrichaceae in the Human Host.* Front Cell Infect Microbiol, 2015. **5**: p. 84.
48. Compare, D., et al., *The Gut Bacteria-Driven Obesity Development.* Dig Dis, 2016. **34**(3): p. 221-9.
49. Iizumi, T., et al., *Gut Microbiome and Antibiotics.* Arch Med Res, 2017. **48**(8): p. 727-734.

50. Malago, J.J., *Contribution of microbiota to the intestinal physicochemical barrier.* Benef Microbes, 2015. **6**(3): p. 295-311.
51. Min, Y.W. and P.L. Rhee, *The Role of Microbiota on the Gut Immunology.* Clin Ther, 2015. **37**(5): p. 968-75.
52. Parker, A., et al., *Host-microbe interaction in the gastrointestinal tract.* Environ Microbiol, 2018. **20**(7): p. 2337-2353.
53. Johansson, M.E., et al., *Normalization of Host Intestinal Mucus Layers Requires Long-Term Microbial Colonization.* Cell Host Microbe, 2015. **18**(5): p. 582-92.
54. Ulluwishewa, D., et al., *Regulation of tight junction permeability by intestinal bacteria and dietary components.* J Nutr, 2011. **141**(5): p. 769-76.
55. Zong, Y., et al., *Chronic stress and intestinal permeability: Lubiprostone regulates glucocorticoid receptor-mediated changes in colon epithelial tight junction proteins, barrier function, and visceral pain in the rodent and human.* Neurogastroenterol Motil, 2018: p. e13477.
56. Nelson, A.M., et al., *Murine norovirus infection does not cause major disruptions in the murine intestinal microbiota.* Microbiome, 2013. **1**(1): p. 7.